The Power of Mathematical Modeling and Simulation in Cardiometabolic Disorders: Personalized Treatment Optimization and Disease Trajectories

DISSERTATION

zur Erlangung des Grades des Doktors der Naturwissenschaften der Naturwissenschaftlich-Technischen Fakultät der Universität des Saarlandes

von

Nina Scherer

Apothekerin

Saarbrücken

2025

Tag des Kolloquiums: 18.09.2025

Dekan: Prof. Dr.-Ing. Dirk Bähre

Berichterstatter: Prof. Dr. Thorsten Lehr

Prof. Dr. Claus Jacob

Vorsitz: Prof. Dr. Andriy Luzhetskyy

Akad. Mitarbeiter: Dr. Michael Ring

Without data you're just another person with an opinion.

(W. Edwards Deming)

Publications included in this thesis

PROJECT I

Scherer N, Kurbasic A, Dings C, et al. The Impact and Correction of Analysis Delay and Variability in Storage Temperature on the Assessment of HbA1c from Dried Blood Spots - an IMI DIRECT Study. Int J Proteom Bioinform. (2019); 4(1): 007-013. (1)

PROJECT II

Türk D, <u>Scherer N</u>, Selzer D, et al. **Significant impact of time-of-day variation on metformin pharmacokinetics**. Diabetologia (2023); 66(6):1024–34. (2)

PROJECT III

Scherer N, Dings C, Boehm M, et al., Alternative Treatment Regimens With the PCSK9 Inhibitors Alirocumab and Evolocumab: A Pharmacokinetic and- Pharmacodynamic Modeling Approach; J Clin Pharmacology (2017); 57(7): 846-854. (3)

Contribution report

To transparently distinguish her involvement in the publications presented within this dissertation, the author assigns her contributions according to the Contributor Roles Taxonomy (CRediT) (4,5).

PROJECT I

Conceptualization, Data curation, Investigation; Formal analysis, Methodology, Visualization, Validation, Writing – original draft, Writing – review & editing

PROJECT II

Conceptualization, Data curation, Formal analysis, Investigation, Methodology, Visualization, Writing – original draft, Writing – review & editing

PROJECT III

Data curation, Formal analysis, Methodology, Validation, Visualization, Writing – original draft, Writing – review & editing

Abstract

This dissertation investigates the potential of mathematical modeling to enhance the management of cardiometabolic diseases. These conditions represent a major global health challenge due to their high prevalence and the complex nature of underlying metabolic risk factors. Utilizing nonlinear mixed-effects (NLME) modeling, the projects presented in this thesis demonstrate that modeling can (i) improve the accuracy of clinical biomarker data, (ii) incorporate biological rhythms into pharmacokinetic analyses, and (iii) support the development of cost-efficient treatment strategies. The methodological focus includes correcting biases in biomarker measurements, capturing circadian variation in drug exposure, and evaluating flexible dosing regimens that balance therapeutic efficacy with cost-effectiveness. By aligning quantitative insights with clinical practice, this work illustrates how data-driven modeling can personalize treatment and optimize healthcare resource allocation. The findings highlight mathematical modeling as a valuable tool for advancing precision medicine in cardiometabolic care through more adaptive, efficient, and individualized treatment approaches.

Zusammenfassung

Diese Dissertation zeigt das Potenzial mathematischer Modellierung zur Verbesserung des Managements kardiometabolischer Erkrankungen auf. Aufgrund der hohen Prävalenz und der komplexen metabolischen Risikofaktoren stellen diese Erkrankungen eine bedeutende globale Gesundheitsherausforderung dar. Diese Arbeit vereint drei Projekte, die jeweils mittels mathematischer Modellierung nichtlinearer gemischter Effekte (NLME) zeigen, wie Modellierungsansätze (i) die Genauigkeit klinischer Messergebnisse von Biomarkern verbessern, (ii) biologische Schwankungen in pharmakokinetische Analysen integrieren und (iii) zur Entwicklung kosteneffizienter Behandlungsstrategien beitragen können. Dabei liegt der methodische Fokus auf der Korrektur von Biomarker-Messungen infolge fehlerhafter Probenlagerung, der Beschreibung und Erklärung von zirkadianen Variationen in der Wirkstoffexposition sowie der Entwicklung flexibler Dosierungsschemata, die therapeutische Wirksamkeit mit ökonomischen Aspekten in Einklang bringen. Durch die Verknüpfung quantitativer Modellierung mit klinischer Anwendung veranschaulicht diese Arbeit, wie datenbasierte Ansätze zur Personalisierung von Therapien und zur effizienteren Nutzung von Gesundheitsressourcen beitragen können. Die Ergebnisse unterstreichen den Mehrwert mathematischer Modellierung als ein Instrument für eine adaptivere, effektivere und individuellere Versorgung von Patienten mit kardiometabolischen Erkrankungen.

Table of Contents

Publ	icati	ons included in this thesis	i
Con	tribu	tion report	ii
Abst	tract		iii
Zusa	amm	enfassung	iv
Abb	revia	tions	vii
1	In	troduction	1
1.1	M	etabolic Syndrome	3
1.2	Di	abetes Mellitus	4
1.2	2.1	Metformin	5
1.3	Lij	oid Disorders	6
1.3	3.1	PCSK9 Inhibitors	8
1.4	IM	II DIRECT Consortium	9
1.5	M	athematical Modelling	10
2	Ol	bjectives of the thesis	11
2.1 diab		bjective 1: Handling of "real-life" data to investigate Disease Progres Patients	
2.2	Ol	bjective 2: The Impact of Circadian Rhythms on Metformin Pharmac	okinetics 12
2.3 Hype		ojective 3: Evaluating new Cost Effective Dosing Regimens for the T	
2.4	Pr	oject included in this thesis	13
3	M	ethods	14
3.1	Ва	ackground	14
3.2	Po	opulation Approach	15
3.3	No	onlinear Mixed-Effects Modeling	16
3.3	3.1	Structural Model	17
3.3	3.2	Statistical Model	18
3.3	3.3	Covariate Model	20
3.4	Es	stimation Method	20
3.5	M	odel Selection and Evaluation	21
3.5	5.1	Objective Function Value and Akaike Information Criterion	21
3.5.2		Relative Standard Error	21
3.5	5.3	Graphical Methods	22
3.6	PE	3PK Modeling Approach	22
4	R	egulte	24

4.1 Storag	Publication I: The Impact and Correction of Analysis Delay and Variability in Temperature on the Assessment of HbA1c from Dried Blood Spots - an IMI	
DIREC	CT Study.	24
4.2 Pharm	Publication II: Significant Impact of Time-of-Day Variation on Metformin acokinetics.	32
	Publication III: Alternative Treatment Regimens With the PCSK9 Inhibitors umab and Evolocumab: A Pharmacokinetic and- Pharmacodynamic Modeling ach	44
5	Discussion and Perspective	
5.1	Modeling as a Tool for Personalization and Optimization	
5.2	Bridging Controlled Trials and Real-World Conditions	55
5.3	Simulation and Decision Support	56
5.4	Data Limitations and Justified Simplifications	57
5.5	Outlook: Al and Model Informed Precision Dosing	57
5.6	Interdisciplinary Collaboration and Public Health Relevance	58
6	Conclusion	59
Bibliog	raphy	60
Appen	dix A: Supplementary material to the publications	67
A 1: Pı	roject II appendix	67
A 2: Pı	roject III appendix	.118
Appen	dix B:	.125
B1: Co	onference Abstracts	.125
B2: Bo	ook Chapters	.125
Danks	agung	.126

Abbreviations

Abbreviation	Definition			
AACE	American Association of Clinical Endocrinologists			
ADME	Absorption, distribution, metabolism and elimination			
Al	Artificial intelligence			
AIC	Akaike Information Criterion			
AMP	Adenosinmonophosphat			
AMPK	AMP-activated protein kinase			
BMI	Body mass index			
ВР	Blood pressure			
CVD	Cardiovascular disease			
DARWIN	Data Analysis and Real World Interrogation Network			
DBS	Dried blood spot			
DIRECT	Dlabetes REsearCh on patient straTification			
EMA	European Medicines Agency			
EU	European Union			
FDA	Food and Drug Administration			
FOCE (I)	First-order conditional estimation (with/ without interaction)			
FPG	Fasting Plasma Glucose			
GMFE	Geometric mean fold error			
GOF	Goodnes-of-fit			
HbA1c	Glycated hemoglobin			
HDL	High-density lipoprotein			
ICA	Individual compartmental analysis			
IDF	International Diabetes Federation			
IFG	Impaired fasting glucose			
IGT	Impaired glucose tolerance			
IIV	Interindividual variability			
IMI	Innovative Medicines Initiative			
IOV	Inter-occasion variability			
LDL	Low-density lipoprotein			
LDLR	LDL-receptor			
LL	Log-likelihood function			

Abbreviation	Definition			
LRT	Likelihood ratio test			
MATEs MID3	Multidrug and toxin extrusion proteins Model-Informed Drug Discovery and Development			
MIDD	Model-informed Drug Development			
MIPD	Model-Informed Precision Dosing			
ML	Machine learning			
MRD	Mean relative deviation			
NCEP-ATP	National Cholesterol Education Program Adult Treatment Panel III			
NLME	Nonlinear Mixed-Effects			
NONMEM®	Program for population analysis			
OCT	Organic cation transporter			
ODE	Ordinary differential equations			
OFV	Objective function value			
PBPK	Physiologically based pharmacokinetics			
PCSK9	Proprotein convertase subtilisin/kexin type 9			
PD	Pharmacodynamic			
PK	Pharmacokinetic			
QSP	Quantitative systems pharmacology			
RCT	Randomized controlled trials			
RSE	Relative standard error			
RUV	Residual unexplained variability			
RWD	Real-world data			
RWE	Real-world evidence			
SAEM	Stochastic approximation expectation-maximization			
SGLT2	Sodium-glucose co-transporter-2			
STS	Standard Two-Stage Approach			
T2DM	Type 2 Diabetes Mellitus			
TG	Triglyceride			
wc	Waist circumference			
WHO	World Health Organization			
WHR	Waist-hip ratio			

1 Introduction

In recent years, the global healthcare landscape has been significantly challenged by the increasing prevalence of cardiometabolic diseases, which encompass a spectrum of conditions affecting the heart, blood vessels, and metabolic processes within the body (6,7). Metabolic syndrome, composed of at least three of the following five components, is becoming an increasingly pressing health problem in the modern world: central adiposity as measured by waist circumference (a marker for visceral adipose tissue), elevated blood sugar (indicative of insulin resistance), elevated triglyceride levels, low high-density lipoprotein (HDL) cholesterol levels, and elevated blood pressure (8). As suspected from the elevated blood sugar, a central comorbidity is Type 2 Diabetes Mellitus (T2DM), a condition characterized by disrupted glucose metabolism and insulin resistance (9,10). Particularly, the increasingly prevalent comorbidities over time, such as obesity, hypertension, or dyslipidemia, further increase the complexity of managing cardiometabolic diseases (11).

Metabolic Syndrome affects up to 30% of the population in industrialized nations, with increasing prevalence among younger age groups (12). In addition to the immediate consequences for those affected, the Metabolic syndrome holds high relevance from a health economic perspective. For instance, in Germany alone, the direct healthcare costs attributed to diabetes, obesity, and hypertension reached approximately 15 billion euros in 2020, with secondary complications further straining healthcare resources (12).

Understanding the complex interplay of genetic, environmental, and lifestyle factors contributing to the development and individual progression of these diseases is therefore essential for long-term early patient assistance and minimizing subsequent damage and costs (13). Moreover, the prevalence of comorbidities, particularly between diabetes and cholesterol disorders, poses additional challenges for patients and healthcare providers (14).

For this reason, there is an urgent need for innovative approaches to understand the underlying mechanisms, predict disease trajectories, and develop effective interventions including new treatment options (6,7).

To address these multifaceted issues, collaborative initiatives like the IMI DIRECT (Innovative Medicines Initiative - Diabetes Research on Patient Stratification) Consortium were initiated and have significantly contributed to this effort. Funded by the European Innovative Medicines Initiative (IMI), this consortium united 20 academic institutions and

five pharmaceutical companies to investigate the progression of T2DM and its therapeutic responses (14). By analyzing data from a cohort of over 3,000 participants across five European countries, the IMI DIRECT Consortium provided critical insights into individual disease progression and variability in treatment responses (11).

As part of the IMI DIRECT Consortium, this dissertation builds on these findings to deepen our understanding of T2DM and related cardiometabolic diseases. The research presented herein focuses on the use of mathematical modeling and pharmacometrics to address the key challenges in the prevention and treatment of these complex conditions. Pharmacometrics is an interdisciplinary field, that applies mathematical models and simulations to analyze the relationships between drugs, patients, and diseases. It includes approaches such as physiologically based pharmacokinetics (PBPK), quantitative systems pharmacology (QSP), and population-based modeling, all of which play a central role in developing accurate and individualized treatment strategies.

This dissertation aims to make meaningful contributions to the field through three distinct projects. Each project employs mathematical modeling and simulation to generate hypotheses, explore research questions, and provide actionable insights for healthcare professionals, patients, and researchers. The overarching goal is to reduce the burden of cardiometabolic diseases, improve patient outcomes, and address gaps in our understanding of these complex conditions (15).

Having established the global relevance of cardiometabolic diseases and the importance of pharmacometrics, the following sections examine in more detail the key components of these conditions: Metabolic Syndrome, T2DM, and lipid disorders.

1.1 Metabolic Syndrome

The metabolic syndrome is a collection of metabolism-related symptoms that increase an individual's risk of developing cardiovascular diseases (CVD), including heart disease, atherogenic dyslipidemia, stroke, and T2DM (16). However, there are various definitions of metabolic syndrome, and the ranking and importance of each parameter is discussed controversy in the literature (17). The relevant metabolic parameters that are associated with the syndrome are increased blood pressure, altered lipid values such as increased triglycerides and decreased HDL cholesterol, overweight, especially abdominal obesity, and increased fasting blood sugar or pre-existing diabetes (13). Each of these symptoms alone poses a risk factor for vascular and cardiovascular diseases (18). When these symptoms co-occur, the risk further increases, leading to the metabolic syndrome often being referred to as the "deadly quartet" (19).

The World Health Organization (WHO) defines metabolic syndrome as an insulin resistance combined with two or more of the other symptoms: abdominal obesity reflected by a high waist/hip ratio or BMI, hypertension, and/or hyperlipidemia (20,21). The National Cholesterol Education Program (NCEP), International Diabetes Federation (IDF), and American Association of Clinical Endocrinologists (AACE) definitions are similar but differ in the selection of essential criteria for diagnosis, the way of combining the criteria, or the cut-off values for specific criteria (22). Table 1 provides a summary of the three commonly used definitions of metabolic syndrome.

In clinical practice, the severity assessment of the metabolic syndrome serves as a tool to predict individual risk for developing cardiovascular diseases and T2DM (23). Various reviews and analyses in the literature have highlighted that CVD is the primary outcome of metabolic syndrome (24). Additionally, the presence of metabolic syndrome can be utilized as a predictive marker for identifying T2DM (25).

Cardiovascular diseases remain the leading cause of death worldwide, accounting for an estimated 17.9 million deaths each year and representing approximately 32 percent of all global mortality. In light of this, it is essential to examine the interconnections between the individual components of metabolic syndrome (21). Building on this foundation, the following chapter turns to one of its key comorbidities: T2DM, with a particular focus on the role of metformin in disease management (26).

Table 1: Definition of metabolic syndrome according to WHO, AACE, NCEP and IDF (according to (27,28))

	WHO (1998)	AACE (2003)	NCEP: ATP III (2005)	IDF (2009)
Definition:	T2DM, IFG, IGT or insulin resistance plus at least 2 of the criteria below	Specific clinical factors plus at least 2 criteria below	At least 3 criteria below	At least 3 criteria below
Glucose/ Hyper- glycemia	IFG, IGT, T2DM	IFG (FPG 110– 125 mg/dL) or IGT (excl. T2DM)	FPG ≥100 mg/dL (incl. T2DM) modified in 2006	FPG ≥100 mg/dL (incl. T2DM)
Abdominal obesity	WHR >0.9 in men and >0.85 in women or BMI >30 kg/m2	BMI ≥25 kg/m2	WC >102 cm in men and >88 cm in women	Population-/ Country specific: WC for Europe ≥ 94 cm in men and ≥80 cm in women
Blood pressure/ Hypertension	≥ 140/90 mmHg	≥130/85 mmHg	≥130/85 mmHg or treated for hypertension	≥130/85 mmHg or treated for hypertension
Triglyceride	≥ 150 mg/dL	> 150 mg/dL	≥150 mg/dL or treated for dyslipidemia	≥ 150 mg/dL or treated for dyslipidemia
HDL- Cholesterol	<35 mg/dL in men or <39 mg/dL in women	<40 mg/dL in men or <50 mg/dL in women	<40 mg/dL in men or <50 mg/dL in women or treated for dyslipidemia	<40 mg/dL in men or <50 mg/dL in women or treated for dyslipidemia

AACE, American Association of Clinical Endocrinologists; BMI, body mass index; BP, blood pressure; FPG, fasting plasma glucose; HDL-C, high-density lipoprotein cholesterol; IDF, International Diabetes Federation; IFG, impaired fasting glucose; IGT, impaired glucose tolerance; NCEP-ATP III, National Cholesterol Education Program Adult Treatment Panel III; T2DM, Type 2 Diabetes Mellitus; TG, triglyceride; WHO, World Health Organization; WHR, waist-to-hip ratio; WC, waist circumference. (Table according to (27,28))

1.2 Diabetes Mellitus

T2DM is a worldwide epidemic, affecting approximately 463 million adults, with an expected rise to 700 million by 2045, as per the IDF (29). T2DM patients are at an increased risk of developing severe health complications, including cardiovascular diseases, blindness, kidney failure, and lower limb amputation. To prevent long-term consequences like microand microangiopathies, oral anti-diabetic agents are considered the first-line therapy (30). Clinical studies have confirmed the efficacy of glucose-lowering medications, particularly metformin, in reducing morbidity and mortality (30,31). Besides normalizing blood glucose levels, controlling blood pressure and cholesterol levels can delay or prevent diabetes complications. Monitoring T2DM patients is crucial, and glycated hemoglobin (HbA1c) is a well-established biomarker for long-term glucose control and the efficacy of therapeutic agents (32). Early diagnosis and identification of high-risk patients are essential to alleviate

the pressure on the healthcare system caused by high patient care costs for treating longterm consequences of T2DM.

Effective management of T2DM involves a multifaceted approach that includes both pharmacological and non-pharmacological interventions. Lifestyle modifications, such as dietary changes and increased physical activity, are fundamental components of T2DM management. Metformin remains the first-line pharmacotherapy for most patients due to its well-documented safety and efficacy profile in improving glycemic control and reducing cardiovascular risk. In recent years, sodium-glucose co-transporter-2 (SGLT2) inhibitors have emerged as a valuable addition to the therapeutic arsenal, particularly for patients at high risk for cardiovascular and renal complications. These agents not only help lower blood glucose but have also been shown to provide additional cardioprotective and nephroprotective benefits (33). This evolving treatment landscape reflects the importance of a comprehensive, individualized approach to diabetes care.

1.2.1 Metformin

Metformin, an oral antidiabetic drug, is recommended as the first-line therapy for T2DM (10). Its therapeutic effect stems from its ability to inhibit hepatic gluconeogenesis and enhance peripheral glucose uptake (34). The precise mechanism of action of metformin is complex and involves multiple pathways (34,35). It has been shown that metformin activates the adenosinmonophosphat (AMP)-activated protein kinase (AMPK) enzyme, which regulates cellular energy homeostasis by modulating the balance between anabolic and catabolic processes (36). AMPK activation results in several downstream effects, including decreased hepatic glucose production, increased glucose uptake and utilization in skeletal muscle and adipose tissues, and improved mitochondrial function (35,36). These actions ultimately lead to a decrease in FPG levels and an improvement in insulin sensitivity (35,36).

In addition to its glucose-lowering effects, metformin has been shown to have beneficial effects on multiple other pathways that contribute to the development of metabolic disorders (37,38). For example, metformin has anti-inflammatory properties, which may contribute to its protective effect against cardiovascular disease (37,38). Additionally, metformin improves endothelial function, reduces oxidative stress, and decreases platelet aggregation, all of which may improve cardiovascular health (37,38). Furthermore, recent studies have suggested that metformin may have anticancer effects, possibly due to its ability to inhibit the growth of cancer cells and reduce the risk of cancer recurrence (39,40)

Even if metformin is a widely used medication for the management of T2DM, it shows a high inter- and intraindividual variability that cannot be explained in detail. It is highly soluble, exhibits a low permeability, and retains a positive charge across a range of physiological pH levels (2,41). Its absorption, distribution, and excretion are primarily mediated by active transport processes involving organic cation transporter (OCT) and multidrug and toxin extrusion proteins (MATEs) (41). OCT1 and OCT3 transporters are responsible for the hepatic uptake of metformin, which is a crucial determinant of its overall pharmacokinetic profile. Variability in the expression and function of these transporters, as well as in MATEs, can contribute to inter- and intra-individual variability in metformin pharmacokinetics. Incomplete transporter-mediated absorption from the upper intestine yields a moderate bioavailability of approximately 50-60%. Metformin is not metabolized and is primarily eliminated through the kidneys, with renal clearance accounting for approximately 90% of its total clearance. Renal excretion is facilitated by OCT2 and MATEs, which mediate the active secretion of metformin into urine. Other factors that can influence the pharmacokinetics of metformin include age, renal function, body weight, and concomitant use of drugs that affect OCTs and MATEs (41).

1.3 Lipid Disorders

With a clear understanding of T2DM and the role of metformin, this section highlights another critical aspect of the metabolic syndrome - lipid disorders, and the innovative treatments being developed to manage them. Along with glucose metabolism disorder, lipid metabolism disorder is another significant component of metabolic syndrome. Lipid metabolism disorders include low-density lipoprotein (LDL) hypercholesterolemia, mixed hyperlipoproteinemia, or high-density lipoprotein (HDL) cholesterol decreased. LDL hypercholesterolemia as one lipid metabolism disorder is directly linked to the high risk of developing atherosclerosis and to the increased cardiovascular risk (42). The connection between hypercholesterolemia and atherosclerosis was described in literature as early as 1913. In the past decades, there was a lot of research ongoing to identify therapeutic interventions to treat hypercholesterolemia that cannot be managed by lifestyle modifications or the standard of care therapy with statins (43).

Cholesterol can enter the bloodstream from the liver or absorbed through the intestine from the diet, and it is transported in the form of lipoproteins, with LDL and HDL playing significant roles. LDL transports cholesterol to body cells that need it, e.g. from the starting substance for hormones or as an essential component of the cell membrane, whereas HDL performs a purifying function by taking up cholesterol deposited on blood vessels and transporting it

back to the liver. However, if LDL is permanently elevated in the blood and the bound cholesterol cannot be released to target cells, it deposits on vessel walls, leading to narrowed arteries and minimized elasticity. In the coronary arteries, the narrowing causes the heart muscle to stop receiving enough blood and thus lack oxygen and nutrients. As a result, angina or complete blockage of a vessel, that is, a heart attack, occurs. Thus, LDL hypercholesterolemia must always be treated because of the increased cardiovascular risk associated with it (43)

According to recommendations of the European Society of Cardiology and European Atherosclerosis Society, an individual target circulation LDL level should be defined depending on the overall cardiovascular risk. For example, if risk is very high, as in established atherosclerosis or T2DM with end-organ damage, LDL cholesterol < 70 mg/dL (< 1.8 mmol/L) should be sought. At lower risk, target levels are higher: < 100 mg/dL (< 2.6 mmol/L) for moderate risk or < 115 mg/dL (< 3.0 mmol/L) for low risk (43).

Therapeutically, lifestyle modifications are effective mainly for hypertriglyceridemia and mixed lipid metabolism disorders. However, elevated circulating LDL levels can usually be reduced by less than 10% (44), whereas the effect on triglycerides is significantly more significant, with up to a 50% reduction (42,45).

If individual target levels are not reached by lifestyle modification, statin-based LDL cholesterol lowering is the first choice of drug therapy. Statin therapy is now standard medication for all forms of atherosclerosis used as a secondary prevention of cardiovascular risks and, if risk factors are present, it is also used in primary prevention (46,47).

However, there are patients who are unable to archive target of LDL levels despite maximally tolerated statin doses, or who are intolerant of statin therapy. Familial hypercholesterolemia, characterized by premature coronary artery disease and a high LDL level, is an extreme form in which available therapies have long prevented the desired levels from being achieved. In 2015, a breakthrough was achieved in the therapy of familial hypercholesterolemia with the newly developed PCSK9 (proprotein convertase subtilisin/kexin type 9) inhibitors (48–50).

1.3.1 PCSK9 Inhibitors

PCSK9-targeting monoclonal antibodies represent a new class of lipid-lowering therapies and have received regulatory approval from both the FDA and EMA for the treatment of heterozygous familial hypercholesterolemia as well as for reducing cardiovascular risk in individuals with established cardiovascular disease (48–51). PCSK9 itself is a plasma protein found in low concentrations, produced and secreted by liver cells. Its primary function is to modulate the number of LDL receptors (LDLR) present on the surface of hepatocytes (52). These receptors are crucial for the removal of LDL cholesterol from the bloodstream. When PCSK9 is present, it attaches to LDLR on hepatocytes and stabilizes the complex formed between LDL and LDLR. This interaction interferes with the normal release of the receptor from the endocytosed vesicle, directing it instead toward lysosomal degradation (51).

As a result, LDLRs bound to PCSK9 are not recycled but are instead targeted for intracellular degradation. Consequently, fewer LDLRs remain available on the surface of hepatocytes, which diminishes LDL clearance from the bloodstream and leads to increased circulating LDL levels (52).

Alirocumab and evolocumab are monoclonal antibodies directed against PCSK9 and are administered subcutaneously by patients themselves at intervals of either two or four weeks (48,50). Inhibiting the interaction between PCSK9 and the LDL receptor (LDLR), or the absence of PCSK9 altogether, prevents the degradation of LDLR. As a result, LDLRs are recycled and accumulate on the surface of hepatocytes, enhancing the clearance of LDL particles from the circulation and thereby lowering plasma LDL levels (53). Clinical trials demonstrated that these agents reduce LDL cholesterol concentrations by approximately 50–60%, offering a highly effective therapeutic option for individuals with elevated LDL. Moreover, outcome studies have shown that this pronounced LDL-lowering effect also translates into a measurable reduction in cardiovascular events, all without a marked increase in adverse effects (53).

However, the costs of treatment are higher than conventional statin therapy, making it burdensome for the healthcare system. The incremental cost is described about \$350,000 per quality adjusted life years when compared to statins in literature (51,54). Therefore, the selection of patients to be administered PCSK9 inhibitors must be well chosen, and the dosing frequency must be optimized in terms of a comprehensive cost-benefit analysis (48–50).

1.4 IMI DIRECT Consortium

Having discussed metabolic syndrome, and in detail T2DM and lipid disorders and their treatment, it's important to mention the role of collaborative initiatives in advancing our understanding of these diseases. One such initiative is the IMI DIRECT Consortium, which has contributed to parts of the research presented in this thesis.

One of the projects included in this dissertation is part of the IMI DIRECT consortium and utilizes data obtained from the IMI DIRECT study. The DIRECT consortium, initially funded by the European Union's IMI, is a collaborative effort comprising 20 academic institutions across Europe and 5 pharmaceutical companies. Launched in February 2012, the project duration spanned seven years, with formal funding concluding in July 2019.

The primary objective of the DIRECT consortium is to investigate the development and progression of T2DM, along with varying responses to treatment. Over 3,000 participants from five European countries were recruited and meticulously studied for up to four years. T2DM patients present as a highly variable condition, individuals with T2DM can experience diverse outcomes, with some witnessing rapidly worsening blood sugar levels over time, while others maintain stability. Additionally, responses to common diabetes drugs can vary, with some experiencing side effects and others not.

Thus, two main aims of the consortium were to identify potential biomarkers that can distinguish patients with a rapid from those with a slow disease progression or to identify patients exhibiting a response to diabetes treatments compared to so-called non responder. This endeavor aims to pave the way for a personalized or stratified medicine approach to T2DM treatment, utilizing both existing and novel therapies.

The DIRECT project was designed to investigate these variations, aiming to understand the underlying reasons for differential responses among individuals with T2DM. By exploring these differences, the project seeks to predict how individuals might respond to treatments, thereby advancing personalized diabetes care.

The data and insights garnered from the IMI DIRECT Consortium have been instrumental in the mathematical modeling approach.

1.5 Mathematical Modelling

Mathematical modeling is a valuable approach for answering a wide range of scientific questions. In the clinical setting, it is crucial to identify the correct drug and dosing regimen for individual patients (55). Similarly, in clinical development, it is important to estimate the appropriate dose for a drug before it is administered to humans. The importance of correct dosing was highlighted by Paracelsus's well-known statement, "All things are poison and not without poison; only the dose makes a thing not a poison" (56). However, the potential of mathematical modeling extends far beyond dosing decisions. It encompasses various applications, from improving data quality to supporting economic evaluations of therapies.

This dissertation combines three different applications of mathematical modeling within the field of metabolic disorders, all of which employ the population modelling approach as the underlying methodology. While the methodological framework and disease area remain consistent across all three projects, each addresses a different scientific question.

- Project I explores the application of mathematical modeling to improve the reliability
 of clinical measurements that are susceptible to bias due to inadequate sample
 handling. A correction method was developed to enhance the precision and
 accuracy of these measurements.
- Project II presents a detailed analysis of the pharmacokinetics of metformin, a wellestablished and widely prescribed antidiabetic drug. This project investigates key factors contributing to variability in drug exposure and the implications for individualized therapy.
- In project III focuses on the economic dimension of pharmacotherapy. Mathematical modeling was used to evaluate the cost-effectiveness of existing high-cost treatment regimens. Based on available data, alternative dosing scenarios were simulated to optimize both clinical outcomes and healthcare expenditures. Using mathematical modeling, new dosing scenarios were developed for recommended and approved therapies for high-cost drugs.

2 Objectives of the thesis

The present cumulative dissertation was conducted within the framework of the IMI DIRECT project, a European research initiative funded by the Innovative Medicines Initiative in collaboration with academic and industrial partners. The overarching aim of IMI DIRECT was to identify novel biomarkers and modeling approaches to stratify individuals at risk of, or living with, T2DM. Being part of this large-scale collaborative project not only provided access to unique and comprehensive datasets but also underlined the scientific relevance and translational potential of the research presented herein.

However, as illustrated in Project I of this thesis, several methodological challenges emerged during the analysis of the IMI DIRECT data. These included pre-analytical variability and measurement inaccuracies, particularly related to HbA1c quantification from Dried Blood Spot (DBS) cards. Addressing such issues requires the development of dedicated correction models to improve data quality and reliability. These limitations highlighted the importance of critical data evaluation. To ensure a broader and more robust scientific foundation, this thesis also includes independent research projects that examine related aspects of cardiometabolic diseases, particularly within the domains of pharmacokinetics and personalized treatment strategies. While each individual project originated from distinct research questions, ranging from correction of individual sample results to individual pharmacokinetic of approved drugs or health economics, they are unified by a shared methodological foundation: the application of quantitative and population-based mathematical modeling. In the context of the individual publications being part of this work, modeling primarily served as a means to support data interpretation, enable predictive simulations, and facilitate hypothesis testing. However, in the context of this dissertation, these projects are intentionally brought together to demonstrate the versatility, adaptability, and translational utility of mathematical modeling in medical research.

Thus, the primary objective of this dissertation is not limited to the isolated outcomes of the three projects but rather lies in showcasing the broader value and applicability of mathematical modeling as a scientific approach. It is emphasized that mathematical models, when carefully designed, applied to appropriate data, and based on valid assumptions within a robust methodological framework, are capable of addressing a broad range of research questions. The overarching aim of this dissertation is therefore to demonstrate how population-based mathematical modeling can be employed as a flexible and powerful approach to solve diverse, real-world problems in the domain of metabolic disorders,

especially T2DM, while the individual projects focus on: improving the precision of clinical measurements (Project I), characterizing the pharmacokinetics of a widely used antidiabetic drug (Project II), and optimizing the cost-effectiveness of therapeutic strategies (Project III).

2.1 Objective 1: Handling of "real-life" data to investigate Disease Progression in Pre-diabetic Patients

Conducted within Work Package 2 of the IMI DIRECT Consortium, this project aimed to investigate the development and progression of T2DM in pre-diabetic individuals. The disease's complexity, driven by multifactorial influences and high inter-individual variability, posed substantial challenges in identifying genuine progression patterns from observational cohort data. One central topic during the data analysis was to ensure reliable data based on accurate data handling. Using the modelling approach, we have identified bias and measurement artifacts. A key achievement of this project was the identification of pre-analytical variables affecting HbA1c measurements from DBS cards and the development of correction models to enhance data precision through mathematical modeling techniques. The project included in this thesis demonstrates for the first time the impact of storage conditions of DBS cards and highlights how mathematical modeling can be used to develop correction methods that enhance the precision and accuracy of clinical measurements and therewith, to discern real disease progression patterns from other influences.

2.2 Objective 2: The Impact of Circadian Rhythms on Metformin Pharmacokinetics

The second research project focused on metformin, the first-line treatment for managing T2DM. Despite its extensive use spanning several years, there exists a critical gap in knowledge regarding Metformin's individual pharmacokinetic (PK) and pharmacodynamic (PD). This study delved into the effect of circadian rhythms on the pharmacokinetics of metformin, aiming to comprehend how the body's internal clock influences the absorption, distribution, metabolism, and excretion of this vital medication. By understanding the circadian variations in metformin's behavior within the body, the precision of dosing regimens can be enhanced in the future, ensuring optimal therapeutic efficacy for patients.

2.3 Objective 3: Evaluating new Cost Effective Dosing Regimens for the Treatment of Hypercholesterolemia

The third project investigated the potential for alternative dosing strategies using newly approved lipid-lowering agents, specifically PCSK9 inhibitors, to manage hypercholesterolemia. This work applied a pharmacokinetic and pharmacodynamic modeling approach to assess how treatment individualization could improve outcomes while also reducing healthcare costs. The objective was to propose evidence-based, cost-efficient regimens that balance clinical benefit and economic feasibility.

2.4 Project included in this thesis

In summary, this dissertation aimed to contribute significantly to the overarching goal of improving the understanding and treatment of cardiometabolic diseases by utilizing the power of mathematical modeling and simulation as a tool for integrating real-world data, identifying clinically relevant patterns, and tailoring medical treatments to patient-specific characteristics.

The projects of this thesis are presented in the following. Each of the projects was published in a peer-reviewed scientific journal.

- I. **Scherer N,** Kurbasic A, Dings C, et al. The Impact and Correction of Analysis Delay and Variability in Storage Temperature on the Assessment of HbA1c from Dried Blood Spots an IMI DIRECT Study. Int J Proteom Bioinform. (2019);4(1): 007-013
- II. Türk D, Scherer N, Selzer D, et al. Significant impact of time-of-day variation on metformin pharmacokinetics. Diabetologia (2023); 66(6):1024–34
- III. **Scherer N,** Dings C, Boehm M, et al., Alternative Treatment Regimens With the PCSK9 Inhibitors Alirocumab and Evolocumab: A Pharmacokinetic and-Pharmacodynamic Modeling Approach; J Clin Pharmacology (2017), 57(7): 846-854

3 Methods

3.1 Background

Pharmacometrics is an integrative scientific and quantitative discipline that uses mathematical models to describe and predict the relationships between drugs, diseases and patients, and to optimize drug therapy. The goal is to contribute to rational decision-making to optimize drug therapies for individual patients and to promote the rational use of medicines in patients. Over recent years, modeling approaches have become increasingly integral to drug development and evaluation (57–61) and pharmacometric modeling has become an established approach for assessing the effectiveness of therapeutic interventions and is recognized by regulatory agencies such as the European Medicines Agency (EMA) and the U.S. Food and Drug Administration (FDA) (62,63). The Model-Informed Drug Discovery and Development (MID3) framework utilizes pharmacometric models to support decisions across all phases of drug development, from dose selection and safety assessment to the design of clinical trials. MID3 contributes to reducing the time and cost required to bring new therapies to market. For instance, it can be used to predict in vitro outcomes or estimate the starting dose for first-in-human trials based on preclinical data (64).

In parallel, Model-Informed Precision Dosing (MIPD) focuses on optimizing drug therapy for individual patients. MIPD integrates PK, PD, and patient-specific variables, such as disease characteristics or comorbidities, to individualize dosing and improve therapeutic outcomes (65).

PK describes how the body absorbs, distributes, metabolizes, and eliminates a drug (ADME), characterizing the relationship between drug administration and its concentration in plasma. PD relates drug concentration to its biological effects, which may be measured using biomarkers such as HbA1c or LDL levels, or via receptor and transporter saturation (66). PD models, including linear models or the Emax model, describe the concentration-effect relationship and allow the prediction of both therapeutic and adverse effects over time (67). Integrated PK/PD models are essential for understanding the dose–exposure–response relationship and supporting evidence-based dose selection.

Despite the availability of such tools, many therapeutic decisions in practice still rely on fixed, empirical dosing regimens (65). This generalized approach neglects interindividual differences and can result in suboptimal outcomes or adverse effects. Pharmacometrics addresses these gaps through various modeling strategies, including:

• Population Modeling:

This approach uses nonlinear mixed-effects (NLME) models to quantify variability in drug response across individuals. Covariates such as body weight, renal function, or comorbidities are evaluated to explain interindividual variability. Population models support clinical trial design, dose optimization, and personalized medicine by predicting individual responses within a broader population framework. Therefore, PK drug concentration-time are typically described using compartmental models, which divide the body into pharmacokinetically distinct spaces reflecting different distribution phases. A system of ordinary differential equations (ODEs) is used to represent the dynamic mass balance of the drug in each compartment, capturing the key pharmacokinetic processes (ADME processes) (55,57).

Physiologically Based Pharmacokinetics (PBPK):

PBPK models simulate drug disposition based on anatomical and physiological parameters. These models are valuable for extrapolating findings from preclinical data to humans, evaluating the effects of physiological changes (e.g., age, organ impairment), and predicting drug–drug interactions (68). In Project II, both PBPK and NLME modeling were used to investigate the pharmacokinetics of metformin under circadian influence.

The following sections describe the population approach that was used in each project included in this thesis in more detail and provides an overview about PBPK modeling in general.

3.2 Population Approach

PK and PD properties of a drug can be analyzed on an individual level using individual compartmental analysis (ICA). However, this approach may fail to capture more complex variability and is limited in its ability to generalize findings across populations. In contrast, population approaches allow for the identification of typical PK/PD behavior and quantification of variability across individuals, enabling more robust and generalizable conclusions (69). Depending on the strategy for data aggregation and analysis, researchers typically distinguish between three different population-level approaches (70).

• Naïve Pooled Analysis:

This method combines all individual data into a single dataset and estimates model parameters as if they originated from one subject. While simple, it does not account for interindividual variability and may result in biased parameter estimates (71).

• Standard Two-Stage (STS) Approach:

In the first stage, individual parameters are estimated using ICA. In the second stage, the mean and variability (e.g., percentiles) are calculated across individuals (72). This method tends to overestimate population variability, as it combines true interindividual variability with residual (unexplained) variability.

Nonlinear Mixed-Effects (NLME) Modeling:

NLME modeling simultaneously analyzes all individual data, describing both the typical PK/PD profile and different sources of variability. It is able to distinguish between interindividual variability (IIV), inter-occasion variability (IOV), and residual error (RSE) (57,73). Furthermore, covariates (e.g., body weight, renal function, age) can be included to explain variability due to specific parameters, thereby improving model predictability. NLME models are suitable for unbalanced designs and data-sparse situations, including cases with limited sampling or pooled data from different studies. These advantages make NLME modeling the preferred method in modern pharmacometrics. Due to its flexibility, robustness, and ability to handle complex and variable datasets, NLME modeling was used in all three projects of this thesis and is described in further detail in the subsequent sections.

3.3 Nonlinear Mixed-Effects Modeling

NLME modeling is a specialized form of nonlinear regression used to analyze pooled data from multiple experimental units with repeated measurements (55,74). In standard population pharmacokinetic/pharmacodynamic (PK/PD) modeling, the experimental unit is typically the individual study participant, and the observations consist of repeated measurements such as biomarker values or drug concentrations.

In this thesis, Projects I and II follow this standard framework in which the experimental units are individual participants, and the observations consist of either HbA1c biomarker values (Project I) or plasma concentrations of metformin (Project II), measured at multiple time points per subject. In contrast, Project III adopts a different structure due to the absence of individual-level data. In this case, the experimental units are entire clinical trials, and the observations are aggregated trial-level outputs, specifically mean concentration—time and mean effect—time curves. Each curve represents a single observation associated with its respective trial, enabling model-based evaluation despite the absence of subject-level data.

The term "mixed-effects" refers to the combination of (i) fixed effects, which represent typical population values for model parameters and the influence of measurable covariates (e.g., weight, age, renal function), and (ii) random effects, which account for observation variability that cannot be solely explained by the fixed effects and the measurement unit specific covariate values. These include interindividual variability (differences between experimental units, e.g. individual subjects), inter-occasion variability (within-subject variability across different measurement occasions), and residual variability (e.g., measurement errors, non-explainable deviations due to model misspecification or unspecific random effects) (75).

NLME modeling allows for simultaneous analysis of data from all individuals, providing robust estimates of both, the model parameter values and the magnitude of sources of variability. This makes it a powerful tool for analysing unbalanced datasets, sparse sampling designs, and pooled data across studies. NLME models typically consist of three hierarchical components (74,76):

- i Structural model: describing the typical PK and/or PD behavior in the population using mathematical functions,
- ii Statistical model: quantifying unexplained variability between and within individuals, often using random effects to capture interindividual and residual variability, and
- iii Covariate model: explaining part of the variability by incorporating individual-specific characteristics (covariates), such as age, weight, or renal function, and relates them to the structural model parameters.

3.3.1 Structural Model

The structural model defines the typical PK or PD profile as a function of time and model parameters. It represents the central tendency of the observed data across the population and serves as the deterministic core of the NLME model. Model development typically follows a sequential and iterative process, beginning with the simplest model structure. Additional parameters are incorporated step by step to capture essential features of the system and improve model fit. This process balances biological plausibility with parsimony. Structural models may be empirical, based on observed patterns, or mechanistic, grounded in physiological understanding, and are characterized by fixed-effect parameters, commonly denoted by θ (theta). In the context of PK modeling, this often involves evaluating one-, two-, or three-compartment models, with either linear elimination or more complex processes such as capacity-limited (saturable) elimination processes.

3.3.2 Statistical Model

The statistical model accounts for variability in structural parameters across a population

through the inclusion of random effects. It enables the estimation of individual-specific

parameters, such as clearance (CL_i), by quantifying differences not captured by fixed effects

alone. Variability in the data can arise from three main sources:

Interindividual variability (IIV): Differences between individuals

• Inter-occasion variability (IOV): Within-subject differences across different

occasions

• Residual unexplained variability (RUV): Unexplained deviations between model

predictions and observations

While variability can theoretically be estimated for any model parameter, the feasibility and

reliability of such estimation depend on data quality, quantity, and the structure of the

available measurements due to the underlying study design. In this work, the inclusion of

IIV was guided by reductions in the objective function value (OFV), the precision of

parameter estimates, and their clinical or biological plausibility.

IIV reflects variation in fixed-effect parameters (θ_k) among individuals in the population and

is modeled using individual-specific random effects represented by $\eta_{k,i}$ values. These

 $\eta_{k,i}$ values are assumed to be symmetrically distributed with a mean of 0. Different

functional forms can be used to implement IIV:

Additive variability:

 $k_{k,i} = \theta_k + \eta_{k,i}$

Proportional variability:

 $k_{k,i} = \theta_k * (1 + \eta_{k,i})$

Exponential variability:

 $k_{k,i} = \theta_k * e^{\eta_{k,i}}$

In these expressions:

• $k_{k,i}$ represents the individual-specific parameter value for subject i within population

k, such as an individual's clearance or volume of distribution.

• θ_k denotes the typical value of this parameter in the population k (the fixed effect).

 $oldsymbol{\eta}_{k,i}$ captures the deviation of individual i from the population mean for parameter $oldsymbol{ heta}_k$

and quantifies interindividual variability.

18

In practice, the exponential model is most commonly applied, as it ensures parameter estimates remain positive—an important requirement for biologically meaningful parameters (e.g., clearance or volume of distribution). However, additive or proportional models may be appropriate in specific scenarios depending on the parameter and dataset.

IOV was not considered within the mathematical models used within the different research projects. Residual variability captures the remaining differences between observed values $(obs_{i,j})$ and individual model predictions $(ipred_{i,j})$ that cannot be explained by fixed or random effects. Here, the index i refers to the experimental unit, typically an individual participant, while the index j denotes a specific observation within that unit, such as a particular sampling time point. This variability is described using residual error terms $\varepsilon_{i,j}$ which are assumed to be normally distributed with mean 0 and constant or variable variance, depending on the error model. Three common residual error models are:

Additive error model: $obs_{i,i} = ipred_{i,i} + \varepsilon_{add,i,i}$

Proportional error model: $obs_{i,j} = ipred_{i,j} * (1 + \varepsilon_{prop,i,j})$

Combined error model: $obs_{i,j} = ipred_{i,j} * (1 + \varepsilon_{prop,i,j}) + \varepsilon_{add,i,j}$

In these expressions:

- index_i refers to the experimental unit i, typically the individual participant,
- $index_j$ refers observation j within that unit i, such as a specific sampling time point of the individual i.
- *obs*_{i,i} denotes the observed measurement,
- $ipred_{i,j}$ is the model-predicted individual value, and
- $\varepsilon_{add\ or\ prop,i,j}$ represents the residual error, either additive or proportional.

The combined model is commonly used as it accounts for both constant variability (e.g. typical for PD measurements) and variability that scales with the magnitude of the prediction (e.g. typical for PK data). The selection of the residual error model was based on diagnostic plots, plausibility, and model performance criteria.

3.3.3 Covariate Model

The covariate model aims to explain the observed outcomes (measurements) and reduce IIV by accounting for individual- or study-specific characteristics that influence PK and PD parameters (77). Covariates typically include (i) demographic variables, such as age, sex, body weight, ethnicity, (ii) clinical laboratory values such as LDL concentrations, (iii) organ function markers such as estimated glomerular filtration rate, (iv) genetic factors, disease stage, comorbidities, and concomitant medications or time-varying covariates, which can be investigated dynamically within NLME models. Covariates may be continuous (e.g., weight, creatinine clearance) or categorical (e.g., sex, age group). Continuous covariates are typically implemented using linear, exponential, or power functions, while categorical variables are introduced through additive, fractional, or exponential effects on one or more parameters, depending on the model structure (55).

The covariate selection is guided by biological plausibility and statistical significance assessed through the change in objective function value (OFV) and the precision of estimated effects (see Section 3.5.1). Covariate models are developed using standard stepwise procedures. In the forward inclusion phase, covariates are sequentially added to the model based on improvements in model fit and predefined significance criteria. Once all relevant covariates are included, the analysis proceeded with a backward elimination step, where each covariate is tested for exclusion using a stricter significance threshold to retain only those with meaningful contributions to the model (77,78). Incorporating relevant covariates strengthens the explanatory power of the NLME model. It improves the model's ability to describe observed variability, enhances parameter interpretability, and supports individualization of drug therapy.

3.4 Estimation Method

In population modeling, the goal is to identify the set of model parameters that best describe the observed data. Several software tools are available for the determination of NLME models. NONMEM® (Nonlinear Mixed-Effects Modeling) is one of the most widely used programs for population analysis of pharmacokinetic and pharmacodynamic data and was applied throughout this thesis. NONMEM® estimates model parameters by maximizing the likelihood that the model can reproduce the observed data (79). Rather than directly maximizing the likelihood function, the algorithm minimizes minus twice the log-likelihood function (–2LL). This quantity is referred to as the OFV. The parameter set corresponding

to the lowest OFV is considered the best fit to the data. The optimization process is carried out iteratively using estimation methods such as first-order (FO) method, first-order conditional estimation with and without interaction (FOCE/FOCE+I) stochastic approximation expectation-maximization (SAEM), depending on the model complexity and data structure (80,81). In all projects included in this thesis, FOCE+I was used as estimation method, considering a correlation between residual and interindividual variability for more precise parameter estimates.

3.5 Model Selection and Evaluation

Model performance was assessed through various numerical and graphical tools.

3.5.1 Objective Function Value and Akaike Information Criterion

During model development, statistical model improvement was assessed using the likelihood ratio test (LRT). This test applies to nested models, i.e. when one model (the simpler one) is a special case of another (the more complex one), such that the more complex model can be reduced to the simpler one by eliminating one or more parameters (55). The LRT compares the objective function values of the two models: a statistically significant improvement is indicated by a drop in OFV. For example, when adding one additional parameter to the model, a decrease in OFV of at least 3.84 is considered statistically significant at the 5% level (p < 0.05), justifying the increase in model complexity (74).

For non-nested models, the Akaike Information Criterion (AIC) was used to compare model performance. The AIC accounts for both goodness-of-fit and model complexity by applying a penalty for the number of estimated parameters: AIC = -2*LL + 2*P where LL is the log-likelihood of the chosen model and P is the number of estimated parameters of the model. Lower AIC values indicate a more parsimonious and better-fitting model.

3.5.2 Relative Standard Error

The precision of parameter estimates was evaluated using the relative standard error (RSE). A smaller RSE indicates higher precision. The absolute standard error of parameters was estimated during the covariance step in NONMEM® (74). Then, the RSE is calculated as the ratio of the absolute standard error to the parameter estimate, multiplied by 100%.

$$RSE = \frac{absolute\ standard\ error}{parameter\ estimate}*100\%$$

3.5.3 Graphical Methods

Graphical analysis, using R software, included routine generation of Goodness of Fit (GOF) plots (82). These plots encompassed measured observations versus population or individual predictions, weighted residuals versus population or individual predictions, and weighted residuals versus time or time after dose. Model parameters were estimated using the FOCE+I method. Based on these individual parameter estimates, weighted residuals were calculated, reflecting the differences between measured observations and predictions. Ideally, plots exhibit random and uniform scattering around the line of identity (for observed vs. predicted plots) or around the zero line (for residual plots), indicating no systematic model bias (70).

3.6 PBPK Modeling Approach

Physiologically based pharmacokinetic (PBPK) models are used to simulate drug pharmacokinetics processes such as ADME in the human body based on mechanistic and physiology-informed principles. The body is represented as a network of interconnected compartments, each reflecting the anatomical and functional properties of specific tissues and organs, such as the lungs, liver, kidneys, brain, muscle, bone, and skin. These compartments are defined by attributes such as organ volume, blood flow, membrane permeability, and tissue composition. Drug movement within and between compartments is governed by systems of ordinary differential equations, allowing time-resolved simulation of pharmacokinetic processes. (83,84).

Several PBPK modeling platforms support this approach by integrating extensive physiological data and providing preconfigured species- and population-specific models. Commonly used tools include PK-Sim® and MoBi® (Open Systems Pharmacology), GastroPlus™, and SimCyp®. These platforms combine system-specific parameters with compound-specific input and study-specific demographic data, which are entered by the modeler during model development. This enables the construction of physiologically whole-body PBPK models tailored to various populations and clinical scenarios (85).

PBPK modeling typically relies on three core components:

- i System-dependent parameters, such as tissue size, blood perfusion, and physiological constraints
- ii Drug-specific/ drug-dependend characteristics, including solubility, partition coefficients, protein binding, and enzyme/transporter affinities
- iii Process-related parameters, which describe dynamic interactions between drug and system.

In contrast to empirical modeling techniques like nonlinear mixed-effects (NLME) modeling, PBPK modeling follows a knowledge-driven, biology-based framework. Models are often developed using a "bottom-up" approach—building on physicochemical properties, in vitro metabolism, and transporter data to predict concentration—time profiles without initially relying on clinical pharmacokinetic data. Once in vivo data become available, model predictions are validated and refined in a "top-down" manner. This includes adjusting uncertain parameters such as permeability or clearance to improve predictive accuracy. The process follows an iterative "learn-confirm-refine" cycle, where simulations are compared to observed data and progressively improved to capture pharmacokinetics across populations and conditions (83).

This integrative framework enables simulation-based extrapolation to a variety of clinical scenarios, including pediatric populations, renal impairment, first-in-human dose predictions, and drug-drug interaction (DDI) assessments. PBPK models can also be extended to include pharmacodynamic components (PBPK/PD), and their utility has been increasingly recognized by regulatory agencies as a central tool within MIDD strategies (84).

In Project II of this thesis, PBPK modeling was applied in parallel with NLME modeling to investigate the mechanistic basis of circadian variation in metformin pharmacokinetics (2). Model development and simulation were performed using PK-Sim® and MoBi®, leveraging their physiologically body models and ability to incorporate circadian-modulated parameters. Model performance was assessed using both qualitative and quantitative diagnostics. Predicted and observed plasma concentration—time profiles were compared visually, and standard goodness-of-fit plots were assessed. Accuracy was further quantified using metrics such as the mean relative deviation (MRD) and geometric mean fold error (GMFE). Full details on model development and evaluation are presented in the associated publication and its supplement (refer to section 4.2 and Appendix A1: Project II Supplement) (2,86)

4 Results

4.1 Publication I: The Impact and Correction of Analysis Delay and Variability in Storage Temperature on the Assessment of HbA1c from Dried Blood Spots - an IMI DIRECT Study (1).



International Journal of Proteomics & Bioinformatics

Research Article

The Impact and Correction of Analysis Delay and Variability in Storage Temperature on the Assessment of HbA1c from Dried Blood Spots - an IMI DIRECT Study - 3

Nina Scherer¹, Azra Kurbasic², Christiane Dings¹, Andrea Mari³, Valerie Nock⁴, Anita M. Hennige⁴, Robert W. Koivula^{2,5}, Markku Laakso⁶, Maritta Siloaho⁶, Tim J. McDonald^{7,8}, Imre Pavo⁹, Giuseppe N. Giordano², Tue H. Hansen¹⁰, Femke Rutters¹¹, Jacqueline M Dekker¹¹, Bernd Jablonka¹², Hartmut Ruetten¹², Ewan R. Pearson¹³, Paul W. Franks² and Thorsten Lehr^{1*}

Genetics, Faculty of Health and Medical Sciences, University of Copenhagen, Copenhagen, Denmark

*Address for Correspondence: Thorsten Lehr, Professor of Clinical Pharmacy, Saarland University, Campus C2 2, 66123 Saarbrucken-Germany, Tel: +496-813-027-0255; Fax: +496-813-027-0258; E-mail: thorsten.lehr@mx.uni-saarland.de

Submitted: 06 June 2019; Approved: 17 July 2019; Published: 19 July 2019

Cite this article: Scherer N, Kurbasic A, Dings C, Mari A, Nock V, et al. The Impact and Correction of Analysis Delay and Variability in Storage Temperature on the Assessment of HbA1c from Dried Blood Spots - an IMI DIRECT Study. Int J Proteom Bioinform. 2019;4(1): 007-013.

Copyright: © 2019 Scherer N, et al. This is an open access article distributed under the Creative Commons Attribution License, which permits unrestricted use, distribution, and reproduction in any medium, provided the original work is properly cited.

¹Department of Clinical Pharmacy, University of Saarland, Saarbrucken, Germany

²Department of Clinical Sciences, Genetic and Molecular Epidemiology Unit, Lund University, Sweden

³C N R Institute of Neuroscience, Padova, Italy

⁴Boehringer Ingelheim International GmbH, Biberach an der Riss, Germany

⁵Oxford Centre for Diabetes, Endocrinology and Metabolism, Radcliffe Department of Medicine, University of Oxford, Oxford, UK

⁶Department of Medicine, University of Eastern Finland and Kuopio, University Hospital, Kuopio, Finland

⁷NIHR Exeter Clinical Research Facility, University of Exeter, Exeter, UK

⁸Blood Sciences, Royal Devon and Exeter NHS Foundation Trust, Exeter, UK

[°]Eli Lilly Regional Operations GmbH, Vienna, Austria

¹⁰ The Novo Nordisk Foundation Center for Basic Metabolic Research, Section of Metabolic

¹¹Epidemiology and Biostatistics, Amsterdam Public Health research institute, VU University Medical Center, Amsterdam, The Netherlands

¹²Sanofi-Aventis Deutschland GmbH, R&D, Frankfurt am Main, Germany

¹³Medical Research Institute, Ninewells Hospital and Medical School, University of Dundee, Dundee, Scotland, UK

ABSTRACT

Aims: Dried Blood Spot (DBS) sampling is a frequently used method to obtain Haemoglobin A1C (HbA1c) in clinical studies of freeliving populations. Under controlled conditions, DBS sampling is a valid and robust alternative to traditional Whole Blood (WB) sampling. The objective of this analysis was to investigate the impact of storage conditions on the validity of HbA1c assessed from DBS collected in free-living and to develop a method to correct for this type of error.

Methods: Overall, 14,243 DBS cards from 2,237 IMI DIRECT participants at risk of developing diabetes were analyzed using non-linear regression analysis. 4,272 HbA1c levels from WB from the same 2,237 participants were used to validate the predictive performance of the method.

Results: The delay between DBS sample collection and analysis, in combination with different storage temperatures, caused inflation of measured HbA1c levels. An E_{max} model was used to correct inflated HbA1c levels according to individual analysis delay and storage temperatures. Corrected HbA1c showed higher agreement to WB results, compared to the uncorrected HbA1c from DBS cards (Pearson correlation coefficients of 0.61 and 0.69 for reported and corrected vs. WB, respectively, $p = 5.92*10^{-36}$). The mean HbA1c derived from WB was $5.6 \pm 0.29\%$ (38 \pm 3.2 mmol/mol); from DBS, $5.8 \pm 0.40\%$ (40.0 \pm 4.4 mmol/mol) and $5.6 \pm 0.33\%$ (38 \pm 3.6 mmol/mol) (before and after correction, respectively).

Conclusions: Analysis delay and storage temperature influence the assessment of HbA1c from DBS cards. This correction method provides an opportunity to account for the storage conditions and to improve the precision and accuracy of DBS card-derived HbA1c levels under field conditions.

Keywords: Analysis delay; Correction method; Dried blood spot cards; HbA1c; IMI DIRECT; NONMEM

ABBREVIATIONS

WB: Whole Blood: DBS: Dried Blood Spot; fsOGTT: Frequently Sampled Oral Glucose Tolerance Test; IMI: Innovative Medicines Initiative; DIRECT: Diabetes Research on Patient Stratification; HPLC: High-Performance Liquid Chromatography; SAEM: Stochastic Approximation Expectation Methods; IMP: Monte Carlo Importance Sampling; OFV: Objective Function Value; AIC: Akaike Information Criterion; AUC: Area under the Curve; FPG: Fasting Plasma Glucose

BACKGROUND AND OBJECTIVE

HbA1c is a well-established biomarker in diabetes mellitus and reflects long-term (4-6 weeks) blood glucose concentrations [1]. The use of HbA1c as a diagnostic measure is part of the "Standards of Care" by the American Diabetes Association based on the recommendations of the International Expert Committee [2]. Further, HbA1c is used as a longitudinal marker to observe disease progression and to evaluate the success of therapeutic intervention [3]. Traditionally, HbA1c is measured using Whole Blood (WB) samples taken by venipuncture. Compared to alternative blood sampling methods, the collection of blood by venipuncture is more expensive and associated with greater participant burden and logistic challenges regarding sample handling and processing [4]. One alternative blood sampling method is to use a dry matrix where a very small volume of blood obtained from finger puncturing is put on a matrix paper [5]. HbA1c can be measured from these Dried Blood Spots (DBS). Assessments using DBS cards are cheaper, safer and more acceptable to study participants than WB sampling [6]. Because of these advantages, the DBS method is highly appealing in research settings. This is especially true in longitudinal or large population-based studies with repeated HbA1c measurements, as the DBS approach can help reduce costs and minimize inconvenience to participants [7].

The comparability of both sampling methods was recently evaluated in a meta-analysis of seventeen heterogeneous studies [8] and DBS validity has been shown under normalized sample collection, transportation and storage settings. Only a few studies focused on the influence of DBS storage conditions, i.e. specific

temperatures or storage times, on the resulting HbA1c measure [9-12]. It was shown that the accuracy and precision to assess HbA1c from DBS cards stored for more than seven days at room temperature is compromised. So far, there is a lack of knowledge about the stability of DBS card-assessed HbA1c under varying conditions that include long-term storage at variable temperatures.

Within the IMI (Innovative Medicines Initiative) DIRECT (Diabetes Research on Patient Stratification) study, more than 2,000 people at risk of developing diabetes were recruited and in total about 14,000 HbA1c values were collected by DBS cards every 4.5 months during an observation period of 48 months to monitor the individual disease progression [13]. As the collection of the DBS cards varied regarding the storage time and condition, this cohort provides a good opportunity to assess the impact of storage conditions on measurement validity. The aim of this analysis was to investigate the effect of long-term storage at different conditions on the reliability of HbA1c levels obtained from DBS cards that were routinely collected in the IMI DIRECT study. Further, the impact of analysis delay was quantified using a mathematical model to correct for storage time. To investigate the predictive performance of the correction method, a comparison of the corrected and the reported HbA1c levels from DBS cards versus HbA1c levels derived from WB analysis, as well as of the HbA1c levels versus other biomarkers for glyceamic control obtained from a Frequently Sampled Oral Glucose Tolerance Test (fsOGTT), was evaluated.

RESEARCH DESIGN AND METHODS

Study Design

This analysis was performed on longitudinal, repeated HbA1c measurements in non-diabetic participants that engaged in a study within the IMI DIRECT consortium. A detailed study description has been published previously [13]. People at risk of developing diabetes were recruited at four different data collection centers (A-D) [13,14]. To study disease progression, DBS cards were used to obtain HbA1c measurements and further, beta cell function and insulin sensitivity were determined using 75 g fsOGTTs at months 0, 18 and 48. For the fsOGTTs, study participants were called into their respective study center A-D. In addition to the fsOGTT samples, fasting blood samples from each patient were taken and immediately stored at -80°C. At the time of our analysis, data from 0 up to 18 months were available and used for model development.

Bioanalytics

At the beginning of the study, each participant and the clinic staff were instructed how to handle the DBS cards according to the internal study protocol: two blood spots were put on the provided filter paper and kept at room temperature for drying for at least 2 hours before packing them in sealed plastic bags. The participants were asked to store the bags at room temperature and send them immediately to their local study center. From there, the cards were shipped to center A within three days for analysis. All shipments from center B. C and D to center A were performed by regular mail resulting in variable timing and storage conditions. Moreover, details concerning sample collection, processing and storage of DBS cards before shipment to center A differed between the centers; many cards were shipped with longer delays than recommended in the study protocol due to numerous logistical barriers.

Only at center A were all participants invited to have their DBS samples taken by a nurse at the clinical site. The DBS cards were registered, dried, immediately stored at -20°C and analyzed within one week.

At center B, participants took their DBS at home and sent them to the study center to be collected and stored at room temperature before being shipped to center A for analysis. Shipment was done every second week but, because samples were collected continuously, storage time at room temperature at center B varied between one to fourteen days.

At center C, some participants came to the center for DBS sampling; others took their samples at home and sent them to the center. The samples were stored at room temperature until shipment to center A for analysis. Usually the DBS cards were shipped on the day of receipt from the patients. When same-day shipment was not possible, the DBS cards were stored at 4-8°C. Shipment from center C to center A took approximately three to seven days.

At center D, DBS samples were collected at home by the participants and hand-delivered or sent by mail to the study center with variable delay (range from one day to more than a week). At the study center, the DBS cards were stored at 4°C before being sent in batches to center A on a monthly basis.

WB samples were used to measure HbA1c for the purposes of this DBS validation study. The analysis of WB samples was undertaken at center E (no data were collected here). The WB samples were assumed to represent the true HbA1c levels for the two available time points (month 0 and 18). The analysis of all WB samples was performed using High-Performance Liquid Chromatography (HPLC) (Tosoh G8 HPLC Analyzer) [15]. The Tosoh G8 HPLC Analyzer utilizes Standard Ion-Exchange method of HbA1c measurement. The HbA1c determination derived from DBS cards was performed at center A using the immunoturbidimetric assay on Konelab 20XT Clinical Chemistry analyzer, both from Thermo Fisher Scientific. The validation of the DBS as sample material was performed at center A. The analytical total Coefficients of Variation (CV %) for DBS were 5.3-6.5%. The concordance between both assays has been investigated elsewhere [16], where WB samples were analyzed using the HPLC method and compared to DBS cards analyzed with HPLC, as well as the immunoturbidimetry method.

Data analysis

The impact of the analysis delay on HbA1c inflation was investigated with a non-linear regression analysis using the software NONMEM (V. 7.3, ICON Development Solutions, Ellicott City, MD, USA) with the graphical user interface Pirana (V. 2.9.5). Throughout the analysis, the Stochastic Approximation Expectation Methods (SAEM) algorithm with the interaction option, followed by a step of Monte Carlo Importance Sampling (IMP) algorithm was used. Model selection was based on several criteria such as the changes in the NONMEM Objective Function Value (OFV) [17], goodness-offit plots, and the precision of parameter estimation [18].

The decrease of the OFV by 3.84 points for the addition of 1 parameter (chi-square, p < 0.05 with 1 degree of freedom) was considered as statistically significant between two nested models [19]. For non-nested models, the Akaike Information Criterion (AIC) was computed to determine if one model was superior to the other. In the current analysis, AIC was defined as OFV+2*number of parameters

The model building process was performed in a stepwise procedure. First, the baseline model was developed by testing different mathematical functions. A linear, E_{max} with and without Hill factor, and several exponential functions were tested to describe the relationship between measured HbA1c levels and analysis delay. Further, a log transformation of analysis delay was tested to account for the non-normal distribution of analysis delay. In a second step, the center was tested as a covariate.

SAS (V. 9.4) was used for dataset preparation. Graphical visualization of NONMEM results was performed with R (V. 3.2.5) and the graphical user interface RStudio (V. 1.0.44)

To validate the correction method, WB-derived HbA1c levels were used. Bland-Altman plots [21] and regression analysis were performed to compare reported and corrected HbA1c from DBS cards with HbA1c from WB samples. For further validation, glucose exposure, reflected by the Area under the Curve (AUC) of the glucose concentration-time profile obtained from the fsOGTT, as well as the Fasting Plasma Glucose (FPG) and 2h-glucose, were employed. Pearson correlation coefficients between these glucose related biomarkers and HbA1c levels were calculated; paired significance tests for correlation differences were computed and used for model evaluation [22].

RESULTS

Dataset

Overall, 2,237 participants fulfilled the inclusion criteria for the IMI DIRECT prediabetes cohort [13], 76% of whom were male. The median age was 62 years (range from 30 to 75 years) at enrollment and the median weight was 84.2 kg (range from 43.0 to 152 kg). 1,275 participants were enrolled at center A, 332 at center B, 147 at center C and 493 at center D. In total, 14,243 HbA1c values obtained from DBS cards were available and used for model development. The validation dataset consisted of 4.272 HbA1c measurements derived from WB samples, 2222 from the fsOGTT performed at month 0, and 2050 at month 18, respectively. The mean HbA1c derived from WB is $5.6 \pm 0.29\%$ (38 ± 3.2 mmol/mol); from DBS, $5.8 \pm 0.40\%$ (40.0 ± 4.4 mmol/mol). A summary of the characteristics of the key variables of the IMI DIRECT cohort is already described elsewhere [23].

Analysis delay was calculated as the time (in days) between DBS

sampling and the DBS assay date. The overall analysis delay in the dataset used for model development ranged from 0 to more than $400\,$ days. Only 10.7% of the samples was analyzed within one day after sample collection and 50.4% within one week. Approximately 90% of the samples were analyzed within a timespan of four weeks. Less than 0.2% of the DBS cards were stored for more than 12 weeks (Figure 1). Detailed information on temperature variation during this time was unavailable. Supplementary figure S1 shows the relationship between analysis delay and reported HbA1c, restricted to a delay of 100 days.

Data analysis

An E_{max} model with Hill factor best described the relationship between analysis delay and inflated HbA1c levels (Equation 1), reflected by the lowest AIC value compared to other tested structural models. The \mathbf{E}_{max} value was estimated for each study center separately to account for differences in DBS card storage conditions. The inclusion of the study center as a covariate was significant (p =7.86*10⁻²¹¹). The maximal inflation of HbA1c reflected by the $\rm E_{max}$ value in center A was small compared with the other three centers (0.411 [mmol/mol] compared to 10.9 [mmol/mol], 7.40 [mmol/mol] and 6.76 [mmol/mol] for centers B, C and D, respectively). The EC50 reflects the analysis time in days that is related to a half maximum inflation. A log transformation of the analysis delay had no benefit on the correct method, so it was reject in the final model. The observed HbA1c levels and the center-specific \mathbf{E}_{\max} functions versus the analysis delay are shown in figure 2; parameter estimates are presented in table 1.

Equation 1:

$$HbAlc_{reported} = HbAlc_{at \ sampling \ date} + \frac{E_{max(center)} * \ analysis \ delay_{DBS \ card}}{ECS0^{Hill} + analysis \ delay_{DBS \ card}} \frac{Hill}{ECS0^{Hill}}$$

To correct reported HbA1c levels, the center-specific E_{max} function was shifted in parallel along the y axis to intersect the reported HbA1clevel. The new intercept of the y axis and the shifted $E_{\mbox{\tiny max}}$ function was noted as the corrected HbA1c level and can be calculated using equation 2.

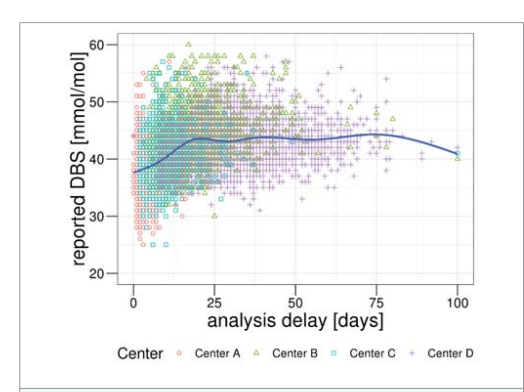


Figure S1: Reported HbA1c levels obtained from the Dried Blood Spot (DBS) cards [mmol/mol] vs. analysis delay (in days) restricted to a delay of 100 days. The blue line indicates a trend line, the shape and color represents the four study centers. The red circles indicate center A, where most of the DBS cards were analysed within 14 days. The green triangles indicate center B, the blue squares and the purple crosses center C and D, respectively

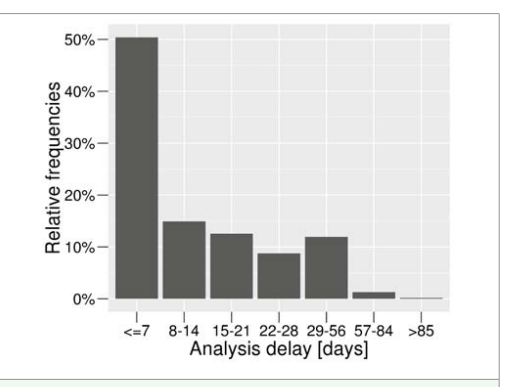


Figure 1: Histogram of the relative frequencies of analysis delay for the Dried Blood Spot (DBS) cards. More than 50% of all DBS cards were analysed in the first week after sampling, while 1.4% were stored for more than 8 weeks.

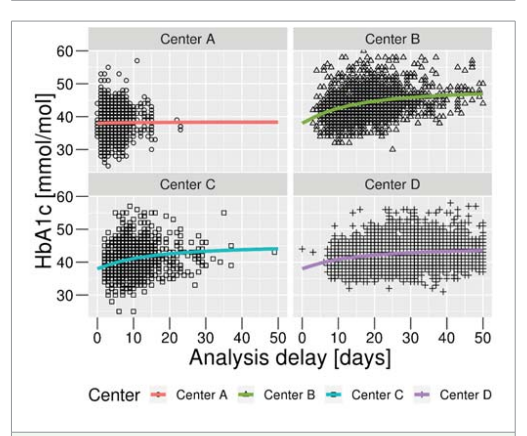


Figure 2: Center-specific Emax functions to describe the relationship between A1c obtained from Dried Blood Spots (DBS) cards and analysis delay. The points, triangles, squares and crosses indicate the reported HbA1c derived from DBS cards of center A, B, C and D, respectively. The colored lines indicate the model prediction for each center (center specific Emax function).

Parameter	Value (RSE[%])*		Description				
Model parameters							
Intercept [mmol/mol]	38.0	(0.2)	Mean HbA1c at sampling date				
E _{max} (Center A) [mmol/mol]	0.411	(85)	Maximal HbA1c increase of Center A				
E _{max} (Center B) [mmol/mol]	10.9	(6)	Maximal HbA1c increase of Center E				
E _{max} (Center C) [mmol/mol]	7.40	(7)	Maximal HbA1c increase of Center C				
E _{max} (Center D) [mmol/mol]	6.76	(6)	Maximal HbA1c increase of Center D				
EC50 [days]	13.4	(11)	Analysis delay of half-maximum HbA1c increase				
Hill	1.15	(9)	Hill factor				
Variability							
PRV [CV%]	8.8	(0.6)	proportional residual variability				

$$\begin{aligned} & \textbf{Equation 2:} \\ & \textit{HbAlc}_{corrected} = \textit{HbAlc}_{reported} - \frac{E_{max(center)} * \textit{analysis delay} \textit{Hill}}{ECS0^{Hill} + \textit{analysis delay} \textit{Hill}} \end{aligned}$$

To validate our correction method, the corrected HbA1c, as well as the reported HbA1c levels from DBS cards, were compared to HbA1c levels derived from WB samples. Mean HbA1c levels derived from DBS cards were 5.8 \pm 0.40% (40.4 \pm 4.39 [mmol/mol]) before and 5.6 \pm 0.33% (38.0 \pm 3.59 [mmol/mol]) after correction. The mean HbA1c derived from WB was $5.6 \pm 0.29\%$ (37.6 ± 3.17 [mmol/mol]).

Figure 3 shows the reported and corrected HbA1c values from DBS cards vs. WB, split into two groups: analysis delay ≤ seven days (within the stability window according to literature), and greater than seven days (outside stability window) [9]. Samples with an analysis delay outside the stability window were corrected appropriately, the corrected HbA1c levels being spread more evenly around the line of identity. Correlation between corrected HbA1c levels from DBS and WB sampling were stronger compared to the reported ones (Pearson correlation coefficient of 0.61 and 0.69 for reported and corrected vs. WB, respectively, $p = 5.92*10^{-36}$). Furthermore, Bland-Altman plots were examined to check for bias in the correction method. After correction, HbA1c levels had significantly better concordance with WB sample results compared to uncorrected HbA1c DBS values (p-value < 2.2*10⁻¹⁶). The mean difference between HbA1c from DBS cards and WB for all samples was -0.2% (-2.16 [mmol/mol]) before, and -0.03% (-0.32 [mmol/mol]) after correction. Figure 4 shows the Bland-Altman plots for each center before and after correction.

Using the HbA1c levels obtained from WB samples as a diagnostic marker for prediabetes (HbA1c <= 48 [mmol/mol] and >= 40 [mmol/mol]) or diabetes (HbA1c > 48 [mmol/mol]), 24% of the samples would be associated with prediabetes and 0.4% with diabetes. Using the reported or the corrected DBS samples, 45% or 23% of the samples results in diagnosis of pre-diabetes and 4.6% and 0.2% in a diagnosis of diabetes, respectively. Using the reported DBS,

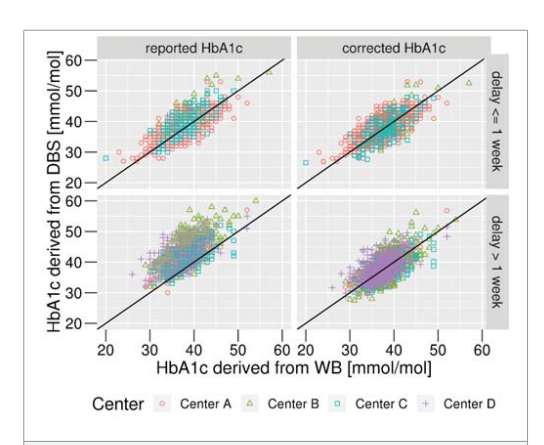


Figure 3: HbA1c levels derived from Dried Blood Spot (DBS) cards (left: reported levels, right: corrected levels) vs. Whole Blood (WB) samples regarding the analysis delay within (top) and outside (bottom) the stability window of one week reported in literature. Each point, triangle, square and cross indicates one observation from one of the four centers. Black lines are lines of identity

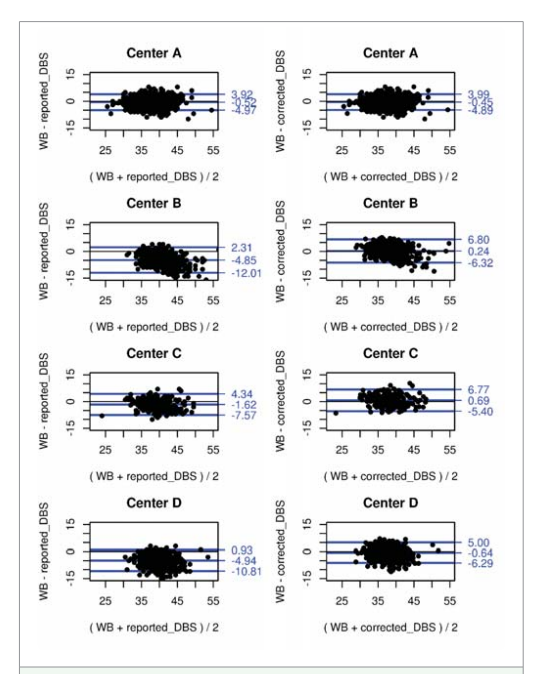


Figure 4: Bland-Altman plots: differences between Whole Blood (WB) HbA1c [mmol/mol] and Dried Blood Spot (DBS) derived HbA1c vs. the mean of the two measurements. The bias between the two methods is represented by the gap between the X axis, corresponding to zero difference in black and the parallel blue line to the X axis. The middle blue line represents the mean difference between the two assays. The upper and lower blue lines represent the agreement limits (1,96*standard deviation). The columns show HbA1c derived from DBS cards, as reported values (reported_DBS, left) and corrected values (corrected_DBS, right). Data are shown separately for each center (A-D) in the panels.

27% of the samples results in a false positive diagnose of pre-diabetes and 4.3% of diabetes. After the correction the false positive rate for diagnosis prediabetes or diabetes is reduced to 0.9% (pre-diabetes) and 0.4% (diabetes).

Further, all HbA1c levels were compared to biomarkers obtained from the fsOGTT. Supplementary figure S2 illustrates a significantly stronger correlation between corrected HbA1c and the AUC of glucose compared to reported HbA1c (r²_uncorrected = 0.274, r²_ corrected = 0.351, $p = 1.61*10^{-19}$). The relationship between the AUC of glucose compared to WB for FPG, the correlation coefficient also increased after correction (r²_uncorrected = 0.248, r²_corrected = 0.342, $p = 1.42*10^{-28}$). Corrected HbA1c and WB showed a similar relationship to 2h-glucose (r²_WB = 0.229, r²_corrected = 0.229), FPG $(r^2 WB = 0.348, r^2 corrected = 0.341)$ and AUC $(r^2WB = 0.358,$ r²_corrected = 0.351); statistically, there were no differences between correlation coefficients (p > 0.30).

DISCUSSION

In this study, we observed a significant increase in HbA1c levels with an increasing analysis delay of the DBS cards under real-life conditions, a topic that has not been investigated previously. The IMI DIRECT study was not explicitly designed to address this research question; however, the huge amount of data collected in IMI DIRECT

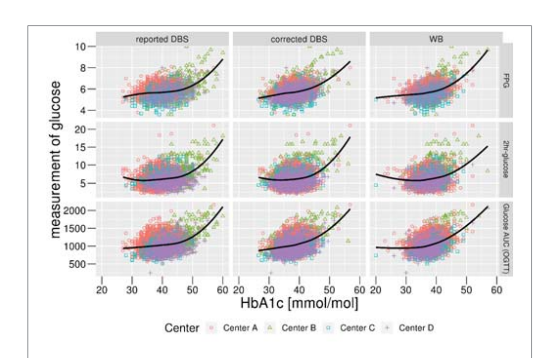


Figure S2: Correlation analysis between HbA1c measurements (reported and corrected HbA1c derived from Dried Blood Spot (DBS) cards and HbA1c derived from Whole Blood (WB)) and fsOGTT related glucose measurements (Fasting Plasma Glucose (FPG), 2h-glucose, Area Under the Curve (AUC)). Each point, triangle, square and cross indicate one observation from one of the four centers. Black lines represent the LOESS regression analysis.

provides a unique possibility to investigate and quantify the impact of up to 400 days of storage.

In accordance with the published literature, DBS cards immediately stored at -20 $^{\circ}\text{C}$ showed a negligible influence of storage time on the resulting HbA1c levels [11]. In our study at center A, the DBS samples were handled in this manner and confirmed this finding. A maximum inflation of 0.04% (0.411[mmol/mol]) during storage is usually not considered as clinically relevant. However, some of the HbA1c values obtained from DBS cards collected at study centers B-D were highly inflated, due to extended storage time at variable storage temperature.

With the exception of the study by Buxton et al., which investigated the stability of DBS cards stored in the freezer for at least three months [11], most of the published stability studies investigated a shorter analysis delay and smaller sample size compared to our analyses. Nevertheless, short-term studies indicate that inflation of HbA1c values is directly related with storage time [9,24].

Fokkema et al. investigated the stability of DBS cards over ten days at room temperature and reported an increase in HbA1c of 0.4% (from 7.2% (55.0 [mmol/mol], day 0) to 7.6% (60.0 [mmol/mol], day 10) [10]. In center B, where cards were stored at room temperature for up to 14 days, our correction method would predict a HbA1c of 7.6% (59.5 [mmol/mol]) assuming an HbA1c level of 7.2% at sampling date and a storage of ten days. Thus, the degree of inflation attributable to extended storage time and variable temperature of our correction method concurs with previous findings.

In addition to the comparison to WB-derived HbA1c levels, we compared our corrected HbA1c levels with glucose related biomarkers obtained from fsOGTTs. We detected a statistically stronger correlation between FPG and AUC of the glucose concentration-time $\,$ profile during the fsOGTT and the corrected HbA1c, in contrast to the reported value. The correlation coefficients after correction are not statistically different from those of WB and the glucose related biomarkers additionally supporting the validity of the presented correction method.

The relationship between analysis delay and HbA1c inflation is described by an \boldsymbol{E}_{\max} model that could possibly be explained by the mechanism of HbA1c formation. Free haemoglobin irreversibly reacts with glucose in a non-enzymatic reaction to form HbA1c [25]. Under ex-vivo conditions, the higher the temperature, the easier the formation of HbA1c in the stored blood sample [26]. Limited by decreasing concentrations of the two reactants over time, an E_{max} model for the description of the change in HbA1c in relation to the analysis delay appropriately captures the reaction. To account for handling and storage temperatures at the four different study centers. specific \mathbf{E}_{\max} values reflected the different conditions. The estimated walues were increasing with increasing storage temperatures; storage at -20°C (center A) is related to a small maximal effect of inflation (0.411 mmol/mol); storage at 4°C (center D) as well as 4-8°C (center C) is related to a maximal increase of 6.76 mmol/mol and 7.40 mmol/mol, respectively; and, storage at room temperature for up to two weeks (center B) had the highest influence on HbA1c, with a maximum effect of 10.9 mmol/mol.

The storage conditions of our DBS samples varied across the four study centers. Within-center specific details of storage conditions for each DBS card were not available. Our correction method uses analysis delay as a predictor for HbA1c inflation during storage. For evaluation of this multicenter study, we have to consider that all DBS samples had to be shipped to center A, where DBS cards were analyzed immediately or frozen at -20°C. The temperature during shipment was assumed to be close to room temperature. As the specific conditions are not known for all samples, our correction method provides an approximation. Precise information about temperature fluctuations during storage, the glucose and haemoglobin concentrations in the sample, as well as humidity levels, all could in theory improve model performance further.

The IMI DIRECT study was conducted to investigate disease progression and not the effect of long-term storage on DBS. Nevertheless, even with this caveat, our correction method appropriately corrects for storage temperature and analysis delay. It remains to be seen whether corrected HbA1c levels can help identify progression subgroups and new biomarkers within the IMI DIRECT

For other researchers to apply our correction method, it might be necessary to adjust the model parameters to their specific study conditions. For example, the \mathbf{E}_{\max} value is expected to be correlated to storage temperature; the higher the temperature, the higher the E_{max} value. Furthermore, baseline HbA1c levels might also have an impact on the E_{max} value, when a broader range of HbA1c levels is considered. In our case, participants at risk of developing diabetes were studied. We hypothesis a negative relation between HbA1c baseline and the possibility of glycation of the not-yet-glycated haemoglobin. If the overall HbA1c baseline is low, an increase in HbA1c due to the high amount of not yet glycated hemoglobin in the samples could be more likely to be observed. However one can also argue that with high HbA1c baseline, plasma glucose might also be higher, increasing the potential for the glycation of proteins. Such dependent relationships should be tested and adjusted for, whenever appropriate.

CONCLUSION

Our study shows that analysis delay and non-ideal storage conditions of DBS samples have a significant impact on the inflation of the resulting HbA1c value. Our developed correction method, however, seems to adequately adjust for HbA1c instability in such instances. Storage conditions of DBS cards should be carefully monitored and controlled, ideally at -20°C; however, whenever this is not possible, our correction method can be used to adjust for the attributable error.

ACKNOWLEDGEMENTS

The work leading to this publication has received support from the Innovative Medicines Initiative Joint Undertaking under grant agreement n°115317 (DIRECT), resources of which are composed of financial contribution from the European Union's Seventh Framework Programme (FP7/2007-2013) and EFPIA companies' in kind contribution. http://www.direct-diabetes.org/

REFERENCES

- 1. Cohen RMC, Haggerty S, Herman WH. HbA1C for the diagnosis of diabetes and prediabetes: Is it time for a mid-course correction? Robert. J Clin . Endocrinol Metab. 2010; 95: 5203-5206. http://bit.ly/2JBB7sq
- 2. Nathan DM, Balkau B, Bonora E, Borch Johnsen K, Buse JB, Colagiuri S. et al. International expert committee report on the role of the A1C assay in the diagnosis of diabetes. Diabetes Care. 2009; 32: 1327-1334. http://bit. lv/2xQRSsX
- 3. American diabetes association. Standards of medical care in diabetes. Diabetes Care. 2014: 37: 14-80.
- 4. McDade TW. Development and validation of assay protocols for use with dried blood spot samples. Am J Hum Biol. 2014; 26: 1-9. http://bit.ly/2JFrZTL
- 5. Mei J V, Alexander JR, Adam BW, Hannon WH. Use of filter paper for the collection and analysis of human whole blood specimens, J Nutr. 2001; 131; 1631-1636. http://bit.ly/2XQ89Ok
- 6. Parker SP. Cubitt WD. The use of the dried blood spot sample in epidemiological studies. J Clin Pathol. 1999; 52: 633-639. http://bit.ly/32ymzkJ
- 7. McDade TW. Williams S. Snodgrass J.J. What a drop can do: dried blood spots as a minimally invasive method for integrating biomarkers into populationbased research. Demography. 2007; 44: 899-925. http://bit.ly/2Gg9jYy
- 8. Affan ET, Praveen D, Chow CK, Neal BC. Comparability of HbA1C and lipids measured with dried blood spot versus venous samples: a systematic rev and meta-analysis, BMC Clin Pathol, 2014; 14; 21, http://bit.lv/30E1DXM
- 9. Mastronardi CA, Whittle B, Tunningley R, Neeman T, Paz Filho G. The use of dried blood spot sampling for the measurement of HbA1C: a cross-sectional study. BMC Clin Pathol. BMC Clinical Pathology; 2015; 15: 13. http://bit.
- 10. Fokkema MR, Bakker AJ, De Boer F, Kooistra J, De Vries S, Wolthuis A. HbA1C measurements from dried blood spots: Validation and patient satisfaction. Clin Chem Lab Med. 2009; 47: 1259-1264. http://bit.ly/2YY4PNN
- 11. Buxton OM, Malarick K, Wang W, Seeman T. Changes in dried blood spot Hb A1C with varied postcollection conditions. Clin Chem. 2009; 55: 1034-1036. http://bit.ly/2JCn5GV

- 12. Jones TG, Warber KD, Roberts BD. Analysis of hemoglobin A1C from dried blood spot samples with the Tina-quantR II immunoturbidimetric method. J Diabetes Sci Technol. 2010; 4: 244-249. http://bit.ly/2xQOZbx
- 13. Koivula RW, Heggie A, Barnett A, Cederberg H, Hansen TH, Koopman AD, et al. Discovery of biomarkers for glycaemic deterioration before and after the onset of type 2 diabetes: Rationale and design of the epidemiological studies within the IMI DIRECT Consortium. Diabetologia. 2014; 57: 1132-1142. http:// hit Iv/2SwCvzH
- 14. http://www.direct-diabetes.org/objectives/wp2.php. DIRECT Objectives.
- 15. Chapelle JP, Teixeira J, Maisin D, Assink H, Barla G, Stroobants AK, et al. Multicentre evaluation of the Tosoh HbA1C G8 analyser. Clin Chem Lab Med. 2010; 48: 365-371. http://bit.ly/2OhX5W3
- 16. Wu Y. Yang X. Wang H. Li Z. Wang T. Evaluation of hemoglobin A1C measurement from filter paper using high-performance liquid chromatography and immunoturbidimetric assay. Scand J Clin Lab Invest. 2017; 77: 104-108. http://bit.ly/2LrNdGQ
- 17. Akaike H. A new look at the statistical model identification. IEEE Trans Autom Control. 1974; 19: 716-723. http://bit.ly/2YUtHpC
- 18. Jonsson EN, Karlsson MO, Xpose An S-PLUS based population pharmacokinetic/pharmacodynamic model building aid for NONMEM. Comput Methods Programs Biomed. 1999; 58: 51-64. http://bit.ly/2Sm2Xvt
- 19. Beal S, Sheiner L. NONMEM Users Guides. San Francisco: NONMEM Project Group University of California. 1998
- 20. Bonate PL. Pharmacokinetic-pharmacodynamic modeling and simulation. 2nd ed. Springer; 2011. http://bit.ly/2LZIZFQ
- 21. Giavarina D. Understanding bland altman analysis. Biochem Med (Zagreb). 2015; 25: 141-151. http://bit.ly/2Lt9J1U
- 22. Revelle W. psych (paired.r), Proced, Psychol, Psychom, Personal, Res. http:// CRAN.R-project.org/package=psych (R Packag. version 1.7.8).
- 23. Koivula RW, Forgie IM, Kurbasic A, Vinuela A, Heggie A, Giordano GN, et al. Discovery of biomarkers for glycaemic deterioration before and after the onset of type 2 diabetes: descriptive characteristics of the epidemiological studies within the IMI DIRECT Consortium. Diabetologia. 2019; 62: 1601. http://bit.ly/2Z6lxxv
- 24. Lakshmy R. Gupta R. Measurement of glycated hemoglobin A1C from dried blood by turbidimetric immunoassay. J Diabetes Sci Technol. 2009: 3: 1203-1206. http://bit.ly/2xWt2ry
- 25. Bunn HF. Shapiro R. McManus M. Garrick L. McDonald MJ. Gallop PM. et al. Structural heterogeneity of human hemoglobin A due to nonenzymatic glycosylation. J Biol Chem. 1979; 254: 3892-3898. http://bit.ly/2Y0ZjbX
- 26. Mortensen HB, Christophersen C. Incubation of hemoglobins isolated by isoelectric, Biochim Biophys Acta, 1982; 707; 154-63.

4.2 Publication II: Significant Impact of Time-of-Day Variation on Metformin Pharmacokinetics (2).

ARTICLE



Significant impact of time-of-day variation on metformin pharmacokinetics

Denise Türk 1 • Nina Scherer 1 • Dominik Selzer 1 • Christiane Dings 1 • Nina Hanke 1 • Robert Dallmann 2 • Matthias Schwab 3.4.5 • Peter Timmins 6 • Valerie Nock 7 • Thorsten Lehr 1 6

Received: 22 November 2022 / Accepted: 31 January 2023 © The Author(s) 2023

Abstract

Aims/hypothesis The objective was to investigate if metformin pharmacokinetics is modulated by time-of-day in humans using empirical and mechanistic pharmacokinetic modelling techniques on a large clinical dataset. This study also aimed to generate and test hypotheses on the underlying mechanisms, including evidence for chronotype-dependent interindividual differences in metformin plasma and efficacy-related tissue concentrations.

Methods A large clinical dataset consisting of individual metformin plasma and urine measurements was analysed using a newly developed empirical pharmacokinetic model. Causes of daily variation of metformin pharmacokinetics and interindividual variability were further investigated by a literature-informed mechanistic modelling analysis.

Results A significant effect of time-of-day on metformin pharmacokinetics was found. Daily rhythms of gastrointestinal, hepatic and renal processes are described in the literature, possibly affecting drug pharmacokinetics. Observed metformin plasma levels were best described by a combination of a rhythm in GFR, renal plasma flow (RPF) and organic cation transporter (OCT) 2 activity. Furthermore, the large interindividual differences in measured metformin concentrations were best explained by individual chronotypes affecting metformin clearance, with impact on plasma and tissue concentrations that may have implications for metformin efficacy.

Conclusions/interpretation Metformin's pharmacology significantly depends on time-of-day in humans, determined with the help of empirical and mechanistic pharmacokinetic modelling, and rhythmic GFR, RPF and OCT2 were found to govern intraday variation. Interindividual variation was found to be partly dependent on individual chronotype, suggesting diurnal preference as an interesting, but so-far underappreciated, topic with regard to future personalised chronomodulated therapy in people with type 2 diabetes.

 $\textbf{Keywords} \ \ Chronopharmacology} \cdot Empirical \ modelling} \cdot Mechanistic \ modelling} \cdot Metformin \cdot Pharmacokinetics \cdot Renal \ excretion \cdot Transporter$

ER

IR

GMFE

Abbreviations

 C_{max} Maximum plasma concentration C_{trough} Trough plasma concentration

Denise Türk and Nina Scherer contributed equally to this study.

☐ Thorsten Lehr thorsten.lehr@mx.uni-saarland.de

Published online: 17 March 2023

- Clinical Pharmacy, Saarland University, Saarbrücken, Germany
- Division of Biomedical Sciences, Warwick Medical School, University of Warwick, Coventry, UK
- ³ Dr. Margarete Fischer-Bosch-Institute of Clinical Pharmacology, Stuttgart, Germany

Extended-release

Immediate-release

Tübingen, Germany

Geometric mean fold error

University of Tübingen, Tübingen, Germany

Cluster of Excellence iFIT (EXC2180) 'Image-guided and Functionally Instructed Tumor Therapies', University of Tübingen,

Departments of Clinical Pharmacology, Pharmacy and Biochemistry,

- Department of Pharmacy, University of Huddersfield, Huddersfield, UK
- Boehringer Ingelheim Pharma GmbH & Co. KG, Biberach, Germany



Research in context

What is already known about this subject?

 Chronotherapy shows benefits for the treatment of various conditions, but the implications for first-line therapy for type 2 diabetes have not been investigated in dedicated clinical trials

What is the key question?

• Does metformin pharmacokinetics exhibit significant intraday variation and what are the underlying causes?

What are the new findings?

- Analysis of clinical data from a large dataset revealed significant intraday variation in metformin pharmacokinetics
- Empirical and mechanistic pharmacokinetic modelling showed that variation in pharmacokinetics could be attributed to rhythms in GFR, renal plasma flow and organic cation transporter 2 activity
- Interindividual variation was found to be partly dependent on individual chronotype, which also affects metformin
 plasma and tissue concentrations

How might this impact on clinical practice in the foreseeable future?

 Metformin pharmacokinetics, which shows pronounced time-of-day-dependent and interindividual variability, might impact metformin efficacy and present opportunities for future optimised chronomodulated therapy for people with type 2 diabetes

$k_{\rm cat}$	Transport rate constant
MATE	Multidrug and toxin extrusion protein
MRD	Mean relative deviation
NLME	Non-linear mixed effects
OCT	Organic cation transporter
PBPK	Physiologically based pharmacokinetic
$PM\Delta T$	Plasma membrane monoamine transporter

RPF Renal plasma flow

Introduction

Metformin is recommended as first-line therapy for type 2 diabetes [1] and predominantly acts in the gastrointestinal system by decreasing glucose uptake from the lumen and increasing glucagon-like peptide-1 secretion [2]. Furthermore, it leads to inhibition of hepatic gluconeogenesis [3] and increased insulin-stimulated glucose uptake into other organs e.g. skeletal muscle [4], resulting in a reduction in blood glucose levels. Recent work suggests that metformin therapy is associated with a preventive effect against cancer and could even be a useful adjuvant in cancer therapy [5].

Metformin is highly soluble, exhibits a low permeability and retains a positive charge over the whole range of physiological pH. Hence, its absorption, distribution and excretion strongly depend on active transport processes to cross biological membranes. Incomplete transporter-mediated absorption from the upper intestine yields a moderate bioavailability of about 55% [6]. Pharmacokinetic metformin data indicate high

inter- and intraindividual variation [6]. Metformin is not metabolised and is mainly excreted in urine passively via glomerular filtration and actively by consecutive action of organic cation transporter (OCT) 2 and multidrug and toxin extrusion proteins (MATEs) [6].

While the pharmacokinetics of metformin is generally well understood, the influence of time-of-day on metformin pharmacology, in particular, has not yet been described. Analysing plasma concentration-time profiles of a twice daily metformin administration from a study conducted with the intention of investigating bioequivalence of different metformin formulations [7] revealed similar mean AUC values during day and night. However, altered plasma curve shapes as well as sizeable time-of-day variations of trough plasma concentrations (C_{trough}) and maximum plasma concentrations (C_{max}) were found. Many body functions, like the GFR and other excretion processes as well as absorption and metabolic processes, underlie intraday variations, resulting in changes of drug exposure and, subsequently, in daily rhythms of efficacy or toxicity [8]. Thus, observed variability in metformin plasma concentrations might be explained by time-of-day dependent pharmacokinetics. To date, however, no dedicated analyses were available in published literature to assess time-dependent alteration of metformin pharmacology in humans.

In general, large interindividual differences in diurnal preference (also referred to as 'chronotype') have been observed, for example as preferred wake-up and sleep times [9]. Chronotherapy, i.e. taking daytime into account for drug administration, might have clinical benefits in various



indications [10–12]. Considering the individual chronotype within the context of personalised precision chronotherapy may improve therapy outcomes, as proposed as a potential treatment option for cancer patients [13].

Here, we (1) investigated whether metformin pharmacokinetics in humans exhibits a significant intraindividual difference depending on time-of-day of administration; (2) quantified the magnitude of the effect using non-linear mixed effects (NLME) pharmacokinetic modelling on a large clinical dataset of individual metformin concentration measurements; (3) generated hypotheses regarding sources of such daily variation and tested the underlying mechanisms using a literature-informed physiologically based pharmacokinetic (PBPK) modelling approach; (4) partly explained interindividual variability based on the model-determined chronotype; and (5) simulated the daily rhythms of metformin concentrations in relevant tissues, which could support the assessment of clinical relevance in future work.

Methods

Clinical dataset Individual metformin measurements from five clinical studies were used. Metformin was administered as immediate- (IR) and extended-release (ER) formulations of 500–2000 mg once to three times daily in single and multiple day regimens. All studies have been approved by the local ethics committees and informed consent was obtained from all participants before study entry. Results from studies II–V have not previously been published. Detailed information on all studies, including number and demographics of participants, inclusion and exclusion criteria and exact dosing/sampling schedules are provided in electronic supplementary material (ESM) Tables 1–5 and ESM Figs 1–5.

Statistical analysis Individual plasma measurements were analysed separately for differences between C_{trough} values measured immediately before the next dose in the morning (' $C_{trough,morning}$ ') and the evening (' $C_{trough,evening}$ ') as well as C_{max} values measured after the morning dose (' $C_{max,morning}$ ') and the evening dose (' $C_{max,evening}$ '). Details on statistical analysis are provided in ESM Section 1.2.

NLME pharmacokinetic modelling An empirical pharmacokinetic model of metformin was implemented in NONMEM (version 7.4.3, ICON Development Solutions, Ellicott City, MD, USA), informed by individual data using NLME techniques. The final model was built and evaluated in a three-step procedure by: (1) developing a structural model by checking one-, two- and three-compartment disposition models as well

as zero-order, first-order and Michaelis-Menten absorption and elimination kinetics; (2) quantifying interindividual and residual variabilities based on the structural model by testing variability on each model parameter; and (3) investigating the effects of the covariates (e.g. sex, age, body weight, serum creatinine, administered dose, formulation, comedication and food intake) using a forward inclusion and backward elimination procedure with significance levels of 5% and 0.1%, respectively.

A function assuming sinusoidal oscillations with a 24 h period (Equation 1) was tested on respective model parameters to identify whether a daily rhythm of metformin absorption, distribution and/or excretion processes improves the description of metformin plasma and urine concentrations:

$$f(t) = AMP \times \sin\left(\frac{2\pi}{24} \times [t + TDEL]\right) + 1 \tag{1}$$

where t = time, AMP = amplitude and TDEL = shift in time. Values for amplitude and shift were optimised by fitting model simulations to observed metformin profiles.

Details on final model selection and evaluation are provided in ESM Section 1.3.

Literature-informed mechanistic PBPK modelling The literature was extensively searched for physiological conditions linked to rhythmicity in absorption, distribution and excretion of metformin, including metformin-specific transporters.

To elucidate the key variables with impact on metformin pharmacokinetics, a mechanistic whole-body PBPK modelling approach was applied, where organs are represented by compartments that are connected via blood flow. The change of drug concentration in these compartments over time is described by differential equations. Mechanistic implementation of transport processes at their respective sites of action allows simulation and prediction of drug concentrations in all relevant organs and body sites. A published whole-body PBPK model of metformin [14] developed via the Open Systems Pharmacology Suite (version 8.0, https://www. open-systems-pharmacology.org/) using metformin studies in healthy volunteers after intravenous and oral administration in fasted and fed state (single and multipledose, dosing range 0.001-2550 mg) was used as a basis for further investigation. The model includes active transport by plasma membrane monoamine transporter (PMAT), OCT1 as well as consecutive action of OCT2 and MATE1.

Time-of-day variation of pharmacokinetic-related processes and physiological conditions identified in the literature was tested with the PBPK model. By modulating relevant model parameter values over time with an oscillation function (Equation 1), the influence of each process on metformin pharmacokinetics was tested separately. Amplitude and acrophase (i.e. clock time of maximal activity) of the tested rhythmic processes were implemented as reported previously or optimised by fitting simulations to observed aggregated metformin plasma concentration—time profiles from study I. The impact of each tested process on metformin pharmacokinetics was evaluated visually and quantitatively by calculating mean relative deviations (MRDs) and geometric mean fold errors (GMFEs) (ESM Equations 1 and 2), to estimate the model accuracy for metformin concentration—time profiles as well as $C_{\rm trough}$ and $C_{\rm max}$ ratios. Details on model extension and performance evaluation are provided in ESM Section 1.4. Information about expression of relevant transport proteins is presented in ESM Table 6.

Results

Clinical dataset The dataset derived from five studies included data on 191 healthy adults (65% men, 18–50 years) with 7476 plasma and 316 urine levels of metformin. Of these, 21.4% of plasma and 100% of urine measurements were observed after administration of IR formulations. Pharmacokinetic profiles covering at least one dosing interval were available for all individuals, with additional C_{trough} measurements for multiple-dose administration studies (studies I and II: 1000 mg twice daily, and study III: 850 mg three times daily) that allowed further investigations of intraday variation in pharmacokinetics.

Statistical analysis Plasma concentration—time profiles from studies I and II were used for the investigation of differences in individual mean C_{trough-morning} and C_{trough,evening} values. Statistical analyses revealed 42% higher mean C_{trough} measurements in the morning compared with the evening (p=0.00016). Moreover, individual C_{trough} measurements exhibited a large intraindividual variability of up to 75%. Linear mixed model analysis that included all individual C_{trough} measurements also confirmed significantly higher C_{trough} measurements in the morning (p<0.0001).

Although differences were less pronounced for $C_{\rm max}$, i.e. 16% higher mean $C_{\rm max}$ values in the morning compared with the evening, measurements were significantly different with p=0.0053 for t test analysis of mean values. Furthermore, for $C_{\rm max}$, large intraindividual variability was observed, with variability up to 52%. In the mixed model analysis, the findings from analysing the means could be confirmed with p=0.0063. A summary of the statistical analysis is shown in Fig. 1a and ESM Figs 6 and 7.

NLME pharmacokinetic modelling All individual plasma and urine measurements from studies I–V were used for model

development and were best described by a two-compartment disposition model with first-order absorption, distribution and clearance. IR formulations were modelled via first-order absorption and ER formulations by a zero-order release preceded the first-order absorption. Interindividual variability could be identified for clearance, central volume of distribution and bioavailability. Implementation of food intake, formulation and dose as significant covariates reduced the interindividual variabilities for clearance, volume of distribution and bioavailability by 14%, 75% and 52%, respectively. Administration after food intake led to a 1.9-fold higher relative bioavailability and a 0.6-fold slower absorption rate constant, but a 5.1-fold increased release duration for the ER formulation. The bioavailability of the ER formulation was 1.1-fold higher compared with the IR formulation. The metformin dose was implemented as a covariate using an exponential function (ESM Equation 3), leading to a decreased relative bioavailability for higher administered doses of metformin.

Daily variation was tested for absorption, distribution as well as clearance parameters. Model performance significantly improved if a daily rhythm on metformin clearance was incorporated (p<1.0 × 10^{-100}), applying an estimated amplitude of 21% and an acrophase at 17:43 hours. Parameter estimates of the model are provided in ESM Table 7, and the model structure is presented in ESM Fig. 8. The performance of the NLME model without and with daily rhythm is presented with plasma concentration—time profiles and goodness-offit plots in Fig. 1b and ESM Figs 9–13, indicating good performance of the model including daily variation, with 95% and 83% of predicted individual metformin plasma and urine concentrations, respectively, within twofold of the observed values.

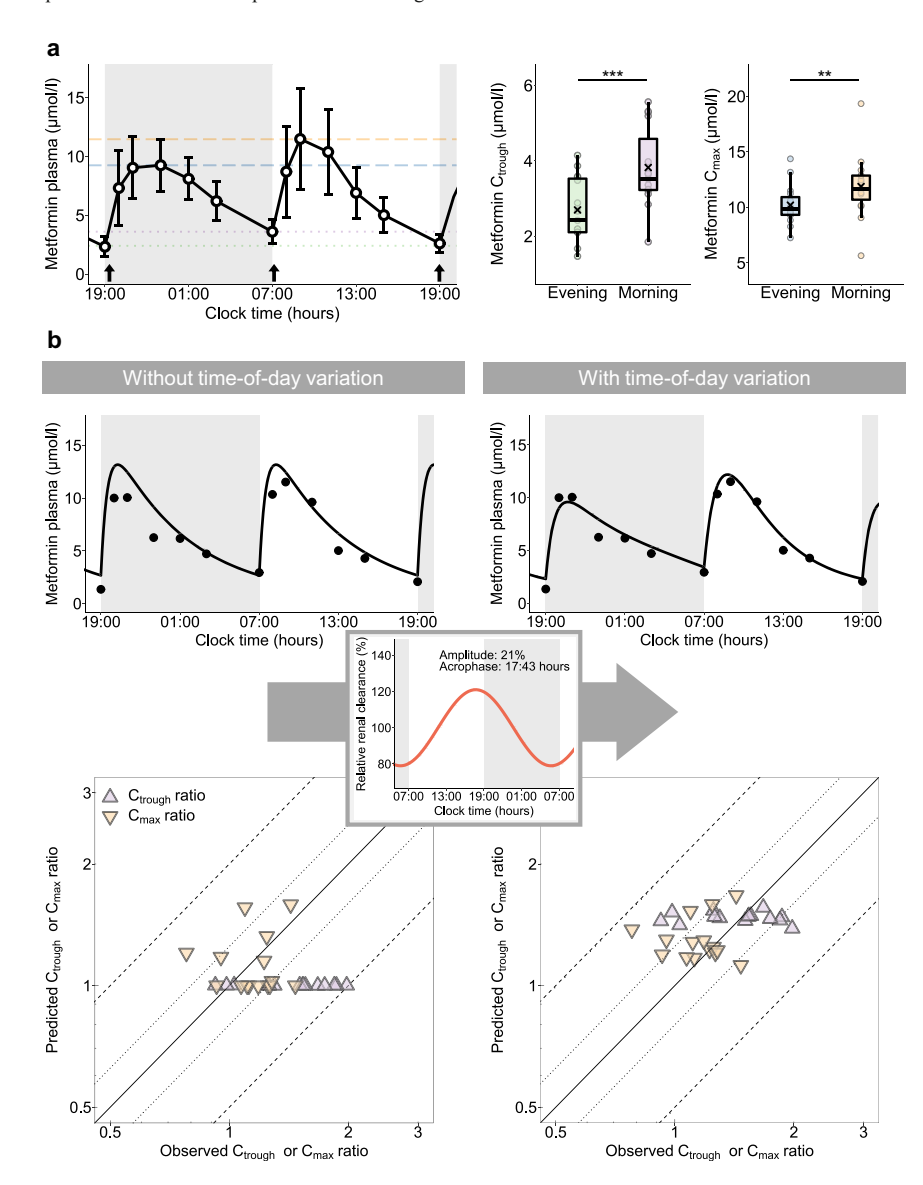
Fig. 1 Investigation of daytime-dependent metformin pharmacokinetics with concentration measurements from study I [7]. (a) Statistically significant differences between trough plasma concentrations (Ctrough) measured in the morning compared with the evening and maximum plasma concentrations (Cmax) measured in the morning compared with the evening were found. Data are shown as arithmetic means \pm SD. Metformin administration (1000 mg twice daily) is indicated by arrows. Grey areas indicate night-time. In the box plots, mean C_{trough} and C_{max} values are indicated by crosses, individual values (n=15) by dots. Boxes represent the distance between first and third quartiles (IQR). Whiskers range from smallest to highest value (<1.5 × IQR). **p<0.01; *p<0.001. (b) Performance of the NLME model without and with time-of-day variation via the estimated oscillation function (insert and Equation 1) applied on clearance. Representative individual plasma concentration-time profiles (n=1) are plotted after twice daily administration of 1000 mg metformin. Dots indicate observed data and lines indicate model predictions. Goodness-of-fit plots show comparisons of all predicted and observed individual C_{trough} and C_{max} ratios after twice daily administration of 1000 mg metformin. The straight solid line marks the line of identity, dotted lines indicate 1.25-fold and dashed lines indicate twofold deviations



 C_{trough} and C_{max} predictions showed smaller errors for the model with rhythmic renal clearance compared with the model assuming constant renal clearance, quantified by a decrease of mean GMFEs from 1.45 to 1.21 for C_{trough} and 1.21 to 1.19 for C_{max} ratios of study I (Fig. 1b and ESM Figs 14 and 15). Comparison of conditional weighted residuals vs time and predicted concentration is presented in ESM Figs 16

and 17. Further details on modelling results are provided in $\operatorname{\mathsf{ESM}}$ Section 2.2.

Literature-informed mechanistic PBPK modelling Previous studies reported daily rhythm in absorption- and distributionrelated physiological conditions, namely gastric pH, gastric





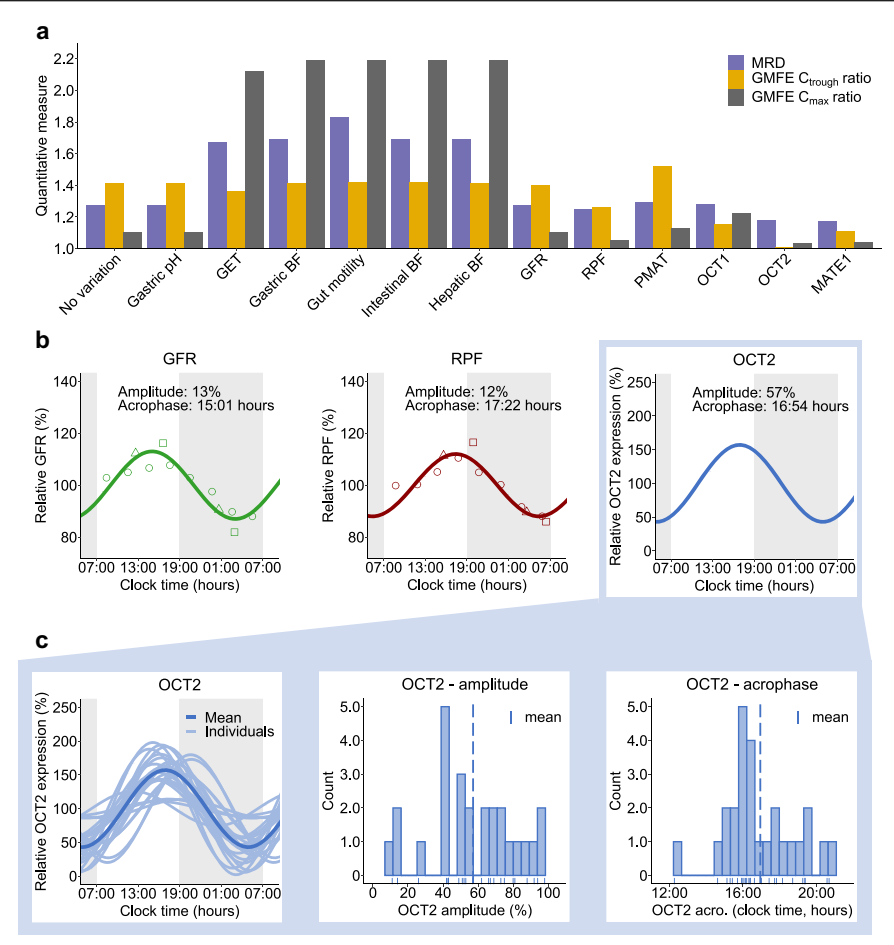


Fig. 2 Implementation of a daily rhythm in the metformin PBPK model. (a) Hypothesis testing. Rhythmic physiological processes and transporter activities tested using the PBPK model with the respective prediction performance metrics, i.e. MRDs and GMFEs. (b, c) Final PBPK model processes with rhythmic excretion. (b) Time-of-day variation of GFR and RPF as reported in the literature [18–20] (measurements from different

reports indicated by dots, triangles and squares) and OCT2 implemented in the final PBPK model. (c) Rhythm of OCT2 was optimised with the PBPK model for each individual, and individual OCT2 parametrisation is shown as distribution of individually optimised OCT2 amplitudes and acrophases (n=26). acro, acrophase; BF, blood flow; GET, gastric emptying time

emptying time, gut motility, blood flow to the gastrointestinal tract and hepatic blood flow, with effects on drug solubility, bioavailability, transit time through the gastrointestinal tract and distribution in the body. For excretion-related processes, rhythmic GFR and renal blood flow have been described (ESM Table 8). In addition, daily variation of active transport processes in the liver and kidney have been observed [8]. No rhythm was reported for PMAT (*SLC29A4*), mainly involved in intestinal absorption of metformin, either in humans or in animals. For OCT1 (*SLC22A1*), the transporter mainly

responsible for metformin uptake into hepatocytes, no human time-series data were available. However, in mice, hepatic Slc22a1 mRNA expression is not rhythmic [15]. Regarding renal transporters, Slc47a1 (MATE1) is not rhythmic [15, 16], while for Slc22a2 (OCT2) expression, one study reported significant daily rhythms [17]. Again, no human expression data were available to investigate SLC22A2 (OCT2) rhythmicity.

These potential factors introducing time-of-day variation were tested in the PBPK model to confirm and explain

findings from the NLME model regarding observed time-ofday variation in metformin pharmacokinetics. Temporal variations of gastrointestinal and distribution-related processes as well as GFR and renal plasma flow (RPF) were modelled with literature values for amplitudes and acrophases, expressing amplitudes from 12-56% (ESM Table 8). However, judging by GMFEs for C_{trough} and C_{max} ratios, rhythmic absorption-, distribution- and passive excretion-related processes on metformin pharmacokinetics did not lead to an improved description of metformin concentration-time profiles, especially not for both Ctrough and Cmax values compared with the base PBPK model without any temporal variation. The daily variation of transport rates was modelled with optimised values for amplitudes and acrophases. Introducing oscillation in PMAT and OCT1 activities resulted in insufficient descriptions of both metformin Ctrough and Cmax ratios, while time-ofday variation in activity of excretion-related transporters, i.e. OCT2 and MATE1, improved descriptions of observed plasma concentrations as well as C_{trough} and C_{max} ratios (Fig. 2a and ESM Figs 18 and 19 under Section 2.3.2). In the final model, metformin plasma concentration-time profiles were modelled incorporating a combination of a daily rhythm in GFR, renal blood flow and OCT2 (Fig. 2b), which is consistent with published findings for human renal physiology [17-20]. PBPK model parameters are listed in ESM Tables 9 and 10 under Section 2.3.3.

Individual differences in the daily rhythms of metformin pharmacokinetics Individual metformin profiles exhibited a large interindividual variability and were insufficiently described using the same rhythmic OCT2 parametrisation for all participants. To account for interindividual variability in OCT2 baseline activity (caused by e.g. genetic polymorphisms), transport rate constant (k_{cat}) values were optimised for individual profiles with mean k_{cat} =57680 1/min (CV=69%;

n=26). Individual chronotypes were estimated by calculating OCT2 amplitudes and acrophases separately for each individual with a mean amplitude of 57% (CV=43%) and mean acrophase at 16:54 hours (CV=39%). The distribution of individual amplitudes and acrophases is shown in Fig. 2c, while no correlation of OCT2 parameters has been determined (ESM Fig. 20). Predicted mean and individual plasma concentration-time profiles from studies I and III are shown in Fig. 3, agreeing with observed higher C_{trough} values before the morning dose and higher C_{max} values after the morning dose when administered every 12 h (Fig. 3a). Highest C_{max} values were predicted during the night for the three-times daily regimen (Fig. 3b). Predicted plasma concentration-time profiles for all studies compared with observed data are shown in ESM Figs 21-25. Goodnessof-fit plots demonstrate that 93% of predicted plasma concentration values from studies I and III lie within twofold of observed values (ESM Fig. 26). Comparisons of predicted and observed C_{trough} and C_{max} ratios are shown in ESM Fig. 27.

Simulations in relevant tissues To investigate the impact of daily modulation of metformin pharmacology on its exposure in tissues, plasma, kidney, liver, fat and muscle tissue concentrations were simulated in steady-state, administering the highest recommended metformin dose of 1000 mg three times daily [21]. Simulated metformin concentration—time profiles for plasma and tissues showed substantial interindividual and intraday variability (Fig. 4a—e) and calculations of metformin peak-to-trough concentration ratios for each dosing interval within 1 day in plasma and tissues revealed intraday, intertissue and interindividual differences (Fig. 4f). As OCT2, the main contributor to metformin rhythm in the model, is expressed at the basolateral membrane of tubular epithelial cells, concentrations in the kidney showed an opposing trend due to a decreased transport of metformin into

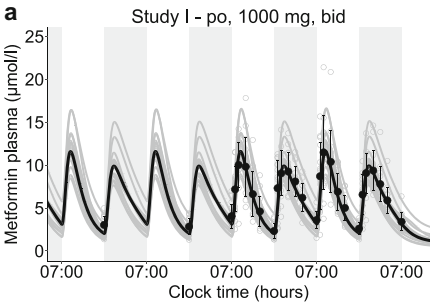
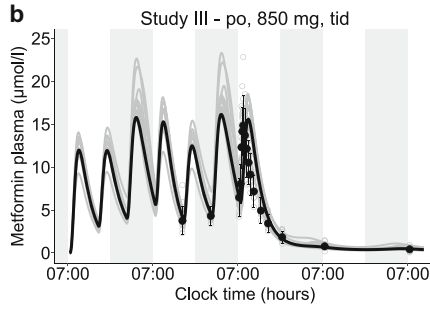


Fig. 3 Mean (black lines) and individual (grey lines) PBPK model predictions of metformin plasma concentration–time profiles compared with measurements from (a) study I (n=15) and (b) study III (n=11) [7,



39]. Closed black dots indicate arithmetic means \pm SD, open grey dots indicate individual measurements. Grey areas indicate night-time. bid, twice daily; po, oral; tid, three times daily

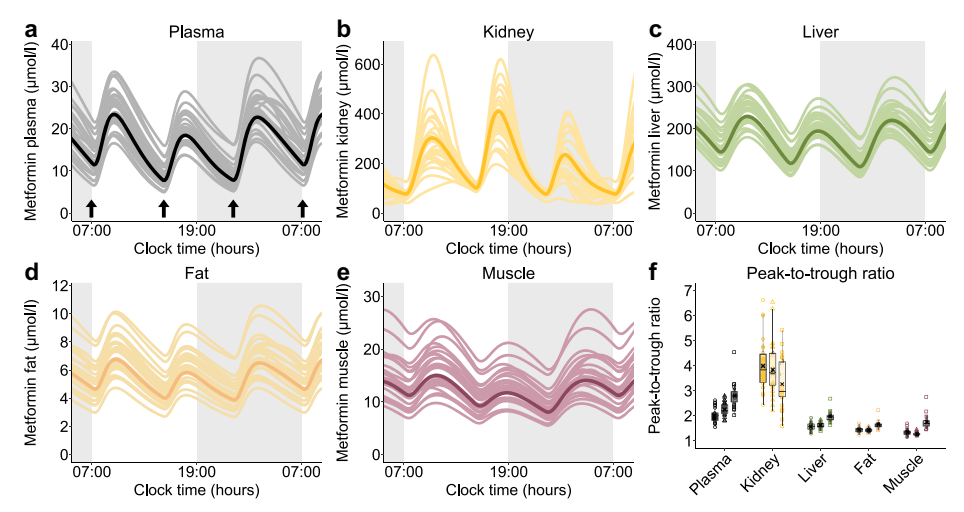


Fig. 4 PBPK model simulations of plasma and tissue concentration—time profiles of an oral administration of three-times daily 1000 mg metformin (highest recommended dose according to the German prescribing information [21]) at 07:00, 15:00 and 23:00 hours (indicated by arrows). (a—e) Comparison of metformin levels in (a) plasma, (b) kidney tissue, (c) liver tissue, (d) fat tissue and (e) muscle tissue. Respective simulations with a mean parameter set of OCT2 $k_{\rm cut}$ amplitude and acrophase are shown as dark lines, simulations with individual parameter sets (n=26) are shown

as light lines. Grey areas indicate night-time. (f) Comparison of metformin peak-to-trough ratios for simulations in plasma and tissues. The three box plots per tissue give peak-to-trough ratios after metformin administration at 07:00, 15:00 and 23:00 hours. Dots (peak 1), triangles (peak 2) and squares (peak 3) show individual peak-to-trough ratios (n=26), crosses indicate mean values. Boxes represent the distance between first and third quartiles (IQR). Whiskers range from smallest to highest value (<1.5 × IQR)

kidney cells at night, leading to increased concentrations in plasma and other tissues.

Discussion

Chronotherapy might have a clinical benefit in various indications, discussed e.g. for therapy of cancer [10], rheumatoid arthritis [11] or metabolic diseases [12]. To date, the implications of chronopharmacology for treatment of type 2 diabetes have not been investigated in dedicated clinical trials. The presented work focused on statistical and in silico analyses of metformin pharmacokinetics covering interindividual variability with the help of NLME and PBPK modelling, revealing intraday changes in pharmacokinetics for metformin plasma and urine concentrations. Mechanistic mathematical modelling of metformin pharmacokinetics allowed the investigation of hypotheses for the underlying chrono-mechanisms and the integration of related findings in the overall context of diabetes therapy.

Statistical analyses showed significant differences between metformin C_{trough} as well as C_{max} values measured in the morning or the evening. To further investigate these differences and variations, empirical and mechanistic pharmacokinetic models were applied, as these methods have been proven useful to (1) test hypotheses and (2) investigate time-of-day

dependence, e.g. for oral bioavailability and clearance of midazolam [22], light-triggered melatonin release [23] and heart rate [24].

The NLME pharmacokinetic modelling analysis led to an accurate description of metformin plasma concentrations, especially C_{trough} and C_{max} measurements, when a daily rhythm for systemic clearance was incorporated. In contrast, rhythms of other processes, e.g. the absorption, did not improve the modelling outcomes. The time-dependent effect on systemic clearance might be predominantly attributed to biologic rhythmic variations of kidney function, as metformin is exclusively eliminated renally. Rhythmic GFR and renal blood flow have been described [18-20] while the variation in GFR cannot be explained by the oscillation of renal blood flow alone [20]. In mice, the circadian clock in podocytes has been found to contribute to a rhythmic GFR [25], but the influence of further systemic factors are not completely understood [26]. However, the NLME estimated amplitude for the oscillation of metformin clearance was more pronounced compared with the published amplitude for GFR (21% vs 13%) [18-20], leading to the hypothesis of an additional daily rhythm in active secretion.

The PBPK modelling approach complemented the empirical NLME model, as it allowed the mechanistic implementation of individual physiology including demographics, kidney function as well as relevant transport proteins. Key processes

from the NLME model were well in line with the independently developed PBPK model, and the additional rhythmic active secretion, proposed by analysing the NLME model outcomes, could be supported with the PBPK approach. Here, metformin plasma concentration-time profiles, especially C_{max} as well as C_{trough}, were best described assuming a combination of rhythmic GFR, renal blood flow and tubular secretion rate. In the literature, there is no unambiguous evidence for rhythmic SLC22A2 compared with SLC47A1 (MATE1). Kidney expression data from mice presented by Zhang et al [16] reveal that Slc47a1 is not rhythmic, similar to Slc22a2, but a slightly more pronounced rhythm in Slc22a2 is shown. Oda et al [17] observed rhythmic Slc22a2 but not Slc47a1 expression profiles in nocturnal mice [17]. Baboons exhibit a rhythm in both SLC22A2 and SLC47A1 expression in the kidney medulla, but not in the kidney cortex, where the relevant proximate tubule cells are located [27]. Unfortunately, expression data of SLC22A2 in human kidney cells are currently not available. However, due to the sequential action of OCT2 and MATEs in tubule cells, discrimination between both processes is challenging and dedicated studies are required to investigate the specific contributions of both OCT2 and MATEs. Model implementation of daily variation for both OCT2 and MATE1, also taking interindividual variability into account, was not feasible using the currently available data. If data from human kidneys become available, the model could be adjusted in future projects.

The influence of other possible rhythmic processes affecting drug pharmacokinetics, i.e. absorption- and distributionrelated mechanisms, was quantified with a PBPK model, because these mechanisms might also affect metformin solubility, distribution and transit time through the gastrointestinal tract, bioavailability and tissue distribution [8]. Food intake has been reported to reduce metformin bioavailability of an IR formulation [28] but was not the main contributor to observed daily variations of metformin pharmacokinetics according to our PBPK model analysis. Only a minor contribution of daily rhythms in other absorption- and distributionrelated processes has been assumed in previous work [15. 28-30]. This was confirmed, as a rhythmic absorption rate reduced NLME model performance, and PBPK modelling of rhythmic absorption- and distribution-related processes showed only a very small effect on plasma concentrationtime profiles (ESM Figs 18 and 19). An altered metformin absorption, however, might have a more pronounced impact on its pharmacokinetics after administration of ER formulations, which was not addressed in this study due to the lack of

Both the NLME and the PBPK models predict higher C_{trough} and C_{max} values of the morning dose compared with the evening dose after twice daily administration. The PBPK model predicts higher C_{max} values during the night when metformin is administered in a three-times daily regimen.

This observation is expected, as maximum GFR, RPF and OCT2 activity are modelled in the late afternoon and minimum activity was assumed in the early morning. Hence, in comparison with the morning dose, higher metformin levels are expected after the night dose administered at 23:30 hours with increased $C_{\rm trough}$ values predicted in the morning due to lower elimination of metformin. Moreover, individual differences in night $C_{\rm max}$ compared with day $C_{\rm max}$ can be attributed to individual chronotypes estimated by the model. For the three-times daily regimen, frequent measurements during the night would be valuable to verify model hypotheses.

Since large interindividual differences in individual chronotypes have been observed [9], 'chronotype' like phase differences were hypothesised and an individual OCT2 parametrisation improved plasma concentration—time predictions. Whereas all data herein are from healthy volunteers, an extension to patients with diabetes or kidney failure might be challenging due to relevant pathophysiological changes. Moreover, rhythms in GFR, RPF and OCT2 could be different in patients compared with healthy individuals [31] and, thus, require further experimental data to adjust our model.

Both of our presented models assume active renal excretion as the main contributor to metformin pharmacokinetics. In our NLME model, a large interindividual variability (CV=68%) was estimated on the clearance processes. Other modelling work, e.g. by Stage and coworkers, identified less variability on the clearance (CV=25%) but found large interoccasion variability (up to CV=94%) on absorption and bioavailability processes [32]. Duong et al presented varying degrees of interindividual variability without modelling daytime variations but incorporated interoccasion variability as a random error term [33]. The comparison of parameter estimates from empirical NLME models is complex, as the models are nonmechanistic and were built for different purposes with different model structures and different datasets. It may be speculated that the modelled interoccasion variability might represent parts of the daytime variation, as the inclusion of daytime variation in our model reduced the interindividual variability on the central volume of distribution and the clearance significantly, by 36% and 11%, respectively.

Disruption of the circadian clock has been associated with the development of various diseases, such as metabolic and cardiovascular disorders [34]. Mistimed sleep, for example in shift workers, has been identified as a risk factor for developing type 2 diabetes [35], as this affects glucose tolerance and insulin sensitivity [36]. Additionally, a disrupted daily rhythm has been described in diabetes patients [37]. In diet-induced obese rats, targeting the disrupted clock using melatonin in combination with metformin led to an improved therapy outcome [38]. However, using chronobiological concepts to optimise the treatment of type 2 diabetes is not adopted in clinical practice yet. In mice, differences in the direct glucose-lowering effect of metformin and in blood lactic acid

levels were observed if metformin was administered in the active or the rest phase of the animals [15], which would support the hypothesis of time-of-day dependent pharmacodynamics. An interesting future research question regarding clinical implication might focus on the extent to which intraday variation of metformin pharmacokinetics affects efficacy and toxicity in humans, i.e. the risk of lactic acidosis, which needs further investigation. Additionally, personalised chronotherapy might improve therapy outcomes for diabetes patients.

Statistical analyses as well as empirical and mechanistic pharmacokinetic modelling were successfully applied to generate and test hypotheses of the underlying chronomechanisms affecting metformin pharmacokinetics. Both modelling approaches suggest that rhythmic renal elimination had the strongest impact on metformin pharmacokinetics. Key variables of renal elimination were the rhythms in GFR, renal blood flow and OCT2-dependent transport rate. More broadly, our analyses demonstrated the strength of combining empirical and mechanistic pharmacokinetic modelling as a powerful toolchain to investigate scenarios with incomplete and missing clinical data. Furthermore, our results suggest a significant impact of chronotype on metformin pharmacology. Thus, this work might be a starting point for the translation of study results to therapy outcomes and risk assessment by individualised chronotherapy.

Supplementary Information The online version contains peer-reviewed but unedited supplementary material available at https://doi.org/10.1007/s00125-023-05898-4

Acknowledgements We thank Bristol Myers Squibb and Boehringer Ingelheim for provision of individual pharmacokinetic data.

Data availability The datasets analysed during the current study from Bristol Myers Squibb (study I) and Boehringer Ingelheim (studies II—V) are not publicly available. Data from Bristol Myers Squibb are however available from the authors upon reasonable request and with the permission of Bristol Myers Squibb. Regarding the data from Boehringer Ingelheim, interested researchers are invited to consult the external research platform Vivli (https://vivli.org/) to request access to anonymised data.

Funding Open Access funding enabled and organized by Projekt DEAL. MS was supported in part by the Robert Bosch Stiftung, Stuttgart, Germany, and the Deutsche Forschungsgemeinschaft (DFG, German Research Foundation) under Germany's Excellence Strategy - EXC 2180 – 390900677. TL received funding from Boehringer Ingelheim Pharma GmbH & Co. KG for personnel costs of NS, CD and NH.

Authors' relationships and activities NH is now an employee of Boehringer Ingelheim Pharma GmbH & Co. KG. VN is an employee of Boehringer Ingelheim Pharma GmbH & Co. KG. DT, NS, DS, CD, RD, MS, PT and TL declare that there are no relationships or activities that might bias, or be perceived to bias, their work.

Contribution statement DT, NS and TL contributed to conception and design. PT and VN procured individual metformin data. DT, NS and TL analysed the data. DT, NS, DS and TL wrote the manuscript. All the

authors contributed to interpretation of the results, critically revised the article and gave final approval of the version to be published. TL is the guarantor of this work.

Open Access This article is licensed under a Creative Commons Attribution 4.0 International License, which permits use, sharing, adaptation, distribution and reproduction in any medium or format, as long as you give appropriate credit to the original author(s) and the source, provide a link to the Creative Commons licence, and indicate if changes were made. The images or other third party material in this article are included in the article's Creative Commons licence, unless indicated otherwise in a credit line to the material. If material is not included in the article's Creative Commons licence and your intended use is not permitted by statutory regulation or exceeds the permitted use, you will need to obtain permission directly from the copyright holder. To view a copy of this licence, visit http://creativecommons.org/licenses/by/4.0/.

References

- American Diabetes Association (2020) 9. Pharmacologic approaches to glycemic treatment: Standards of medical care in diabetes—2020. Diabetes Care 43(Supplement 1):S98–S110. https://doi.org/10.2337/dc20-S009
- McCreight LJ, Bailey CJ, Pearson ER (2016) Metformin and the gastrointestinal tract. Diabetologia 59(3):426–435. https://doi.org/ 10.1007/s00125-015-3844-9
- Rena G, Hardie DG, Pearson ER (2017) The mechanisms of action of metformin. Diabetologia 60(9):1577–1585. https://doi.org/10. 1007/s00125-017-4342-z
- Galuska D, Nolte LA, Zierath JR, Wallberg-Henriksson H (1994) Effect of metformin on insulin-stimulated glucose transport in isolated skeletal muscle obtained from patients with NIDDM. Diabetologia 37(8):826–832. https://doi.org/10.1007/BF00404340
- Coyle C, Cafferty FH, Vale C, Langley RE (2016) Metformin as an adjuvant treatment for cancer: a systematic review and metaanalysis. Ann Oncol 27(12):2184–2195. https://doi.org/10.1093/ annone/mdw410
- Graham GG, Punt J, Arora M et al (2011) Clinical pharmacokinetics of metformin. Clin Pharmacokinet 50(2):81–98. https://doi.org/10.2165/11534750-00000000-00000
- Timmins P, Donahue S, Meeker J, Marathe P (2005) Steady-state pharmacokinetics of a novel extended-release metformin formulation. Clin Pharmacokinet 44(7):721–729. https://doi.org/10.2165/ 00003088-200544070-00004
- Dallmann R, Brown SA, Gachon F (2014) Chronopharmacology: new insights and therapeutic implications. Annu Rev Pharmacol Toxicol 54(1):339–361. https://doi.org/10.1146/annurevpharmtox-011613-135923
- Roenneberg T, Kuehnle T, Juda M et al (2007) Epidemiology of the human circadian clock. Sleep Med Rev 11(6):429–438. https://doi. org/10.1016/j.smrv.2007.07.005
- Sancar A, Van Gelder RN (2021) Clocks, cancer, and chronochemotherapy. Science 371(6524):eabb0738. https://doi. org/10.1126/science.abb0738
- Buttgereit F, Smolen JS, Coogan AN, Cajochen C (2015) Clocking in: chronobiology in rheumatoid arthritis. Nat Rev Rheumatol 11(6):349–356. https://doi.org/10.1038/nrrheum.2015.31
- Wallace A, Chinn D, Rubin G (2003) Taking simvastatin in the morning compared with in the evening: randomised controlled trial. BMJ 327(7418):788. https://doi.org/10.1136/bmi.327.7418.788
- Zhou J, Wang J, Zhang X, Tang Q (2021) New insights into cancer chronotherapies. Front Pharmacol 12(December):741295. https:// doi.org/10.3389/fphar.2021.741295



- Hanke N, Türk D, Selzer D et al (2020) A comprehensive wholebody physiologically based pharmacokinetic drug-drug-gene interaction model of metformin and cimetidine in healthy adults and renally impaired individuals. Clin Pharmacokinet 59(11): 1419–1431. https://doi.org/10.1007/s40262-020-00896-w
- Henriksson E, Huber A-L, Soto EK et al (2017) The liver circadian clock modulates biochemical and physiological responses to metformin. J Biol Rhythms 32(4):345–358. https://doi.org/10. 1177/0748730417710348
- Zhang R, Lahens NF, Ballance HI, Hughes ME, Hogenesch JB (2014) A circadian gene expression atlas in mammals: implications for biology and medicine. Proc Natl Acad Sci U S A 111(45): 16219–16224. https://doi.org/10.1073/pnas.1408886111
- Oda M, Koyanagi S, Tsurudome Y, Kanemitsu T, Matsunaga N, Ohdo S (2014) Renal circadian clock regulates the dosing-time dependency of cisplatin-induced nephrotoxicity in mice. Mol Pharmacol 85(5):715–722. https://doi.org/10.1124/mol.113. 08805
- Wesson LG (1964) Electrolyte excretion in relation to diurnal cycles of renal function. Medicine (Baltimore) 43(5):547–592. https://doi.org/10.1097/00005792-196409000-00002
- van Acker BAC, Koomen GCM, Koopman MG, Krediet RT, Arisz L (1992) Discrepancy between circadian rhythms of inulin and creatinine clearance. J Lab Clin Med 120(3):400–410
- Koopman MG, Koomen GCM, Krediet RT, de Moor EA, Hoek FJ, Arisz L (1989) Circadian rhythm of glomerular filtration rate in normal individuals. Clin Sci 77(1):105–111. https://doi.org/10. 1042/cs0770105
- Merck (2022) Glucophage® 500 mg/- 850 mg/- 1000 mg Filmtabletten. Fachinformation. https://www.fachinfo.de/pdf/ 000959. Accessed 30 May 2022
- van Rongen A, Kervezee L, Brill M et al (2015) Population pharmacokinetic model characterizing 24-hour variation in the pharmacokinetics of oral and intravenous midazolam in healthy volunteers.
 CPT Pharmacometrics Syst Pharmacol 4(8):454–464. https://doi.org/10.1002/pss4.12007
- Peng HT, Bouak F, Vartanian O, Cheung B (2013) A physiologically based pharmacokinetics model for melatonin - effects of light and routes of administration. Int J Pharm 458(1):156–168. https:// doi.org/10.1016/j.ijpharm.2013.09.033
- Lott D, Lehr T, Dingemanse J, Krause A (2018) Modeling tolerance development for the effect on heart rate of the selective SIP 1 receptor modulator ponesimod. Clin Pharmacol Ther 103(6): 1083–1092. https://doi.org/10.1002/cnt.877
- Ansermet C, Centeno G, Nikolaeva S, Maillard MP, Pradervand S, Firsov D (2019) The intrinsic circadian clock in podocytes controls glomerular filtration rate. Sci Rep 9(1):1–9. https://doi.org/10.1038/ s41598-019-52682-9
- Wuerzner G, Firsov D, Bonny O (2014) Circadian glomerular function: from physiology to molecular and therapeutical aspects. Nephrol Dial Transplant 29(8):1475–1480. https://doi.org/10. 1093/ndt/eff525
- Mure LS, Le HD, Benegiamo G et al (2018) Diurnal transcriptome atlas of a primate across major neural and peripheral tissues. Science 359(6381):eaao0318. https://doi.org/10.1126/science. aao0318

- Sambol NC, Brookes LG, Chiang J et al (1996) Food intake and dosage level, but not tablet vs solution dosage form, affect the absorption of metformin HCl in man. Br J Clin Pharmacol 42(4): 510–512. https://doi.org/10.1111/j.1365-2125.1996.tb00017.x
- Desai D, Wong B, Huang Y et al (2014) Surfactant-mediated dissolution of metformin hydrochloride tablets: wetting effects versus ion pairs diffusivity. J Pharm Sci 103(3):920–926. https://doi.org/10.1002/jps.23852
- Vidon N, Chaussade S, Noel M, Franchisseur C, Huchet B, Bemier JJ (1988) Metformin in the digestive tract. Diabetes Res Clin Pract 4(3):223–229. https://doi.org/10.1016/s0168-8227(88)80022-6
- Mohandas R, Douma LG, Scindia Y, Gumz ML (2022) Circadian rhythms and renal pathophysiology. J Clin Invest 132(3):e148277. https://doi.org/10.1172/JC1148277
- Stage TB, Wellhagen G, Christensen MMH, Guiastrennec B, Brøsen K, Kjellsson MC (2019) Using a semi-mechanistic model to identify the main sources of variability of metformin pharmacokinetics. Basic Clin Pharmacol Toxicol 124(1):105–114. https:// doi.org/10.1111/bcpt.13139
- Duong JK, Kumar SS, Kirkpatrick CM et al (2013) Population pharmacokinetics of metformin in healthy subjects and patients with type 2 diabetes mellitus: simulation of doses according to renal function. Clin Pharmacokinet 52(5):373–384. https://doi.org/10. 1007/s40262-013-0046-9
- Kervezee L, Kosmadopoulos A, Boivin DB (2020) Metabolic and cardiovascular consequences of shift work: the role of circadian disruption and sleep disturbances. Eur J Neurosci 51(1):396–412. https://doi.org/10.1111/ein.14216
- Vetter C, Devore EE, Ramin CA, Speizer FE, Willett WC, Schemhammer ES (2015) Mismatch of sleep and work timing and risk of type 2 diabetes. Diabetes Care 38(9):1707–1713. https://doi.org/10.2337/dc15-0302
- Mason IC, Qian J, Adler GK, Scheer FAJL (2020) Impact of circadian disruption on glucose metabolism: implications for type 2 diabetes. Diabetologia 63(3):462–472. https://doi.org/10.1007/ s00125_019_05059_6
- Peng X, Fan R, Xie L et al (2022) A growing link between circadian rhythms, type 2 diabetes mellitus and alzheimer's disease. Int J Mol Sci 23(1):504. https://doi.org/10.3390/ijms23010504
- Thomas AP, Hoang J, Vongbunyong K, Nguyen A, Rakshit K, Matveyenko AV (2016) Administration of melatonin and metformin prevents deleterious effects of circadian disruption and obesity in male rats. Endocrinology 157(12):4720–4731. https://doi.org/10. 1210/en.2016-1309
- Boehringer Ingelheim Pharma GmbH & Co. KG (2014) Bioavailability of BI 1356 BS and metformin after coadministration compared to the bioavailability of BI 1356 BS alone and metformin alone in healthy male volunteers. ClinicalTrials.gov Identifier: NCT02183506. National Library of Medicine, Bethesda MD; https://clinicaltrials.gov/ct2/show/NCT02183506. Accessed 13 Sep 2022

Publisher's note Springer Nature remains neutral with regard to jurisdictional claims in published maps and institutional affiliations.



4.3 Publication III: Alternative Treatment Regimens With the PCSK9 Inhibitors Alirocumab and Evolocumab: A Pharmacokinetic and-Pharmacodynamic Modeling Approach (3).



Alternative Treatment Regimens With the PCSK9 Inhibitors Alirocumab and Evolocumab: A Pharmacokinetic and Pharmacodynamic Modeling Approach

The Journal of Clinical Pharmacology 2017, 57(7) 846–854 © 2017, The American College of Clinical Pharmacology DOI: 10.1002/jcph.866

Nina Scherer¹, Christiane Dings¹, Michael Böhm, MD², Ulrich Laufs, MD², and Thorsten Lehr, PhD¹

Abstract

Alirocumab and evolocumab are 2 human monoclonal antibodies that inhibit the proprotein convertase subtilisin/kexin type 9 (PCSK9). These antibodies can potently lower low-density lipoprotein cholesterol (LDLc) serum concentrations. The aims of this analysis were to develop a pharmacokinetic (PK) and pharmacodynamic (PD) model for both antibodies, to simulate and investigate different dosage and application regimens, and finally, to note the effects on LDLc levels. Alirocumab was clinically studied and approved with 2 doses, 75 and 150 mg every 2 weeks (Q2W), whereas evolocumab was tested and approved with 2 dosing intervals, 140 mg Q2W and 420 mg Q4W. Data were digitized from published studies describing alirocumab and evolocumab PK, as well as LDLc levels in humans for various single and multiple doses. Alirocumab dosages ranged between 75 and 300 mg and evolocumab from 7 to 420 mg. The analysis was performed using a nonlinear mixed-effects modeling technique. A 2-compartment model with first-order absorption and saturable elimination described the PK of both antibodies best. LDLc levels were described by a turnover model with zero-order synthesis rate decreased by the antibodies and a first-order degradation rate that was increased by the antibodies. Simulations show a comparable effectiveness for alirocumab 75 mg Q2W and 150 mg Q3W as well as evolucmab 140 mg Q2W and 420 mg Q5W, respectively. This is the first PK/PD model describing the link between alirocumab and evolocumab PK and LDLc concentrations. The model may serve as an important tool to simulate different dosage regimens in order to optimize therapy.

Keywords

alirocumab, evolocumab, PCSK9, PK/PD modeling, NONMEM, simulation

Epidemiologic and genetic evidence shows that low-density lipoprotein cholesterol (LDLc) serum concentration is an important modifiable risk factor for cardiovascular diseases (CVD). Large clinical trials with LDLc-lowering medications, such as statins, confirmed that LDLc reduction potently reduces cardiovascular morbidity and mortality. Statins are recommended as the first line of therapy for the prevention of CVD. However, many high-risk patients do not attain the recommended LDLc levels under treatment with statins. Especially for patients with statin intolerance or familial hyperlipidemia, there is a need for new therapeutic strategies to lower LDLc levels.

One recently discovered target is proprotein convertase subtilisin/kexin type 9 (PCSK9). In the absence of PCSK9, circulating LDLc binds to the LDLc receptor (LDLR) on the surface of hepatocytes. In turn, the formed LDLR-LDLc complex is internalized by endocytosis. LDLc is degraded in lysosomes while the LDLR is recycled and moved back to the cell surface. If present, PCSK9 binds to LDLRs on the surface of hepatocytes, and subsequently the LDLR-PCSK9-LDLc complex occurs and is internalized.

PCSK9-bound LDLRs are marked for intracellular degradation, leading to a reduced number of LDLRs on hepatocytes. As a consequence, LDLc concentrations increase.⁷

Alirocumab and evolocumab are 2 fully humanized monoclonal antibodies that bind selectively and with high affinity to PCSK9, preventing it from binding to the LDLR. Therefore, the number of available LDLRs on hepatocytes is increased, and in turn, more LDLc can be removed from the circulation. Since 2015, both antibodies have been approved by the European

Klinische Pharmazie, Universität des Saarlandes, Saarbrücken, Germany ² Klinik für Innere Medizin III, Kardiologie, Angiologie und Internistische Intensivmedizin, Universitätsklinikum des Saarlandes, Homburg/Saar, Germany

Submitted for publication 24 August 2016; accepted 5 December 2016.

Corresponding Author:

Thorsten Lehr, PhD, Junior Professor of Clinical Pharmacy, Saarland University, Campus C2 2, 66123 Saarbrücken, Germany Email: thorsten.lehr@mx.uni-saarland.de

There are no disclosures, conflicts of interests, or use of a professional medical writing company.

Scherer et al 847

Medicines Agency and the US Food and Drug Administration for the treatment of patients with elevated cholesterol levels.^{8–11} The recommended dosing regimen for alirocumab is 75 mg administered every 2 weeks (Q2W). If the LDLc response is insufficient, the dose may be increased to the maximum dose of 150 mg Q2W. For evolocumab, the recommended dosing regimen is 140 mg Q2W or 420 mg Q4W. These new first-in-class medications were shown to be highly effective in large randomized clinical trials. LDLc reductions of 62% (alirocumab) and 61% (evolocumab) were observed after subcutaneous (sc) administration of 150 mg Q2W alirocumab or 140 mg Q2W or 420 mg Q4W evolocumab.^{12,13}

These studies showed that the occurrence of cardio-vascular safety events within 1 year was significantly reduced with alirocumab and evolocumab treatment compared with standard therapy. 12,13

The PK of alirocumab and evolocumab is mainly driven by their characteristics as monoclonal human antibodies. 14,15 The absolute bioavailability (F) after sc administration is 85% for alirocumab and 72% for evolocumab. 14,15 The volume of distribution is 3.0-3.8 L for alirocumab and 3.3 L for evolocumab, 14,15 indicating a limited tissue distribution. Both antibodies showed at least 2 different elimination pathways, ie, proteolytic and target-mediated elimination. The relative contributions of these different elimination pathways to the overall elimination process are dependent on the drug concentration:^{14,15} The proteolytic elimination is relevant only at high antibody concentrations when the target-mediated pathway is saturated, whereas the nonlinear target-mediated elimination is more prominent in the low concentration range. The half-lives range from 17 to 20 days for alirocumab and from 11 to 17 days for evolocumab and are reduced in patients with statin coadministration (eg, about 12 days for alirocumab). 14,15 Statins induce PCSK9 expression. 16-18 resulting in increased target-mediated elimination of the antibodies.¹⁴ Thus, the area under the plasma concentration-time curve of both antibodies is reduced under statin comedication.15

Even though these new treatment options are highly effective and provide an excellent opportunity for the treatment of elevated cholesterol levels, very little is known about their quantitative PK/PD relationship. Some patients show an above-average response to PCSK9 inhibitors. However, the long-term safety of very low LDLc levels (eg, below 30 mg/dL) is not yet fully understood. Furthermore, the treatment costs are very high. As a consequence, alternative dosing regimens may be valuable to individualize treatment and to reduce the treatment cost.

The aims of this analysis were to describe and predict the PK as well as the PD of both antibodies.

In addition, the resulting PK/PD model was used to investigate different dosing regimens that were not clinically tested and to compare these to the recommended regimens.

Methods

Data Set

Serum concentrations of alirocumab and evolocumab and LDLc levels, recorded as the change from baseline, were derived from mean curves of clinical trial data.

For alirocumab, data from 6 studies were digitized and used for model development: 4 phase 1 studies investigated the PK after single-dose administration. Mean serum concentrations for doses of 50 mg, 75 mg, 100 mg, 150 mg, 200 mg, and 250 mg were reported. ¹⁹ The phase 2 study DF111565 investigated the PD after multiple dosings of 50 mg, 100 mg, and 150 mg Q2W as well as 200 mg and 300 mg Q4W. ¹⁹ Stein et al reported the PD of alirocumab after single-dose administration of 50 mg, 100 mg, 150 mg, and 250 mg. ²⁰ Lunven et al examined the PK and PD of alirocumab after single sc administration at 3 different injection sites in healthy volunteers. ²¹

For evolocumab, data from 6 studies were used for model development. Dias et al reported 2 phase 1 studies that investigated the PK and PD of evolocumab: 21 mg and 420 mg were administered intravenously, and doses between 7 mg and 420 mg were administered sc to healthy subjects (Study 20080397). ^{22,23} Furthermore, hypercholesterolemic adults received 14 or 35 mg weekly, 140 or 280 mg Q2W, or 420 mg Q4W. ^{22,23} Study 20080398 investigated the PK of evolocumab following multiple dosing of 140 mg Q2W and 420 mg Q4W sc in subjects with hyperlipidemia on top of stable doses of statins. ²² Phase 2 dose-finding studies investigated the PD after multiple dosing of 70 mg Q2W, 140 mg Q2W, 280 mg Q4W, and 420 mg Q4W administered to patients with elevated LDLc levels. ¹⁴

Data Analysis

Data analysis and simulations were performed using nonlinear mixed-effects modeling techniques implemented in the software NONMEM (V 7.3, ICON Development Solutions, Ellicott City, Maryland) with the graphical user interface Pirana (V 2.9.2). To consider the different study sizes for each mean curve, the random and residual errors were weighted by the inverse square root of the number of subjects. ^{24,25} Throughout the analysis, first-order conditional estimation with INTERACTION was used, and interstudy variability was modeled using exponential random-effects models. Model selection was based on several criteria such as the changes in the NONMEM objective function value, ²⁶ goodness-of-fit plots, and the precision with which model parameters were

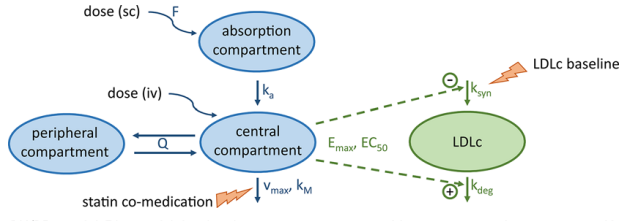


Figure 1. Schematic of the PK/PD model. F, bioavailability; k_a , absorption rate constant; V_{max} , maximum elimination rate; K_m , antibody concentration at half-maximum elimination; Q, intercompartmental clearance; EC_{50} , drug concentration at half-maximum drug effect; E_{max} , maximum drug effect on k_{syn} and k_{deg} ; k_{syn} , zero-order LDLc synthesis rate constant; k_{deg} , first-order LDLc degradation rate constant; LDLc, low-density lipoprotein cholesterol; sc, subcutant source is intervenous.

estimated.²⁷ A reduction in the objective function value by 3.84 points was considered a criterion of superiority comparing 2 nested models (X^2 , P < .05, 1 degree of freedom).²⁸ Graphical visualization of NONMEM results was performed with R (V 3.2.0) and the graphical user interface RStudio (V 0.98.1103). For digitization, the software GetData Graph Digitizer (V 2.26) was used.

The model-building process was performed stepwise. First the PK model was developed for both antibodies For each antibody, 1-, 2- and 3-compartment models as well as target-mediated drug-disposition models were tested. Different absorption and elimination kinetics (zero-order, first-order, Michaelis-Menten) were investigated. The final PK model was parameterized in terms of volumes of distribution and absorption and elimination parameters. Second, the PK model parameters were fixed to develop the PK/PD model. Different linear, exponential, Emax, and turnover models were evaluated to describe the LDLc change over time. Direct links to plasma concentration and effect compartment models were explored. LDLc baseline level as well as statin comedication were considered as covariates.

Internal model evaluation was performed by visual predictive checks based on 5000 simulations using the final PK/PD model. Medians and 90% confidence intervals of the predictions were plotted and overlaid with the observed data.

External model evaluation was performed by comparing model-predicted median LDLc levels with long-term data on both antibodies from studies reported by Robinson et al and Sabatine et al. ^{12,13} In both studies patients were cotreated with statins.

Simulations

To investigate alternative treatment regimens with equivalent effectiveness in comparison to the standard dosing recommendations, steady-state simulations with and without statin comedication were performed based on the final model including interstudy and residual variability. Each simulation consisted of 2000 individuals. For alirocumab the recommended dosing regimen is 75 mg Q2W or 150 mg Q2W if a change from baseline of more than 60% is required. Simulations for the 2 recommended doses were performed using dosing intervals of 2, 3, and 4 weeks. For evolocumab, 2 equivalent dosing regimens are recommended: 140 mg Q2W and 420 mg Q4W. Simulations with administration of 140 mg evolocumab every 2, 3, and 4 weeks as well as 420 mg every 4, 5, and 6 weeks were performed.

Additionally, simulations starting from different LDLc baselines between 100 mg/dL and 240 mg/dL were performed to investigate the optimal dosing regimen aiming to attain specific goals in LDLc reduction.

Results

Data Set

Data from 12 different studies were pooled for analysis (Supplemental Table S1). Dose ranges from 50 to 300 mg and 7 to 420 mg were covered for alirocumab and evolocumab, respectively. The final data set comprised 103 and 100 mean plasma concentrations and 86 and 209 mean LDLc measurements for alirocumab and evolocumab, respectively. The mean LDLc baseline levels were available for each study. The median LDLc baseline levels across the studies were 128.2 mg/dL (range 117.2-142.2 mg/dL) and 120.5 mg/dL (range 100-134 mg/dL) for alirocumab and evolocumab, respectively.

PK/PD Model

Plasma concentration-time profiles of alirocumab and evolocumab were best described by a 2-compartment model with first-order absorption and a saturable Michaelis-Menten elimination process (Figure 1). Statin comedication increased the maximum elimination rate (V_{max}) of alirocumab and evolocumab by 1.25- and 1.19-fold, respectively. A turnover

Scherer et al 849

Table 1. Parameter Estimates From the PK/PD Model for Alirocumab and Evolocumab

Parameter	Value, R	SE (%)	
	Alirocumab	Evolocumab	Description
Fixed effects			
k _a , day-1	0.262 (30)	0.302 (7)	First-order absorption rate constant
V ₂ , L	2.70 (37)	3.72 (4)	Volume of distribution of central compartment
V ₃ , L	2.64 (19)	3.6 (19)	Volume of distribution of peripheral compartment
$Q, L day^{-1}$	1.29 (6)	0.167 (18)	Intercompartmental clearance
F, %	85.0 (fixed)	84.9 (4)	Bioavailability
V _{max} , mg day⁻¹	25.2 (33)	14.3 (14)	Maximum elimination rate
K _m , mg L ⁻¹	41.6 (37)	14.3 (31)	Antibody conc at half-maximum elimination
effect _{statin}	1.25 (4)	1.19 (4)	Proportional effect of statin comedication on V _{max}
k_{deg} , day^{-1}	0.138 (12)	0.229 (9)	First-order LDLc degradation rate constant
EC ₅₀ , mg L ⁻¹	7.99 (9)	4.45 (21)	Drug conc at half-maximum drug effect
E _{max}	0.784 (4)	0.610 (7)	Maximum drug effect on k _{syn} and k _{deg}
Random effects ^a			- /
ω ² E _{max} , CV%	8.45 (21)	34.5 (23)	Variance of interunit random effects on Emax
Residual effects ^a	, ,	. ,	
PRV, %	11.0 (13)	4.25 (14)	Proportional residual variability (PK model)
ARV (SD)	0.00065 (62)	0.358 (47)	Additive residual variability (PK model)
ARV (SD)	17.5 (26)	53.3 (20)	Additive residual variability (PD model)

RSE, residual standard error

^aAll unit-level random and residual effects for arm data are weighted by $n: \omega_a^1 = \omega_{a,\text{raw}}^2 / n$ and $\sigma_b^2 = \sigma_{b,\text{raw}}^2 / n$, where ω_a^2 is the unit-level variance for parameter σ and σ_b^2 is the residual variance for σ for median unit size (n); $\omega_{a,\text{raw}}^2$ is the unweighted unit-level variance for parameter σ , and $\sigma_{b,\text{raw}}^2$ is the unweighted residual variance for b that NONMEM reports. Random effects and proportional residual variance for σ that σ has σ and σ . The median σ values for the alirocumab PK and PD data set are 8 and 20, respectively; the median σ for both the evolocumab data sets is 6.

model with zero-order synthesis and first-order degradation rate best described LDLc levels over time. Higher drug concentrations in the central compartments of alirocumab and evolocumab were found to decrease the synthesis rate and to increase the elimination rate of LDLc mediated by an $E_{\rm max}$ model

The PK/PD model parameter estimates are presented in Table 1. All model parameters were precisely estimated with residual standard errors ≤50%. A small interstudy variability on the maximum drug effect was identified for alirocumab (%CV 8.45) and evolocumab (%CV 34.5). Observed vs model-predicted antibody plasma concentration and LDLc changes (goodness-of-fit plots, Supplemental Figure S1) are randomly distributed around the line of identity, indicating good descriptive properties of the final PK/PD model. The visual predictive checks (Figure 2, Supplemental Figures S2 and S3) demonstrate good descriptive performance with neither under- nor overestimation.

For evolocumab an sc bioavailability of 84.9% was estimated. For alirocumab no intravenous data were available, and the sc bioavailability was fixed to the literature value of 85%. 15 The sum of the central and peripheral volumes of distribution was estimated as 7.32 L for evolocumab and 5.34 L for alirocumab. The maximum drug effect was estimated in the same range

for both compounds (evolocumab, 0.610; alirocumab, 0.784).

External model evaluation showed a good predictive performance. The evaluation study¹² for alirocumab included 2341 patients at high risk for cardiovascular events. The patients were randomly assigned in a 2:1 ratio to receive either alirocumab (150 mg Q2W) or placebo. All patients received statin comedication and were monitored for 78 weeks. The observed LDLc change from baseline after 78 weeks of treatment with 150 mg Q2W was –58% excluding nonadherent patients.¹² The model predicted a median change of –67 0% after 78 weeks

In the evolocumab evaluation study, ¹³ 4465 patients were randomly assigned in a 2:1 ratio to receive either evolocumab (140 mg Q2W or 420 mg Q4W) or standard therapy to investigate long-term data on safety, side-effect profile, and LDLc reduction. A total of 2976 patients received evolocumab plus standard therapy, and the median follow-up was 11.1 months. The observed LDLc change from baseline following administration of 140 mg evolocumab Q2W for 12 weeks was –61%. A corresponding reduction of –58.4% was observed following administration of 420 mg evolocumab for 48 weeks. ¹³ The model-predicted LDLc changes from baseline at steady-state+ doses of 140 mg Q2W and 420 mg Q4W were –59.1% and –67.0%, respectively.

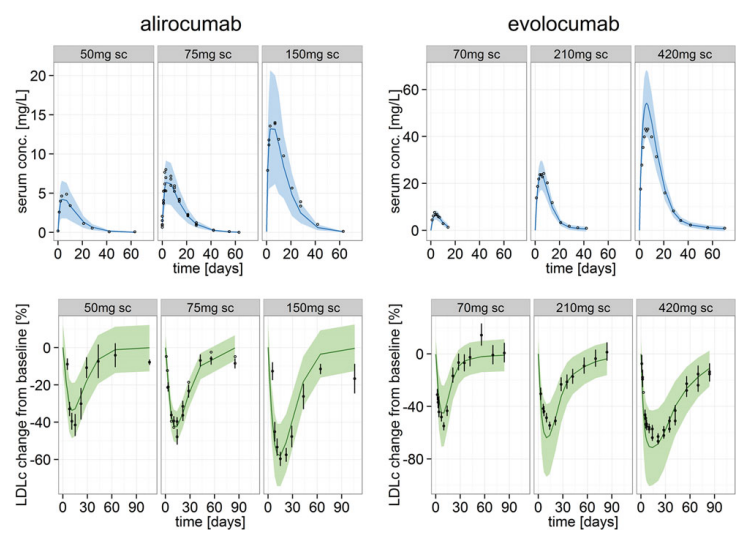


Figure 2. Selected visual predictive checks. Observed and model-predicted drug concentrations (upper) and LDLc change from baseline (lower) following administration of alirocumab (left) and evolocumab (right). Observations (circles) and \pm 1 SE (bars) are shown. Lines and bands indicate the predicted median and 90% confidence interval of the predictions of 5000 individuals. LDLc, low-density lipoprotein cholesterol; sc, subcutaneous.

Simulation for Different Dosing Regimes

The final PK/PD model was used to simulate different dosing regimens under steady-state conditions to investigate alternative treatment regimens. Median LDLc change from baseline and median LDLc profiles with and without statin comedication are presented in Figure 3. The simulations revealed a comparable LDLc change for 75 mg alirocumab Q2W and 150 mg Q3W as well as for 140 mg evolocumab Q2W and 420 mg Q5W, respectively. Due to the decreased PCSK9 antibody exposure under statin comedication, ^{16–18} a smaller LDLc change from baseline is achieved for patients with statin comedication compared to patients without statin comedication.

To visualize the effect of different LDLc baseline levels on the levels reached at steady-state, the recommended dosing regimens were simulated for LDLc baseline levels between 100 mg/dL and 240 mg/dL without statin comedication. Assuming a baseline LDLc level of 240 mg/dL, the administration of 75 mg alirocumab Q2W results in an LDLc level of 106 mg/dL; a baseline LDLc level of 120 mg/dL results in an LDLc level of 52.9 mg/dL. For 150 mg alirocumab Q2W, the resulted LDLc levels are 76.3 mg/dL (baseline 240 mg/dL) or 38.1 mg/dL (baseline 120 mg/dL). After administration of 140 mg evolocumab Q2W, the LDLc level reaches 77.1 mg/dL (baseline 240 mg/dL) or 38.5 mg/dL (baseline 120 mg/dL), and for 420 mg Q4W, 123 mg/dL (baseline 240 mg/dL) or

61.6 mg/dL (baseline 120 mg/dL). The simulated LDLc concentration-time profiles are visualized in Figure 4.

Discussion

This analysis presents the first PK/PD model for the novel PCSK9-targeting antibodies alirocumab and evolocumab. The model allows assessing the LDLclowering effects of both antibodies when administered with different dosing regimens.

A 2-compartment model adequately described the PK of each antibody, which is in accordance with literature models for monoclonal antibodies.^{29–31} The volume of distribution in the central compartment was estimated as 3.72 L and 2.70 L for evolocumab and alirocumab, respectively, approximating the plasma volume of 4 L. The saturable clearance pathway is assumed to represent a target-mediated pathway of elimination, which is frequently observed for monoclonal antibodies.31 The low number of PK samples collected during the elimination phase made it difficult to properly estimate the parameters of a target-mediated drug-disposition model. In turn, Michaelis-Menten kinetics was used to capture the nonlinearity in the antibody elimination. A published PK/PD model of another PCSK9-targeting antibody described the elimination with a parallel first-order and Michaelis-Menten kinetic,³² supporting the hypothesis that the target (ie, PCSK9) impacts the elimination of the drug.

85 I

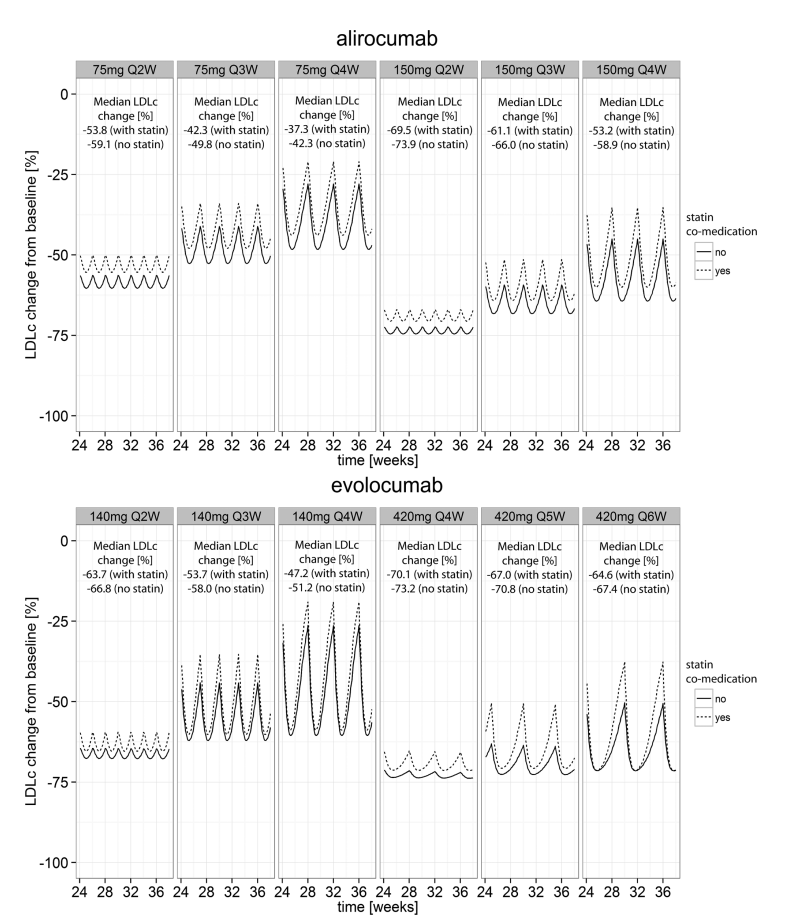


Figure 3. Predicted LDLc change from baseline using the final PK/PD model for different dosing regimens for alirocumab (upper) and evolocumab (lower). The lines indicate the predicted median of the predictions in 2000 individuals without statin comedication (solid line) and with statin comedication (dashed line). LDLc, low-density lipoprotein cholesterol; PK/PD, pharmacokinetic/pharmacodynamic; QnW, dosing once every n weeks.

Based on the mechanism of action of PCSK9 antibodies, an indirect response model was used to link the antibody exposure to the LDLc level. The binding of the antibodies to PCSK9 results in an increased uptake of LDLc into liver cells. Therefore, LDLc degradation increases due to the higher availability of LDLRs on the cell membrane. Additionally, via negative feedback, elevated intracellular cholesterol levels result in a decreased LDLc synthesis.³³

Our model was developed using mean curves digitized from literature rather than individual patients' profiles, which were not accessible. Due to the lack of individual data, the influence of patient-specific factors, ie, covariates such as age, weight, sex, and organ

function, on the PK or PD could not be determined. Thus, our model is not able to predict individual LDLc levels and can only reflect the variability between different studies. However, 2 important covariates, statin comedication and LDLc baseline levels, were available for each study and could be successfully integrated into the model. Comedication with statins significantly decreases the exposure to both PCSK9 antibodies. This is triggered by the statin-induced increased expression of PCSK9 $^{16-18}$ resulting in an increased target-mediated elimination of the antibodies. 14 In our model, this effect was best described by 1.25- and 1.19-fold increases in $V_{\rm max}$ of the elimination of alirocumab and evolocumab, respectively. The results are in line with

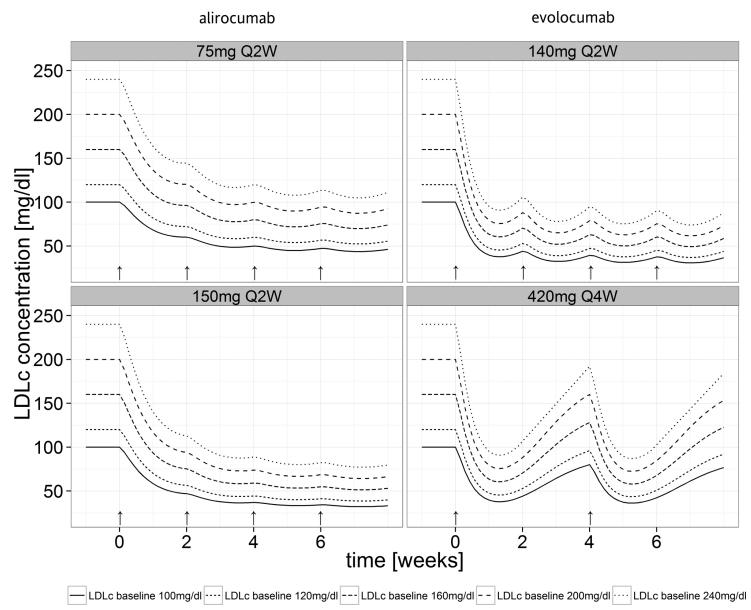


Figure 4. Model predictions for the recommended dosing regimens for subjects with different baseline levels for alirocumab (left) and evolocumab (right). The arrows indicate the dosing of 75 mg or 150 mg alirocumab or 140 mg or 420 mg evolocumab, respectively. Lines indicate the predicted median of 2000 individuals. LDLc, low-density lipoprotein cholesterol; QnW, dosing once every n weeks.

literature reports in which the AUC of alirocumab was reduced by 39% and the clearance of evolocumab was increased by 20% under statin comedication. 14,15 Simulations revealed that the statin comedication also has a marked effect on the LDLc change from baseline. Thus, patients under statin comedication achieved a smaller reduction of LDLc levels compared to patients without statin comedication (Figure 3). The implemented statin effect predicted by our model reflects a median effect of low-, moderate-, and high-dose statin therapy and describes the change in the PK of the antibodies under statin steady-state conditions. The additional PD effects of statins or other cholesterol-lowering drugs are not incorporated in the model because the data did not provide the necessary information and should be integrated in a future extension of the presented

LDLc baseline levels were identified as another significant covariate to predict the absolute LDLc reduction in patients (Figure 4), whereas the percentage change from baseline is independent from the baseline levels. The recommended LDLc target levels are idependent on different risk factors of the patients. In a high-risk patient, the recommended LDLc levels should be below 100 mg/dL. Model simulations indicated that a baseline level of 240 mg/dL requires the

administration of 150 mg alirocumab Q2W to reach the desired LDLc level, whereas 75 mg Q2W was estimated as sufficient for a baseline level of 200 mg/dL and below.

Overall, the final PK/PD models showed a good descriptive performance over a wide dose range. Even more important, our models showed a good predictive performance for the outcome of 2 long-term clinical studies that were not used for model development. All patients in these studies received treatment with statins at the maximum tolerated dose with or without other lipid-lowering therapy. For alirocumab, the model slightly overpredicted the LDLc change from baseline (-67.0%) compared to the observed outcome (-58%). For evolocumab, the model also slightly overpredicted the outcome (observed -58%, predicted -59.1% for 140 mg Q2W; -67.0% for 420 mg Q4W). This slight difference may have been caused by noncompliant patients in the study population. As no information on the compliance was provided for the evolocumab study population, we assumed a compliance of 100% for the simulations. This assumption may not reflect reality, especially as an increase in the observed LDLc levels in the statin-treated control group indicated the existence of nonadherent patients. Furthermore, all patients in the evaluation study received high-dose therapy with Scherer et al 853

statins. As discussed previously, we did not distinguish among high-, moderate-, and low-dose statin comedication during model development. Therefore, it is reasonable that the effect of high-dose statin comedication on the PK of both antibodies is underestimated.

The PK/PD model allowed the prediction of alternative dosing regimens. Simulations confirmed that dosing regimens for alirocumab of 150 mg Q2W should be used if a decrease of LDLc levels of more than 60% is required. The simulations allowed us to choose individualized dosing and application strategies. For example, the model indicates that alirocumab 150 mg Q3W is equivalent to 75 mg Q2W, pointing out a potential alternative treatment regimen if less-frequent dosing is favored. For evolocumab, the simulations show that 420 mg Q5W may be similarly effective compared to 140 mg Q2W.

Conclusion

To conclude, the PK/PD models showed excellent descriptive and predictive performance. Alternative dosing regimens for alirocumab and evolocumab may present very important opportunities to adjust therapies according to individual responses, the baseline LDLc, and the desired target LDLc. In addition, alternative application strategies could reduce treatment costs. Finally, the presented model may offer a valuable tool for future PK/PD research on PCSK9-targeting antibodies.

References

- Castelli WP, Anderson K, Wilson PWF, Levy D. Lipids and risk of coronary heart disease. The Framingham Study. Ann Epidemiol. 1992;2(1/2):23–28.
- Collins R, Armitage J, Parish S, Peter S, Peto R. MRC/BHF Heart Protection Study of cholesterol lowering with simvastatin in 20,536 high-risk individuals: a randomised placebo-controlled trial. *Lancet*. 2002;360(6):7–22.
- Piepoli MF, Hoes A, Agewall S, et al. European guidelines on cardiovascular disease prevention in clinical practice. Eur Heart J. 2016;37(29):2315–2381.
- Jones PH, Nair R, Thakker KM. Prevalence of dyslipidemia and lipid goal attainment in statin-treated subjects from 3 data sources: a retrospective analysis. J Am Heart Assoc. 2012;1(6):1–11.
- Vallejo-Vaz AJ, Seshasai SRK, Cole D, et al. Familial hypercholesterolaemia: a global call to arms. *Atherosclerosis*. 2015;243(1):257–259.
- Natarajan P, Kathiresan S. PCSK9 inhibitors. Cell. 2016; 165(5):1037.
- Urban D, Pöss J, Böhm M, Laufs U. Targeting the proprotein convertase subtilisin/kexin type 9 for the treatment of dyslipidemia and atherosclerosis. J Am Coll Cardiol. 2013;62(16):1401– 1408.
- FDA product information. Praluent (alirocumab): United States product information. 2015. http://www.accessdata. fda.gov/drugsatfda_docs/label/2015/125559Orig1s000lbledt.pdf. Updated July 2015.

 FDA Product Information (revised: 8/2015). Repatha (evolocumab): United States product information. 2015. http:// www.accessdata.fda.gov/drugsatfda_docs/label/2015/125522 s000lbl.pdf.

- European Medicines Agency. European public assessment report for Repatha (evolocumab). 2015. http://www.ema.europa .eu/ema/index.jsp?curl=pages/medicines/human/medicines/ 003766/human_med_001890.jsp&mid=WC0b01ac058001d124. Undated August 2015.
- European Medicines Agency. European public assessment report for Praluent (alirocumab), 2015. http://www.ema.europa.eu/ ema/index.jsp?curl=pages/medicines/human/medicines/003882/ human_med_001915.jsp&mid=WC0b01ac058001d124. Updated September 2015.
- Robinson JG, Farnier M, Krempf M, et al. Efficacy and safety of alirocumab in reducing lipids and cardiovascular events. N Engl J Med. 2015;372(16):1489–1499.
- Sabatine MS, Giugliano RP, Wiviott SD, et al. Efficacy and safety of evolocumab in reducing lipids and cardiovascular events. N Engl J Med. 2015;372(16):1500–1509.
- Amgen Inc. EMDAC meeting briefing document (Evolocumab): background information for Endocrinologic and Metabolic Drugs Advisory Committee. 2015. http://www.fda.gov/downloads/AdvisoryCommittees/CommitteesMeeting Materials/Drugs/EndocrinologicandMetabolicDrugsAdvisory Committee/UCM450072.pdf.
- Smith JP. Food and Drug Administration Center for Drug Evaluation and Research. Briefing document: Praluent (alirocumab) injection. The Endocrinologic and Metabolic Drugs Advisory Committee Meeting. 2015. http://www.fda. gov/downloads/Advisory/Committees/CommitteesMeeting Materials/Drugs/EndocrinologicandMetabolicDrugsAdvisory Committee/UCM449865.pdf.
- Mayne J, Dewpura T, Raymond A, et al. Plasma PCSK9 levels are significantly modified by statins and fibrates in humans. *Lipids Health Dis*. 2008;7(1):22.
- Welder G, Zineh I, Pacanowski MA, Troutt JS, Cao G, Konrad RJ. High-dose atorvastatin causes a rapid sustained increase in human serum PCSK9 and disrupts its correlation with LDL cholesterol. J Lipid Res. 2010;51(9):2714–2721.
- Careskey HE, Davis RA, Alborn WE, Troutt JS, Cao G, Konrad RJ. Atorvastatin increases human serum levels of proprotein convertase subtilisin/kexin type 9. J Lipid Res. 2008;49(2):394-209
- Chung SM, Earp J, Vaidyanathan J, Mehrotra N. Center for Drug Evaluation and Research: Clinical Pharmacology and Biopharmaceutics Review (Praluent- Alirocumab) (Application Number 125559Orig1s000). 2014. http://www.accessdata.fda .gov/drugsatfda_docs/nda/2015/125559Orig1s000ClinPharmR. pdf.
- Stein EA, Mellis S, Yancopoulos GD, et al. Effect of a monoclonal antibody to PCSK9 on LDL cholesterol. J Chem Inf Model. 2012;366(25):1108–1118.
- Lunven C, Paehler T, Poitiers F, et al. A randomized study of the relative pharmacokinetics, pharmacodynamics, and safety of alirocumab, a fully human monoclonal antibody to PCSK9, after single subcutaneous administration at three different injection sites in healthy subjects. *Cardiovasc Ther*. 2014;32(6):297– 301.
- Suryanarayana S, Earp J, Mehrotra N, Jaya V. Center for Drug Evaluation and Research: Clinical Pharmacology and Biopharmaceutics Review (Repatha-Evolocumab) (Application Number 125559Orig1s000). 2014. http://www.accessdata.fda. gov/drugsatfda_docs/nda/2015/125522Orig1s000ClinPharmR. pdf.

- 23. Dias CS, Shaywitz AJ, Wasserman SM, et al. Effects of AMG 145 on low-density lipoprotein cholesterol levels: results from 2 randomized, double-blind, placebo-controlled, ascending-dose phase 1 studies in healthy volunteers and hypercholesterolemic subjects on statins. J Am Coll Cardiol. 2012;60(19):1888–1898.
- Ocampo-Pelland AS, Gastonguay MR, French JF, Riggs MM. Model-based meta-analysis for development of a population-pharmacokinetic (PPK) model for vitamin D₃ and its 25OHD₃ metabolite using both individual and arm-level data. *J Pharmacokinet Pharmacodyn*, 2016;43(2):191–206.
- Ahn JE, French JL. Longitudinal aggregate data model-based meta-analysis with NONMEM: approaches to handling within treatment arm correlation. J Pharmacokinet Pharmacodyn. 2010;37(2):179–201.
- Akaike H. A new look at the statistical model identification. IEEE Trans Autom Control. 1974;19(6):716–723.
- Jonsson EN, Karlsson MO. Xpose—an S-PLUS based population pharmacokinetic/pharmacodynamic model building aid for NONMEM. Comput Methods Programs Biomed. 1999;58(1):51–64.
- Beal S, Sheiner L. NONMEM Users Guides. San Francisco: NONMEM Project Group University of California; 1998.
- Fronton L, Pilari S, Huisinga W. Monoclonal antibody disposition: a simplified PBPK model and its implications for the

- derivation and interpretation of classical compartment models. J Pharmacokinet Pharmacodyn. 2014;41(2):87–107.
- Mould DR, Sweeney KR. The pharmacokinetics and pharmacodynamics of monoclonal antibodies—mechanistic modeling applied to drug development. Curr Opin Drug Discov Dev. 2007;10(1):84–96.
- Dirks NL, Meibohm B. Population pharmacokinetics of therapeutic monoclonal antibodies. Clin Pharmacokinet. 2010;49(10):633–659.
- Budha NR, Leabman M, Jin JY, et al. Modeling and simulation to support phase 2 dose selection for RG7652, a fully human monoclonal antibody against proprotein convertase subtilisin/kexin type 9. AAPS J. 2015;17(4):881–890.
- DeBose-Boyd RA. Feedback regulation of cholesterol synthesis. Cell Res. 2008;18(6):609–621.
- Grundy SM, Cleeman JI, Bairey Merz CN, et al. Implications of recent clinical trials for the National Cholesterol Education Program Adult Treatment Panel III guidelines. Circulation. 2004;110(2):227–239.

Supporting Information

Additional Supporting Information may be found in the online version of this article at the publisher's website

5 Discussion and Perspective

This dissertation highlights the potential of pharmacometric modeling, particularly NLME models, to improve the understanding and management of cardiometabolic diseases. By applying advanced quantitative methods to existing clinical and observational data, the three projects presented in this work contribute to the optimization of established therapies, the refinement of clinical biomarkers, and the personalization of treatment strategies. Each project addresses distinct aspects of T2DM and hypercholesterolemia, illustrating the versatility of modeling in solving disease-specific challenges. Collectively, the results underscore the value of pharmacometric modeling in advancing precision medicine, improving therapeutic outcomes, and promoting a more cost-efficient healthcare system.

In the pharmaceutical industry, randomized controlled trials (RCT) remain the gold standard for assessing the efficacy, safety, and pharmacological properties of new drugs under controlled and standardized conditions. However, such trials often fail to capture the variability and complexity of real-world clinical practice (87). The final trial datasets are typically generated to answer predefined questions outlined in the study protocols. Additional exploratory analyses are seldom conducted, partly due to time constraints and competitive pressures associated with drug development and market access in the pharmaceutical industry.

This thesis follows a complementary strategy. All three projects are based on existing datasets and demonstrate how NLME modeling can be used not only to analyze but also to generate and validate hypotheses. In doing so, it extends the scientific value of previously collected data and supports decisions that go beyond the original scope of the clinical trials.

5.1 Modeling as a Tool for Personalization and Optimization

By reanalyzing existing clinical and observational datasets, the three projects presented herein demonstrate how advanced quantitative methods can optimize established therapies, refine biomarker measurements, and personalize treatment strategies.

In Project 1, NLME modeling was applied to correct HbA1c values measured from dried blood spots by adjusting for variability in storage temperature and analysis delay. While the initial objective was to classify patients into subgroups with different rates of disease progression, it became evident that measurement bias due to pre-analytical variation exceeded the expected biological signal. This was particularly problematic in a prediabetic

cohort, where glycemic changes are typically small. A correction model was therefore developed to adjust for these biases, enabling the accurate identification of individual disease trajectories. Although no new biomarkers predictive of rapid progression could be identified, the corrected progression rates correlated well with established clinical risk factors such as waist-to-hip ratio and postprandial glucose levels. This modeling approach significantly improved the validity of HbA1c as a biomarker in this setting and highlights the importance of considering sample handling effects, even for robust matrices like DBS (88). These insights are especially relevant for decentralized studies, resource-limited settings, and the use of real-world data (RWD), where sample standardization is often limited.

In the case of metformin (Project 2), a substance that has been used for many years to treat T2DM, has traditionally not been studied in relation to human circadian rhythms. However, this dissertation demonstrates that modern mathematical modeling approaches can derive valuable insights even from limited and retrospective datasets. While earlier studies may not have accounted for these time-dependent influences, the modeling in this case has made a crucial contribution to filtering out new insights from the available data. These findings not only provide theoretical insights but also have the potential to improve patient care by offering dosing regimens that are better aligned with individual circadian rhythms.

Project 3 applies PK/PD modeling to evaluate flexible dosing regimens for PCSK9 inhibitors. Through simulations of less frequent administration schedules, the study contributes to the evidence that modeling can support cost-effective, adherence-friendly treatment solutions without compromising efficacy.

5.2 Bridging Controlled Trials and Real-World Conditions

A key strength of pharmacometric modeling lies in its ability to integrate and interpret real-world data (RWD). While RCTs provide high internal validity, they often lack generalizability due to strict inclusion criteria and controlled conditions. In contrast, RWD reflects clinical variability in patient heterogeneity inherent in patient behavior, healthcare delivery, and treatment adherence. However, it also presents challenges, including missing data, inconsistencies, and potential bias (87). Project 1 addressed these limitations directly by correcting variability in HbA1c measurements and highlighting the importance of systematic data quality assessment, even within the context of well-structured prospective studies. This underscores the need to critically evaluate and pre-process real-world data before drawing clinical conclusions. By correcting for biases and systematically modeling sources of

variability, this work bridges the gap between controlled trial results and practical clinical application as illustrated by the HbA1c correction model.

Despite its limitations, RWD offer considerable potential. When appropriately modeled, they enable the investigation of treatment effects across diverse patient populations, thereby improving the external validity of clinical findings.

Regulatory frameworks, particularly within the EU, are increasingly supportive of the use of real-world evidence (RWE) in decision-making processes. In this context, the EMA emphasized in its Real-World Evidence Framework to Support EU Regulatory Decision-Making (89) that RWE can be used to support assessments both before and after the authorization of medicinal products. Moreover, targeted EU-level initiatives, such as the DARWIN EU® network, are being implemented to facilitate access to RWD and promote their systematic use in regulatory processes (89).

5.3 Simulation and Decision Support

One of the most impactful applications of pharmacometric modeling is its capacity to simulate clinical scenarios. Simulations allow for the exploration of "what-if" questions under defined assumptions, supporting clinical decision-making in areas where trial data may be limited.

In Project 2, time-dependent variations in metformin pharmacokinetics were investigated, highlighting the potential of chronotherapy. In Project 3, alternative dosing regimens for PCSK9 inhibitors were simulated to assess the potential for less frequent dosing while maintaining LDL reduction.

Such simulations provide a low-risk, data-driven framework for optimizing treatment strategies. One regulatory initiative that exemplifies the increasing institutional support for model-informed decision-making is the MIDD Paired Meeting Program established by the U.S. Food and Drug Administration (FDA). This program provides selected sponsors with the opportunity to engage directly with FDA staff to discuss and refine MID3 approaches during medical product development (90).

5.4 Data Limitations and Justified Simplifications

Pharmacometric models inevitably require simplifications of complex biological systems to ensure tractability, identifiability, and interpretability. However, these simplifications must remain consistent with the model's intended use.

In Project 3, aggregate-level data from published clinical trials required assumptions regarding population variability and model structure. Despite these limitations, the model produced reliable estimates and supported the evaluation of cost-efficient treatment alternatives.

Similarly, in Project 1, pre-analytical error was not ignored but explicitly modeled and corrected, thereby preserving the validity of clinical conclusions. These examples demonstrate how transparent handling of limitations, combined with data-driven refinements, can ensure robust and trustworthy modeling outcomes.

5.5 Outlook: Al and Model Informed Precision Dosing

The integration of artificial intelligence (AI) and machine learning (ML) into pharmacometric modeling opens new possibilities for improving individualized therapy for the future. These data-driven methods are particularly well-suited to handle large and complex, high-dimensional datasets and can be used to adapt to patient-specific characteristics in real time.

An early example emerged in 2017, when Fraunhofer MEVIS and Siemens Healthineers started their collaboration on the development of clinical decision support systems using deep learning algorithms. The goal was to consolidate relevant patient data from diverse sources into a single, user-friendly interface, thereby reducing both the cognitive workload and time demands placed on clinicians as one increasingly important aspect in light of healthcare workforce shortages. The system also incorporated disease-specific clinical guidelines to assist in evidence-based decision-making (91). By linking each patient case to a structured knowledge base, the algorithm could identify treatment strategies that had demonstrated success in similar clinical contexts.

As healthcare increasingly moves forward to precision medicine, such adaptive, modelbased approaches such as MIPD are expected to play a central role in supporting individualized treatment decisions. MIPD combines mechanistic pharmacometric models with patient-specific data and, increasingly, Al-enhanced tools to tailor dosing regimens more accurately than traditional one-size-fits-all approaches. A recent example of Alassisted precision medicine is the Clairity Breast platform, which supports clinicians in identifying a patient's five-year breast cancer risk using Al-based image analysis. In June 2025, the U.S. FDA granted De Novo authorization for this first-in-class device, which predicts future cancer risk based solely on imaging data (92).

5.6 Interdisciplinary Collaboration and Public Health Relevance

The work presented in this dissertation was made possible through the collaborative framework of the IMI DIRECT consortium, which provided access to extensive datasets and expertise from multiple scientific domains. This illustrates the importance of interdisciplinary collaboration in advancing complex, translational research.

Beyond individual-level optimization, the findings of this work offer broader public health benefits. Improved biomarker reliability (Project 1) supports better population-level monitoring of diabetes. Cost-effective treatment regimens (Project 3) may reduce long-term healthcare expenditures. Collectively, the projects contribute to a more efficient, data-informed healthcare system. The collaborative, multi-institutional structure of the IMI DIRECT consortium illustrates how shared resources and expertise can accelerate advances in biomarker discovery, disease stratification, and clinical innovation. These elements represent essential building blocks for the successful implementation of precision medicine.

6 Conclusion

This dissertation demonstrates how advanced pharmacometric modeling techniques, particularly NLME models, can be leveraged to improve the management of cardiometabolic diseases such as T2DM and hypercholesterolemia. Across three independent yet thematically connected projects, this work highlights the added value of reanalyzing existing clinical and observational datasets through model-based approaches. Rather than generating new data, the emphasis was placed on making more efficient and meaningful use of available information, thereby extending the utility of previously collected data for personalized medicine, improved biomarker interpretation, and optimized treatment strategies.

Collectively, the findings presented in this thesis for three different research topics support the notion that pharmacometric modeling is a valuable instrument in the implementation of precision medicine, especially in the context of chronic and multifactorial diseases. The integration of RWD with biases in regard to sample management and the simulation of individualized treatment pathways, all this contributes to narrowing the gap between controlled trial environments and everyday clinical practice.

Looking ahead, the growing availability of RWD and the ongoing development of AI and ML technologies will open new possibilities for adaptive, data-driven modeling. These methods have the potential to transform static population-level recommendations into dynamic, patient-specific treatment strategies, which are continuously refined through additional real-time feedback.

Finally, the work described conducted within the collaborative framework of the IMI DIRECT consortium underscores the importance of interdisciplinary research in tackling complex health challenges. By combining expertise in clinical pharmacology, endocrinology, pharmacometrics, and data science, this dissertation exemplifies how integrated approaches can yield robust and broadly applicable solutions in modern healthcare.

Bibliography

- 1. Scherer N, Kurbasic A, Dings C, Mari A, Nock V, Hennige AM, et al. The Impact and Correction of Analysis Delay and Variability in Storage Temperature on the Assessment of HbA1c from Dried Blood Spots an IMI DIRECT Study. Int J Proteom Bioinform (2019) ;4(1): 2019;007–13.
- 2. Türk D, Scherer N, Selzer D, Dings C, Hanke N, Dallmann R, et al. Significant impact of time-of-day variation on metformin pharmacokinetics. Diabetologia. 2023 Jun 1;66(6):1024–34.
- 3. Scherer N, Dings C, Böhm M, Laufs U, Lehr T. Alternative Treatment Regimens With the PCSK9 Inhibitors Alirocumab and Evolocumab: A Pharmacokinetic and Pharmacodynamic Modeling Approach. J Clin Pharmacol. 2017 Jul 1;57(7):846–54.
- 4. Holcombe AO. Contributorship, Not Authorship: Use CRediT to Indicate Who Did What. Publications. 2019 Jul 2;7(3):48.
- 5. Brand A, Allen L, Altman M, Hlava M, Scott J. Beyond authorship: attribution, contribution, collaboration, and credit. Learned Publishing. 2015 Apr;28(2):151–5.
- 6. Sattar N, Gill JMR, Alazawi W. Improving prevention strategies for cardiometabolic disease. Nat Med. 2020 Mar 9;26(3):320–5.
- 7. Sattar N. Gender aspects in type 2 diabetes mellitus and cardiometabolic risk. Best Pract Res Clin Endocrinol Metab. 2013 Aug;27(4):501–7.
- 8. Alberti KGMM, Zimmet P, Shaw J. Metabolic syndrome—a new world-wide definition. A Consensus Statement from the International Diabetes Federation. Diabetic Medicine. 2006 May 20;23(5):469–80.
- American Diabetes Association. Diagnosis and Classification of Diabetes Mellitus.
 Diabetes Care. 2014;37(Suppl 1):S81–S90. Available from: Diagnosis and
 Classification of Diabetes Mellitus | Diabetes Care | American Diabetes Association [cited 2025 Apr 17].
- American Diabetes Association. Standards of Medical Care in Diabetes—2019
 Abridged for Primary Care Providers. Clinical Diabetes. 2019 Jan 1;37(1):11–34.
- 11. Danaei G, Finucane MM, Lu Y, Singh GM, Cowan MJ, Paciorek CJ, et al. National, regional, and global trends in fasting plasma glucose and diabetes prevalence since 1980: systematic analysis of health examination surveys and epidemiological studies with 370 country-years and 2·7 million participants. The Lancet. 2011 Jul;378(9785):31–40.
- 12. Moebus S, Hanisch J, Bramlage P, Lösch C, Hauner H, Wasem J, et al. Regional Differences in the Prevalence of the Metabolic Syndrome in Primary Care Practices in Germany. Dtsch Arztebl Int. 2008 Mar 21.
- 13. Grundy SM. Metabolic Syndrome Pandemic. Arterioscler Thromb Vasc Biol. 2008 Apr;28(4):629–36.

- 14. McCarthy MI. Genomics, Type 2 Diabetes, and Obesity. New England Journal of Medicine. 2010 Dec 9;363(24):2339–50.
- 15. Eddy DM, Schlessinger L, Kahn R. Clinical Outcomes and Cost-Effectiveness of Strategies for Managing People at High Risk for Diabetes. Ann Intern Med. 2005 Aug 16;143(4):251.
- 16. Alberti KGMM, Eckel RH, Grundy SM, Zimmet PZ, Cleeman JI, Donato KA, et al. Harmonizing the Metabolic Syndrome. Circulation. 2009 Oct 20;120(16):1640–5.
- 17. Kaur J. A Comprehensive Review on Metabolic Syndrome. Cardiol Res Pract. 2014;2014:1–21.
- 18. Guembe MJ, Fernandez-Lazaro CI, Sayon-Orea C, Toledo E, Moreno-Iribas C, Cosials JB, et al. Risk for cardiovascular disease associated with metabolic syndrome and its components: a 13-year prospective study in the RIVANA cohort. Cardiovasc Diabetol. 2020 Dec 22;19(1):195.
- 19. Kaplan NM. The deadly quartet. Upper-body obesity, glucose intolerance, hypertriglyceridemia, and hypertension. Arch Intern Med. 1989 Jul 1;149(7):1514–20.
- 20. World Health Organization (WHO). Definition, diagnosis and classification of diabetes mellitus and its complications: report of a WHO consultation. Part 1, Diagnosis and classification of diabetes mellitus [Internet]. Geneva: WHO; 1999 Available from: WHO_NCD_NCS_99.2.pdf [cited 2024 Dec 12].
- 21. World Health Organization. Cardiovascular diseases (CVDs) [Internet]. Geneva: WHO; 2017. Available from: https://www.who.int/news-room/fact-sheets/detail/cardiovascular-diseases-%28cvds%29 [cited 2025 Apr 29].
- 22. Grundy SM, Cleeman JI, Daniels SR, Donato KA, Eckel RH, Franklin BA, et al. Diagnosis and Management of the Metabolic Syndrome. Circulation. 2005 Oct 25;112(17):2735–52.
- 23. Wilson PWF, D'Agostino RB, Parise H, Sullivan L, Meigs JB. Metabolic Syndrome as a Precursor of Cardiovascular Disease and Type 2 Diabetes Mellitus. Circulation. 2005 Nov 15;112(20):3066–72.
- 24. Gami AS, Witt BJ, Howard DE, Erwin PJ, Gami LA, Somers VK, et al. Metabolic Syndrome and Risk of Incident Cardiovascular Events and Death. J Am Coll Cardiol. 2007 Jan;49(4):403–14.
- 25. Ford ES, Li C, Sattar N. Metabolic Syndrome and Incident Diabetes. Diabetes Care. 2008 Sep 1;31(9):1898–904.
- 26. Inzucchi SE, Bergenstal RM, Buse JB, Diamant M, Ferrannini E, Nauck M, et al. Management of Hyperglycemia in Type 2 Diabetes, 2015: A Patient-Centered Approach: Update to a Position Statement of the American Diabetes Association and the European Association for the Study of Diabetes. Diabetes Care. 2015 Jan 1;38(1):140–9.

- 27. Shin J, Lee J, Lim S, Ha H, Kwon H, Park Y, et al. Metabolic syndrome as a predictor of type 2 diabetes, and its clinical interpretations and usefulness. J Diabetes Investig. 2013 Jul 28;4(4):334–43.
- 28. Bagry HS, Raghavendran S, Carli F, Warner DS, Warner MA. Metabolic Syndrome and Insulin Resistance. Anesthesiology. 2008 Mar 1;108(3):506–23.
- 29. IDF Diabetes Atlas 10th edition. 2021.
- 30. Khunti K, Wolden ML, Thorsted BL, Andersen M, Davies MJ. Clinical Inertia in People With Type 2 Diabetes. Diabetes Care. 2013 Nov 1;36(11):3411–7.
- 31. Knowler WC, Barrett-Connor E, Fowler; Sarah E., Hamman RF. Reduction in the Incidence of Type 2 Diabetes with Lifestyle Intervention or Metformin. New England Journal of Medicine. 2002 Feb 7;346(6):393–403.
- 32. Draznin B, Aroda VR, Bakris G, Benson G, Brwon FM, Freeman R. 2. Classification and Diagnosis of Diabetes: *Standards of Medical Care in Diabetes—2021*. Diabetes Care. 2021 Jan 1;44(Supplement_1):S15–33.
- 33. Zinman B, Wanner C, Lachin JM, Fitchett D, Bluhmki E, Hantel S, et al. Empagliflozin, Cardiovascular Outcomes, and Mortality in Type 2 Diabetes. New England Journal of Medicine. 2015 Nov 26;373(22):2117–28.
- 34. Bailey CJ, Turner RC. Metformin. New England Journal of Medicine. 1996 Feb 29;334(9):574–9.
- 35. Rena G, Pearson ER, Sakamoto K. Molecular mechanism of action of metformin: old or new insights? Diabetologia. 2013 Sep 9;56(9):1898–906.
- 36. Foretz M, Guigas B, Bertrand L, Pollak M, Viollet B. Metformin: From Mechanisms of Action to Therapies. Cell Metab. 2014 Dec;20(6):953–66.
- 37. Cameron AR, Morrison VL, Levin D, Mohan M, Forteath C, Beall C, et al. Anti-Inflammatory Effects of Metformin Irrespective of Diabetes Status. Circ Res. 2016 Aug 19;119(5):652–65.
- 38. Rutter MK, Parise H, Benjamin EJ, Levy D, Larson MG, Meigs JB, et al. Impact of Glucose Intolerance and Insulin Resistance on Cardiac Structure and Function. Circulation. 2003 Jan 28;107(3):448–54.
- 39. Franciosi M, Lucisano G, Lapice E, Strippoli GFM, Pellegrini F, Nicolucci A. Metformin Therapy and Risk of Cancer in Patients with Type 2 Diabetes: Systematic Review. PLoS One. 2013 Aug 2;8(8):e71583.
- 40. Agarwal N, Rice SPL, Bolusani H, Luzio SD, Dunseath G, Ludgate M, et al. Metformin Reduces Arterial Stiffness and Improves Endothelial Function in Young Women with Polycystic Ovary Syndrome: A Randomized, Placebo-Controlled, Crossover Trial. J Clin Endocrinol Metab. 2010 Feb 1;95(2):722–30.
- 41. Graham GG, Punt J, Arora M, Day RO, Doogue MP, Duong JK, et al. Clinical Pharmacokinetics of Metformin. Clin Pharmacokinet. 2011 Feb;50(2):81–98.

- 42. Grundy SM, Stone NJ, Bailey AL, Beam C, Birtcher KK, Blumenthal RS, et al. 2018 AHA/ACC/AACVPR/AAPA/ABC/ACPM/ADA/AGS/APhA/ASPC/NLA/PCNA Guideline on the Management of Blood Cholesterol. J Am Coll Cardiol. 2019 Jun;73(24):e285–350.
- 43. Ference BA, Ginsberg HN, Graham I, Ray KK, Packard CJ, Bruckert E, et al. Lowdensity lipoproteins cause atherosclerotic cardiovascular disease. 1. Evidence from genetic, epidemiologic, and clinical studies. A consensus statement from the European Atherosclerosis Society Consensus Panel. Eur Heart J. 2017 Aug 21;38(32):2459–72.
- 44. Malhotra A, Shafiq N, Arora A, Singh M, Kumar R, Malhotra S. Dietary interventions (plant sterols, stanols, omega-3 fatty acids, soy protein and dietary fibers) for familial hypercholesterolaemia. Cochrane Database of Systematic Reviews. 2014 Jun 10.
- 45. Hegele RA, Ginsberg HN, Chapman MJ, Nordestgaard BG, Kuivenhoven JA, Averna M, et al. The polygenic nature of hypertriglyceridaemia: implications for definition, diagnosis, and management. Lancet Diabetes Endocrinol. 2014 Aug;2(8):655–66.
- 46. Taylor F, Huffman MD, Macedo AF, Moore TH, Burke M, Davey Smith G, et al. Statins for the primary prevention of cardiovascular disease. Cochrane Database of Systematic Reviews. 2013 Jan 31;2021(9).
- 47. Baigent C, Blackwell L, Emberson J. Efficacy and safety of more intensive lowering of LDL cholesterol: a meta-analysis of data from 170 000 participants in 26 randomised trials. The Lancet. 2010 Nov;376(9753):1670–81.
- 48. Sabatine MS, Giugliano RP, Keech AC, Honarpour N, Wiviott SD, Murphy SA, et al. Evolocumab and Clinical Outcomes in Patients with Cardiovascular Disease. New England Journal of Medicine. 2017 May 4;376(18):1713–22.
- 49. Sabatine MS, Giugliano RP, Wiviott SD, Raal FJ, Blom DJ, Robinson J, et al. Efficacy and Safety of Evolocumab in Reducing Lipids and Cardiovascular Events. New England Journal of Medicine. 2015 Apr 16;372(16):1500–9.
- 50. Robinson JG, Farnier M, Krempf M, Bergeron J, Luc G, Averna M, et al. Efficacy and Safety of Alirocumab in Reducing Lipids and Cardiovascular Events. New England Journal of Medicine. 2015 Apr 16;372(16):1489–99.
- 51. Kaddoura R, Orabi B, Salam AM. Efficacy and safety of PCSK9 monoclonal antibodies: an evidence-based review and update. J Drug Assess. 2020 Jan 1;9(1):129–44.
- 52. Natarajan P, Kathiresan S. PCSK9 Inhibitors. Cell. 2016 May;165(5):1037.
- 53. Kaddoura R, Orabi B, Salam AM. Efficacy and safety of PCSK9 monoclonal antibodies: an evidence-based review and update. J Drug Assess. 2020 Jan 1;9(1):129–44.

- 54. Arrieta A, Page TF, Veledar E, Nasir K. Economic Evaluation of PCSK9 Inhibitors in Reducing Cardiovascular Risk from Health System and Private Payer Perspectives. PLoS One. 2017 Jan 12;12(1):e0169761.
- 55. Bonate PL. Pharmacokinetic-Pharmacodynamic Modeling and Simulation . 2nd ed. Springer Science & business Media; 2011.
- 56. Bödeker W, Moebus S. Das Paracelsus-Prinzip "Allein die Dosis macht, dass ein Ding (k)ein Gift sei" ein nicht mehr zeitgemäßer Lehrsatz und ätiologischer Mythos. Prävention und Gesundheitsförderung. 2024 May 15;19(2):165–70.
- 57. Powell JR, Gobburu JVS. Pharmacometrics at FDA: Evolution and Impact on Decisions. Clin Pharmacol Ther. 2007 Jul 30;82(1):97–102.
- 58. Gobburu JVS. Pharmacometrics 2020. The Journal of Clinical Pharmacology. 2010 Sep 7;50 (S9).
- 59. U.S. Department of Health and Human Services Food and Drug Administration, Center for Drug Evaluation and Research (CDER), Center for Biologics Evaluation and Research (CBER). Population Pharmacokinetics - Guidance for Industry (FDA-2019-D-2398) [Internet]. 2022. Available from: https://www.fda.gov/regulatoryinformation/search-fda-guidance-documents/population-pharmacokinetics [cited 2024 Nov 1].
- 60. COMMITTEE FOR MEDICINAL PRODUCTS FOR HUMAN USE (CHMP). Guideline on reporting the results of population pharmacokinetic analyses [Internet]. 2008

 Available from: https://www.ema.europa.eu/en/documents/scientificguideline/guideline-reporting-results-population-pharmacokinetic-analyses_en.pdf [cited 2024 Nov 1].
- 61. Gobburu JVS, Marroum PJ. Utilisation of Pharmacokinetic- Pharmacodynamic Modelling and Simulation in Regulatory Decision-Making. Clin Pharmacokinet. 2001;40(12):883–92.
- 62. FDA. Population Pharmacokinetics; Guidance for Industry; Availability [Docket No. FDA-2019-D-2398]. 2022 Apr.
- 63. EMA. Guideline on reporting the results of population pharmacokinetic analyses (Reference Number: CHMP/EWP/185990/06). 2008.
- 64. Zou P, Yu Y, Zheng N, Yang Y, Paholak HJ, Yu LX, et al. Applications of Human Pharmacokinetic Prediction in First-in-Human Dose Estimation. AAPS J. 2012 Jun 10;14(2):262–81.
- Darwich AS, Polasek TM, Aronson JK, Ogungbenro K, Wright DFB, Achour B, et al. Model-Informed Precision Dosing: Background, Requirements, Validation, Implementation, and Forward Trajectory of Individualizing Drug Therapy. Annu Rev Pharmacol Toxicol. 2021 Jan 6;61(1):225–45.
- 66. Sheiner LB, Rosenberg B, Marathe V V. Estimation of population characteristics of pharmacokinetic parameters from routine clinical data. J Pharmacokinet Biopharm. 1977 Oct 17;5(5):445–79.

- 67. Holford NHG, Sheiner LB. Kinetics of pharmacologic response. Pharmacol Ther. 1982 Jan;16(2):143–66.
- 68. Nestorov I. Whole-body physiologically based pharmacokinetic models. Expert Opin Drug Metab Toxicol. 2007 Apr 11;3(2):235–49.
- 69. Duffull SB, Wright DFB, Winter HR. Interpreting population pharmacokinetic-pharmacodynamic analyses a clinical viewpoint. Br J Clin Pharmacol. 2011 Jun 12;71(6):807–14.
- 70. Titze MI. Novel approaches for translational research in oncology: pharmacometric modeling of oncolytic virus dynamics and a new tyrosine kinase inhibitor (Dissertation) 2017 Available from: doi:10.22028/D291-26984.
- 71. Sheiner LB, Beal SL. Evaluation of methods for estimating population pharmacokinetic parameters. I. Michaelis-menten model: Routine clinical pharmacokinetic data. J Pharmacokinet Biopharm. 1980 Dec 1;8(6):553–71.
- 72. Sheiner LB, Beal SL. Evaluation of methods for estimating population pharmacokinetic parameters II. Biexponential model and experimental pharmacokinetic data. J Pharmacokinet Biopharm. 1981 Oct 1;9(5):635–51.
- 73. Steimer JL, Mallet A, Golmard JL, Boisvieux JF. Alternative Approaches to Estimation of Population Pharmacokinetic Parameters: Comparison with the Nonlinear Mixed-Effect Model. Drug Metab Rev. 1984 Jan 22;15(1–2):265–92.
- 74. Mould D, Upton R. Basic Concepts in Population Modeling, Simulation, and Model-Based Drug Development. CPT Pharmacometrics Syst Pharmacol. 2012 Sep 26;1(9):1–14.
- 75. Tornøe CW, Agersø H, Jonsson EN, Madsen H, Nielsen HA. Non-linear mixed-effects pharmacokinetic/pharmacodynamic modelling in NLME using differential equations. Comput Methods Programs Biomed. 2004 Oct;76(1):31–40.
- 76. Dings C. Modelling the impact of (non-)pharmaceutical interventions during covid-19 (Dissertation) 2024 Available from: doi:10.22028/D291-44384.
- 77. Wählby U, Jonsson EN, Karlsson MO. Comparison of stepwise covariate model building strategies in population pharmacokinetic-pharmacodynamic analysis. AAPS PharmSci. 2002 Dec 10;4(4):68–79.
- 78. Hutmacher MM, Kowalski KG. Covariate selection in pharmacometric analyses: a review of methods. Br J Clin Pharmacol. 2015 Jan 19;79(1):132–47.
- 79. Beal SL, Sheiner LB. NONMEM Users Guide. University of California. 1989.
- 80. Beal SL, Sheiner L.B. NONMEM Users Guide: Conditional Estimation Methods. University of California. 1998.
- 81. Wang Y. Derivation of various NONMEM estimation methods. J Pharmacokinet Pharmacodyn. 2007 Sep 21;34(5):575–93.
- 82. Karlsson MO, Savic RM. Diagnosing Model Diagnostics. Clin Pharmacol Ther. 2007 Jul;82(1):17–20.

- 83. Jones H, Rowland-Yeo K. Basic Concepts in Physiologically Based Pharmacokinetic Modeling in Drug Discovery and Development. CPT Pharmacometrics Syst Pharmacol. 2013 Aug 14;2(8):1–12.
- 84. Rowland M, Peck C, Tucker G. Physiologically-Based Pharmacokinetics in Drug Development and Regulatory Science. Annu Rev Pharmacol Toxicol. 2011 Feb 10;51(1):45–73.
- 85. Kuepfer L, Niederalt C, Wendl T, Schlender J, Willmann S, Lippert J, et al. Applied Concepts in PBPK Modeling: How to Build a PBPK/PD Model. CPT Pharmacometrics Syst Pharmacol. 2016 Oct 19;5(10):516–31.
- 86. Hanke N, Türk D, Selzer D, Ishiguro N, Ebner T, Wiebe S, et al. A Comprehensive Whole-Body Physiologically Based Pharmacokinetic Drug—Drug—Gene Interaction Model of Metformin and Cimetidine in Healthy Adults and Renally Impaired Individuals. Clin Pharmacokinet. 2020 Nov 25;59(11):1419–31.
- 87. Kostis JB, Dobrzynski JM. Limitations of Randomized Clinical Trials. Am J Cardiol. 2020 Aug;129:109–15.
- 88. Drolet J, Tolstikov V, Williams B, Greenwood B, Hill C, Vishnudas V, et al. Integrated Metabolomics Assessment of Human Dried Blood Spots and Urine Strips. Metabolites. 2017 Jul 15;7(3):35.
- 89. EMA. Real-world evidence framework to support EU regulatory decision-making (EMA/289699/2023). 2023.
- 90. U.S. Food and Drug Administration. Model-Informed Drug Development Paired Meeting Program [Internet]. Silver Spring (MD): FDA; 2023. Available from: https://www.fda.gov/drugs/development-resources/model-informed-drug-development-paired-meeting-program [cited 2025 Apr 12].
- 91. Imaging technology news: Siemens Healthineers & Fraunhofer MEVIS. Research Alliance on Clinical Decision Support [Internet]. Available from: https://www.itnonline.com/content/siemens-healthineers-and-fraunhofer-mevis-announce-research-alliance-clinical-decision. 2017 (press release) [cited 2025 Apr 12].
- 92. Clairity. Clairity Becomes the First FDA-Authorized AI Platform for Breast Cancer Prediction Historic Milestone for Women's Health [Internet]. Sunnyvale (CA): Business Wire; 2025 Jun 02 [cited 2025 Jul 17]. Available from: https://www.businesswire.com/news/home/20250602896762/en/ADDING-MULTIMEDIA-Clairity-Becomes-the-First-FDA-Authorized-AI-Platform-for-Breast-Cancer-Prediction-Historic-Milestone-for-Womens-Health. 2025. (press release) [cited 2025 Apr 12].

Appendix A: Supplementary material to the publications

A 1: Project II appendix
Supplementary material to Project II

Diabetologia

Significant impact of time-of-day variation on metformin pharmacokinetics

Electronic supplementary material (ESM)

Denise Türk¹, Nina Scherer¹, Dominik Selzer¹, Christiane Dings¹, Nina Hanke¹, Robert Dallmann²,

Matthias Schwab $^{3,4,5},\, Peter\, Timmins ^{6},\, Valerie\, Nock ^{7}\, and\, Thorsten\, Lehr ^{1}\,$

Denise Türk and Nina Scherer contributed equally to this study.

¹ Clinical Pharmacy, Saarland University, Saarbrücken, Germany

² Division of Biomedical Sciences, Warwick Medical School, University of Warwick, Coventry, UK

³ Dr. Margarete Fischer-Bosch-Institute of Clinical Pharmacology, Stuttgart, Germany

 4 Departments of Clinical Pharmacology, Pharmacy and Biochemistry, University of Tübingen,

Tübingen, Germany

⁵ Cluster of Excellence iFIT (EXC2180) 'Image-guided and Functionally Instructed Tumor Therapies',

University of Tübingen, Tübingen, Germany

⁶ Department of Pharmacy, University of Huddersfield, Huddersfield, UK

⁷ Boehringer Ingelheim Pharma GmbH & Co. KG, Biberach, Germany

Corresponding Author:

Thorsten Lehr

Email: thorsten.lehr@mx.uni-saarland.de

ORCID of the author(s): Denise Türk: orcid.org/0000-0002-4047-402X, Robert Dallmann:

orcid.org/0000-0002-7490-0218, Peter Timmins: orcid.org/0000-0002-5840-0678, Thorsten Lehr:

orcid.org/0000-0002-8372-1465

Funding: MS was supported in part by the Robert Bosch Stiftung, Stuttgart, Germany, and the Deutsche

Forschungsgemeinschaft (DFG, German Research Foundation) under Germany's Excellence Strategy -

EXC 2180 – 390900677. TL received funding from Boehringer Ingelheim Pharma GmbH & Co. KG for

personnel costs of NS, CD and NH. Authors' relationships and activities: NH is now an employee of

Boehringer Ingelheim Pharma GmbH & Co. KG. VN is an employee of Boehringer Ingelheim Pharma

GmbH & Co. KG. DT, NS, DS, CD, RD, MS, PT and TL declare that there are no relationships or activities

that might bias, or be perceived to bias, their work.

1 ESM Methods

1.1 Clinical dataset

ESM Table 1. Information on study I (metformin bioavailability study by Timmins et al. [1])

Study number	1			
Title ^a	Steady-State Pharmacokinetics of a Novel Extended-Release Metformin Formulation			
Summary	The objective of this study was (1) to assess metformin steady-state pharmacokinetics when administered as extended-rele			
	tablet and (2) to compare it with those of metformin when administered as immediate-release tablet			
Study type ^a	Bioavailability study			
Number of participants ^a	16 (healthy volunteers)			
Females (%) ^a	44			
Age (years), Weight (kg), Height (cm) ^{a,b}	27 (19-40), 71 (53-103), 172 (160-193)			
Inclusion Criteria ^a	 Adults 			
	 Good health based upon recent medical history, laboratory determinations and physical examination 			
	Informed consent before enrolment			
Exclusion criteria ^a	 Bodyweight >15% higher or lower than desirable weight-for-height range Smoking more than 10 cigarettes per day History of gastrointestinal disease or recent use of medication 			
	Blood donation within last 60 days that might affect the gastrointestinal tract			
	History of clinically significant allergies to biguanides Pregnant or nursing women			
	Exposure to any investigational agent within 60 days of			
	enrolment or participation in any other clinical trials			
	concurrent with this study			
Study design ^a	Open label- randomised, multiple dose, five-regimen, two sequence clinical study (no wash-out between treatments)			
	1) Metformin extended-release 500 mg once daily (n=16)			
	2) Metformin extended-release 1000 mg once daily (n=16)			
	3) Metformin extended-release 1500 mg once daily (n=15)			
	4) Metformin extended-release 2000 mg once daily (n=8) or Metformin immediate-release 1000 mg twice daily (n=7)			
	5) Metformin extended-release 2000 mg one daily (n=7) or Metformin immediate-release 1000 mg twice daily (n=7)			
Outcome measures ^a	C _{max} (immediate-release: evening dose), t _{max} (immediate-release: evening dose), AUC _{0-infinity} on day 1, AUC ₀₋₂₄ post-dose (for			
	immediate-release: sum of AUC ₀₋₁₂ morning and evening), t _{1/28} (immediate-release: evening dose)			
Feeding state ^a	Fed			
Metformin regimen ^a	Oral, tablet, once daily, 7 days (500, 1000, 1500, 2000 mg)			
-	Oral, tablet, twice daily, 7 days (1000 mg)			

ESM Table 1. continued

Study number			
Maximum daily metformin dose ^a	2000 mg		
Metformin formulation ^a	Extended-release (once daily administrations), immediate-release (twice daily administrations)		
Daytime of metformin administration ^a	Once daily administrations:		
	• 19:30 hours		
	Twice daily administrations		
	 19:30 hours on day 1, 07:30 hours and 19:30 hours on days 2-7 		
Metformin plasma sampling schedule	 Serial samples: Predose (19:30 hours), 1 h (20:30 hours), 2 h (21:30 hours), 4 h (23:30 hours), 6 h (01:30 hours), 8 h (03:30 hours), 12 h (07:30 hours), 16 h (11:30 hours), 20 h (15:30 hours), 24 h (19:30 hours) after drug administration (evening dose) on days 1, 6, 7, 13, 14, 20, 21, 27, 28, 34 and 35 (for various treatments) 		
	• Immediate-release: Predose (07:30 hours), 1 h (08:30 hours), 2 h (09:30 hours), 4 h (11:30 hours), 6 h (13:30 hours), 8 h (15:30 hours), 12 h (19:30 hours), 13 h (20:30 hours), 14 h (21:30 hours), 16 h (23:30 hours), 18 h (01:30 hours), 20 h (03:30 hours) and 24 h (07:30 hours) after each morning dose on days 27, 28, 34 and 35		
	 Additional predose samples before evening dose on days 4, 5, 11, 12, 18, 19, 25, 26, 32 and 33 		

a Information extracted from the publication by Timmins et al. [1], b values for age, weight and height are given as mean (range). C_{max}, maximum plasma concentration; t_{1/2β}, terminal elimination half-life; t_{max}, time to reach C_{max}

ESM Table 2. Information on study II (metformin clinical phase I study by Boehringer Ingelheim [2])

Study number	II					
ClinicalTrials.gov Identifier ^a	NCT02172248 (https://clinicaltrials.gov/ct2/show/NCT02172248)					
Study ID ^a	1245.6					
Official title ^a	Relative Bioavailability of Both BI 10773 and Metformin After Coadministration Compared to Multiple Oral Doses of BI 10773 (50 mg q.d.					
	Metformin (1000 mg b.i.d.) Alone to Healthy Male Volunteers (an Open-label, Randomised, Crossover, Clinical Phase I Study)					
Study summary ^a	The objective was to investigate a possible drug-drug interaction between BI 10773 and metformin when co-administered as multiple oral doses.					
	Therefore, the relative bioavailabilities of BI 10773 and metformin were determined when both drugs were given in combination compared with BI					
	10773 or metformin given alone.					
Study type ^a	Interventional (Clinical Trial)					
Number of participants ^a	16 (Healthy volunteers)					
Females (%) ^a	0					
Age (years), Weight (kg), Height (cm)b,c	32.2 (18-48), 81.3 (60-94), 180.1 (168-192)					
GFR (ml/min/1.73m ²) ^b	82.7 (calculated from baseline serum creatinine according to MDRD equation)					
Inclusion Criteria ^a	 Healthy male volunteers according to the following criteria: Based upon a complete medical history, including the physical examination, including the physical examination, vital signs (BP, PR), 12-lead ECG, clinical laboratory tests Age 18 to 50 years BMI 18.5 to 29.9 kg/m² Signed and dated written informed consent prior to admission to the study in accordance with GCP and the local legislation 					
Exclusion criteria ^a	 Any finding of the medical examination (including BP, PR and ECG) deviating from normal and of clinical relevance Any evidence of a clinically relevant concomitant disease Gastrointestinal, hepatic, renal, respiratory, cardiovascular, metabolic, immunological or hormonal disorders Surgery of the gastrointestinal tract (except appendectomy) Diseases of the central nervous system (such as epilepsy) or psychiatric disorders or neurological disorders History of relevant orthostatic hypotension, fainting spells or blackouts Chronic or relevant acute infections History of relevant allergy/hypersensitivity (including allergy to drug or its excipients) Intake of drugs with a long half-life (> 24 hours) within at least one month or less than 10 half-lives of the respective drug prior to administration or during the trial Participation in another trial with an investigational drug within two months prior to administration or during the trial Smoker (> 10 cigarettes or > 3 cigars or > 3 pipes/day) Inability to refrain from smoking on trial days Alcohol abuse (more than 100 ml within four weeks prior to administration or during the trial) Excessive physical activities (within one week prior to administration or during the trial) Any laboratory value outside the reference range that is of clinical relevance Inability to comply with dietary regimen of trial site Inability to comply with dietary regimen of trial site 					

ESM Table 2. continued

Study number	II	
Study arms ^a	Experimental: Sequence ABC Treatment A: BI 10773 once daily from day 1 to 5 Treatment B: BI 10773 once daily from day 1 to 4 and metformin twice daily from day 1 to 3 and once in the morning on day 4 Treatment C: metformin twice daily from day 1 to 3 and once in the morning on day 4	daily from day 1 to 3 and once in the morning on day 4
Outcome measures ^a	Primary Outcome Measures ■ AUC _{τ,ss} , C _{max,ss}	 Secondary Outcome Measures C_{24,N} of BI 10773, C_{12,N} of metformin, λ_{z,ss}, t_{x,ss}, t_{max,ss}, MRT_{po,ss}, CL/F_{ss}, V_z/F_{ss}, Ae_{t1-t2,ss}, fe_{t1-t2,ss}, CL_{R,ss} of BI 10773 and metformin, UGE Number of patients with abnormal findings in physical examination, number of patients with clinically significant changes in vital signs (BP, PR), number of patients with abnormal findings in 12-lead ECG, number of patients with abnormal changes in clinical laboratory tests, number of patients with adverse events, assessment of tolerability by investigator on a 4-point scale
Feeding state ^b	Fasted	u 1 point 35000
Metformin regimen ^a	Oral, 1000 mg, twice daily, 4 days	
Maximum daily metformin dose ^a	2000 mg	
Metformin formulation ^b	Immediate-release tablet	
Daytime of metformin administration ^{b,d}	08:00 hours, 20:00 hours (Days 1-3); 08:00 hours (Day 4)	
Metformin plasma sampling schedule ^{b,d}	Days 2-3: C _{trough}	Days 4-7: full profile
	 24 h (08:00 hours), 36 h (20:00 hours), 48 h (08:00 hours) and 60 h (20:00 hours) after first metformin administration 	 72 h (08:00 hours), 72.33 h (08:20 hours), 72.67 h (08:40 hours), 73 h (09:00 hours), 74 h (10:00 hours), 74.5 h (10:30 hours), 75 h (11:00 hours), 76 h (12:00 hours), 78 h (14:00 hours), 80 h (16:00 hours), 82 h (18:00 hours), 84 h (20:00 hours), 86 h (22:00 hours), 96 h (08:00 hours), 108 h (20:00 hours), 120 h (08:00 hours) and 144 h (08:00 hours) after first metformin administration

^a Information extracted from https://clinicaltrials.gov/ct2/show/NCT02172248, ^b information extracted from the study report, ^c values for age, weight and height are given as mean (range), ^d planned time, actual administration and sampling time is known and was used for model development. Ae_{11-12,55}, amount of analyte eliminated in urine at steady state over a uniform dosing interval τ; AUC_{τ,5}, area under the concentration-time curve of the analyte in plasma at steady state over a uniform dosing interval τ; b.i.d., twice daily; BP, blood pressure; C_{12,N}, concentration of analyte in plasma at 12 hours post-drug administration after administration of the Nth dose; C_{24,N}, concentration of analyte in plasma at 24 hours post-drug administration after administration of the Nth dose; C₁C₁F₅₅, apparent clearance of the analyte in the plasma after extravascular administration at steady state; C_{max,55}, renal clearance of the analyte at steady state; C_{max,55}, maximum measured concentration of the analyte in plasma at steady state over a uniform dosing interval τ; GCP, good clinical practice; MRT_{po,55}, mean residence time of the analyte in the body at steady state after oral administration; PR, pulse rate; q.d., once daily; t_{5,55}, terminal half-life of the analyte in plasma at steady state following extravascular administration; λ_{2,55}, terminal half-life of the analyte in plasma

ESM Table 3. Information on study III (metformin clinical phase I study by Boehringer Ingelheim [3])

Study number	III				
ClinicalTrials.gov Identifiera	NCT02183506 (https://clinicaltrials.gov/ct2/show/NCT02183506)				
Study IDa	1218.4				
Official title ^a	Bioavailability of Both BI 1356 BS and Metformin After Co-administration Compared to the Bioavailability of Multiple Oral Doses of BI 1356 BS 10 mg				
	Daily Alone and Metformin 850 mg Three Times a Day Alone in Healthy Male Volunteers (an Open-label, Randomized, Crossover Study)				
Study summary ^a	Investigate the bioavailability of BI 1356 BS and of metformin after concomitant multiple oral administration of 10 mg BI 1356 BS tablets and 3 x 850 m				
	metformin in comparison to BI 1356 BS and metformin given alone				
Study type ^a	Interventional (Clinical Trial)				
Number of participants ^a	16 (Healthy volunteers)				
Females (%) ^a	0				
Age (years), Weight (kg), Height (cm)b,c	32.2 (22-44), 81.8 (62-106), 176.6 (163-190)				
GFR (ml/min/1.73m ²) ^b	86.2 (calculated from baseline serum creatinine according to MDRD equation)				
Inclusion Criteria ^a	 Healthy males according to the following criteria, based upon a complete medical history, including the physical examination, vital signs (BP, PR), 12-lead ECG, clinical laboratory tests, no finding deviating from normal and of clinical relevance, no evidence of a clinically relevant concomitant disease Age ≥ 21 and Age ≤ 50 years BMI (Body Mass Index) ≥ 18.5 and ≤ 29.9 kg/m² Ability to give signed and dated written informed consent prior to admission to the study in accordance with GCP and the local legislation 				
Exclusion criteria ^a	 Gastrointestinal, hepatic, renal, respiratory, cardiovascular, metabolic, immunological or hormonal disorders Surgery of the gastrointestinal tract (except appendectomy) Diseases of the central nervous system (such as epilepsy) or psychiatric disorders or neurological disorders History of relevant orthostatic hypotension, fainting spells or blackouts Chronic or relevant acute infections History of allergy/hypersensitivity (including drug allergy) which is deemed relevant to the trial by the investigator or during the conduct of this trial) Excessive physical activities (within one week prior to administration or during the conduct of this trial) Any laboratory value outside the normal reference range that is of clinical relevance Inability to refrain from smoking during the conduct of this trial Blood donation (more than 100 ml within four weeks prior to administration or during the conduct of this trial) Excessive physical activities (within one week prior to administration or during the conduct of this trial) Any laboratory value outside the normal reference range that is of clinical relevance Inability to refrain from smoking during the conduct of this trial Excessive physical activities (within one week prior to administration or during the conduct of this trial) Any laboratory value outside the normal reference range that is of clinical relevance No adequate contraception (condom use plus another form of contraception e.g. spermicide, oral contraceptive taken by female partner, sterilisation) during the whole study period from the time of the first intake of study drug until one month after the last intake of drug Participation in another trial with an investigational drug within two months prior to administration or during the conduct of this trial 				

ESM Table 3. continued

Study number	III				
Study arms ^a	Daily administration of BI 1356 BS alone (day 1 to day 6) followed by the combined treatment of BI 1356 BS with metformin (day 7 to day 9)				
Outcome measures ^a	Primary Outcome Measures	Secondary Outcome Measures			
	 AUC of the analytes in plasma at different time points, C_{max} of the analytes in plasma at different time points 	 t_{max,ss}, C_{min,ss}, λ_{z,ss}, t_{1/2,ss}, MRT_{po,ss}, CL/F_{ss}, V_z/F_{ss}, DPP-IV activity, fe_{τ,ss}, CL_{R,ss} Number of patients with adverse events, number of patients with clinically abnormal changes in laboratory values, number of patients with clinically relevant changes in vital signs 			
Feeding state ^b	Fed				
Metformin regimen ^a	Oral, 850 mg, three times daily, 3 days				
Maximum daily metformin dose ^a	2550 mg				
Metformin formulation ^b	Immediate-release tablet				
Daytime of metformin administration ^{b,d}	07:30 hours, 15:30 hours, 23:30 hours (Days 1-2); 07:30 hours (Day 3)				
Metformin plasma sampling scheduleb,d	Day 2: Ctrough	Days 3-5: full profile			
	31.83 h (15:20 hours) and 39.83 h (23:20 hours) after first metformin administration	 47.83 h (07:20 hours), 48.25 h (07:45 hours), 48.5 h (08:00 hours), 48.75 h (08:15 hours), 49 h (08:30 hours), 49.5 h (09:00 hours), 50 h (09:30 hours), 50.5 h (10:00 hours), 51 h (10:30 hours), 52 h (11:30 hours), 54 h (13:30 hours), 56 h (15:30 hours), 60 h (19:30 hours), 72 h (07:30 hours) and 96 h (07:30 hours) after first metformin administration 			

a Information extracted from https://clinicaltrials.gov/ct2/show/NCT02183506, b information extracted from the study report, c values for age, weight and height are given as mean (range), d planned time, actual administration and sampling time is known and was used for model development. BP, blood pressure; CL/F_{ss}, apparent clearance of the analyte in the plasma after extravascular administration at steady state; CL_{R,SS}, renal clearance of the analyte at steady state; C_{min,SS}, minimum concentration of the analytes in plasma at steady state; C_{max}, maximum concentration; C_{trough}, trough plasma concentration; DPP-IV, dipeptidylpeptidase 4; ECG, electrocardiogram; fe_{t,SS}, fraction of the dose excreted unchanged in urine at steady state over a uniform dosing interval τ; GCP, good clinical practice; MRT_{PO,SS}, mean residence time of the analyte in the body at steady state after oral administration; PR, pulse rate; t_{x,SS}, terminal half-life of the analyte in plasma at steady state over a uniform dosing interval τ; UGE, urinary glucose excretion; V₂/F_{SS}, apparent volume of distribution during the terminal phase λ₂ at steady state following extravascular administration; λ_{2,SS}, terminal half-life of the analyte in plasma

ESM Table 4. Information on study IV (metformin clinical phase I study by Boehringer Ingelheim [4])

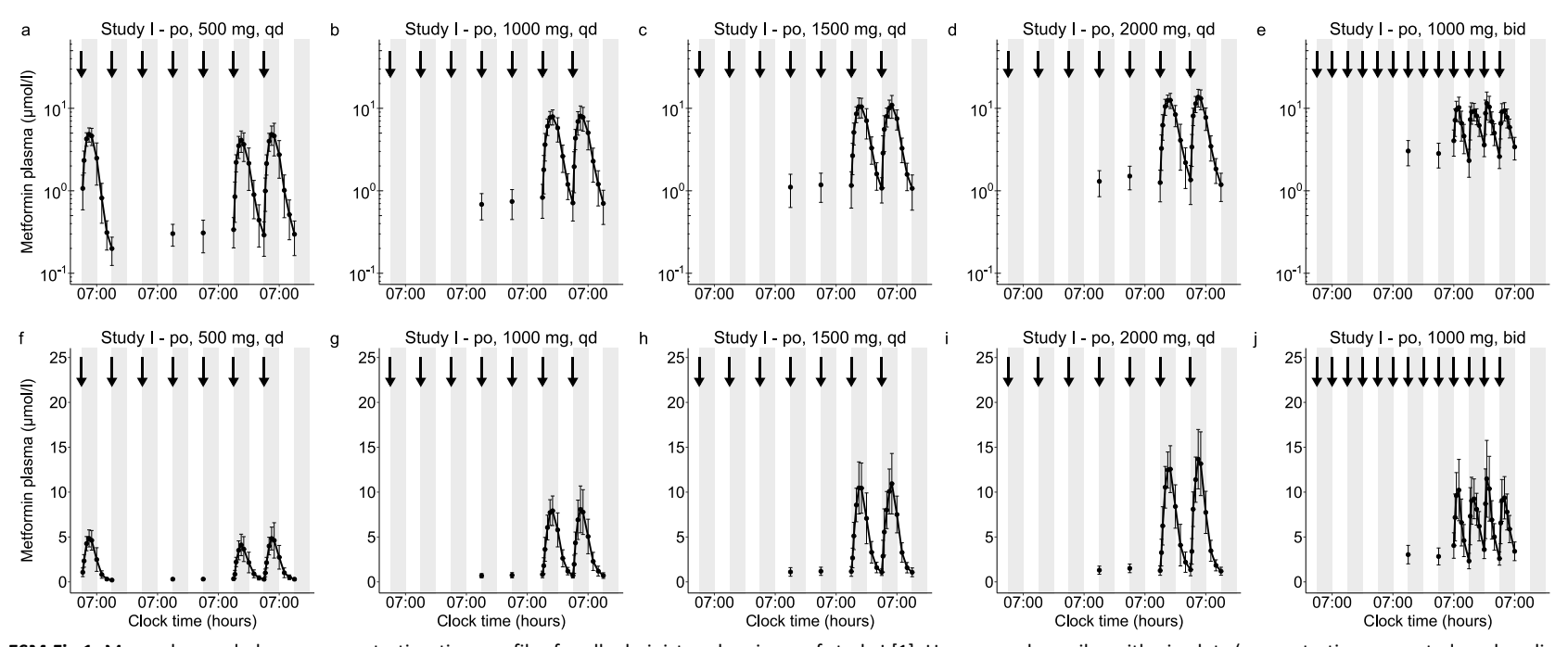
Study number	IV				
ClinicalTrials.gov Identifier ^a	NCT01845077 (https://clinicaltrials.gov/ct2/show/NCT01845077)				
Study ID ^a	1288.8				
Official title ^a	Relative Bioavailability of Two Newly Developed Extended Release FDC Tablet Strengths (5mg/1000mg and 2.5 mg/750 mg) of Linagliptin/Metfor				
	Extended Release Compared With the Free Combination of Linagliptin and Metformin Extended Release in Healthy Subjects (an Open-label, Randomised,				
	Single Dose, Two-way Crossover Study)				
Study summary ^a	The purpose of the trial is to demonstrate the relative bioavailability of 2 newly developed fixed dose combination (FDC) tablets containing linagliptin 8				
	metformin and the single tablets of linagliptin and metformin when administered singularly				
Study type ^a	Interventional (Clinical Trial)				
Number of participants ^a	72 (Healthy volunteers)				
Females (%) ^a	42				
Age (years), Weight (kg), Height (cm)b,c	31.3 (18-49), 72.8 (47-100), 169.5 (147-198)				
Inclusion Criteria ^a	Healthy males or females Subjects must be able to understand and comply with study				
	Age 18 -50 years requirements				
	BMI 18.5 to 29.9 kg/m²				
Exclusion criteria ^a	Any deviation from healthy condition				
Study arms ^a	FDC1000 Fasted vs. L+M1000 Fasted FDC1000 Fed vs. L+M1000 Fed FDC1500 Fasted vs. L+M1500 Fasted				
	• 1 FDC tablet (5 mg linagliptin/1000mg metformin FDC) vs. 3 single tablets (1 x 5 mg metformin FDC) vs. 3 single tablets (1 x 5 mg metformin FDC) vs. 4 single				
	linagliptin + 2 x 500 mg metformin) (and vice linagliptin + 2 x 500 mg metformin) (and linagliptin + 3 x 500 mg metformin) (and				
0	versa) vice versa) vice versa)				
Outcome measures ^a	Primary Outcome Measures Secondary Outcome Measures				
Feeding state (Metformin dose) ^a	 AUC₀₋₇₂ and C_{max} of linagliptin , AUC_{0-tz} and C_{max} of metformin AUC_{0-infinity} of linagliptin, AUC_{0-infinity} of metformin Fasted (1000mg), Fed (1000mg), Fasted (1500mg) 				
Metformin dosing regimen ^a	Oral, single dose				
Maximum daily metformin dose ^a	1000/1500 mg				
Metformin formulation ^a	Extended-release tablet				
Daytime of metformin administration ^{b,d}	08:00 hours				
Metformin plasma sampling schedule ^{a,b,d}	20 min (08:20 hours), 40 min (08:40 hours), 1 h (09:00 hours), 1.5 h (09:30 hours), 2 h (10:00 hours), 3 h (11:00 hours), 4 h (12:00 hours), 5 h (13:00				
metrorium prasina sampling senedale	hours), 6 h (14:00 hours), 8 h (16:00 hours), 10 h (18:00 hours), 12 h (20:00 hours), 16 h (00:00 hours), 24 h (08:00 hours), 36 h (20:00 hours), 48 h (08:00 hours), 26 h (20:00 hours), 27 h (20:00 hours), 28 h (20:00 hours),				
	hours) and 72 h (08:00 hours) after metformin administration				
	Hours, and 72 in 100.00 Hours, are mentioning administration				

^a Information extracted from https://clinicaltrials.gov/ct2/show/NCT01845077, ^b information extracted from the study report, ^c values for age, weight and height are given as mean (range), ^d planned time, actual administration and sampling time is known and was used for model development. AUC₀₋₇₂, area under the concentration-time curve in plasma over the time interval 0 to 72 hours; AUC_{0-infinity}, area under the concentration-time curve in plasma over the time interval from 0 extrapolated to infinity based on predicted last concentration values; AUC₀₋₁₂, area under the concentration-time curve in plasma over the time interval from 0 to the last quantifiable data point; C_{max}, maximum concentration; FDC, fixed dose combination

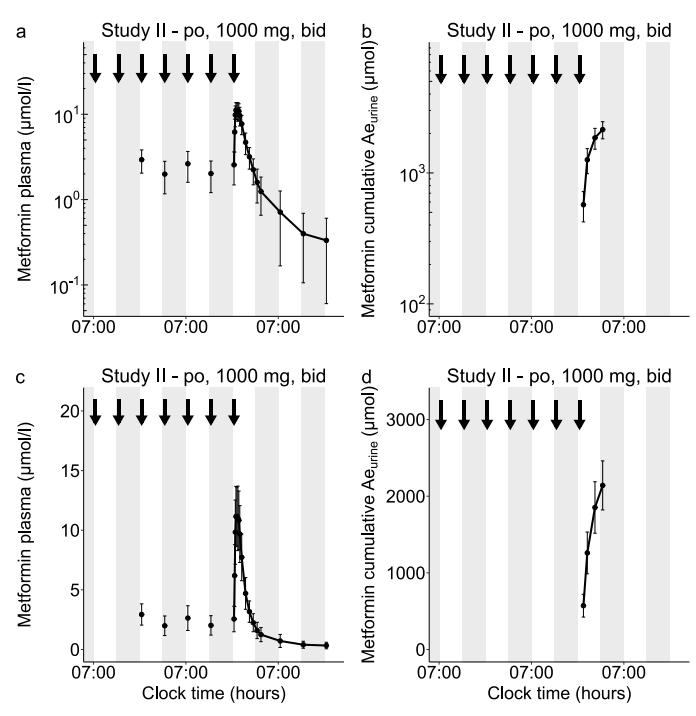
ESM Table 5. Information on study V (metformin clinical phase I study by Boehringer Ingelheim [5])

Study number	V				
ClinicalTrials.gov Identifier ^a	NCT01975220 (https://clinicaltrials.gov/ct2/show/NCT01975220)				
Study ID ^a	1276.13				
Official title ^a	Relative Bioavailability of Two Newly Developed FDC Tablet Strengths (25mg/1000mg and 12.5mg/750mg) of Empagliflozin/Metformin Extended				
	Release Compared With the Free Combination of Empagliflozin and Metformin Extended Release in Healthy Subjects (an Open-label, Randomis				
	Dose, Two-way Crossover Study)				
Study summary ^a	The purpose of this trial is to demonstrate the relative bioavailability of 2 newly developed (FDC) tablets containing empagliflozin & metformin and the				
	single tablets of empagliflozin and metformin when administered singularly				
Study type ^a	Interventional (Clinical Trial)				
Number of participants ^a	72 (Healthy volunteers)				
Females (%) ^a	42				
Age (years), Weight (kg), Height (cm)b,c	32.5 (19-50), 74.3 (50-115), 169.5 (149-198)				
Inclusion Criteria ^a	 Healthy males or females Subjects must be able to understand and comply with study 				
	Age 18-50 years requirements				
	BMI 18.5 to 29.9 kg/m²				
Exclusion criteria ^a	Any deviation from healthy condition				
Study arms ^a	<u>High Dose, Fasted</u> <u>Low Dose, Fasted</u>				
	• 1 FDC tablet (25 mg empagliflozin/1000 mg • 1 FDC tablet (25 mg empagliflozin/1000 mg • 2 FDC tablets (2 x 12.5 mg metformin FDC) vs. 3 single tablets (25 mg metformin) vs. 3 single tablets (1 x 25 mg empagliflozin/750 mg metformin) vs. 4				
	empagliflozin + 2 x 500 mg metformin) (and empagliflozin + 2 x 500 mg metformin) (and single tablets (1 x 25 mg empagliflozin + 3 x				
	vice versa) vice versa) 500 mg metformin) (and vice versa)				
Outcome measures ^a	<u>Primary Outcome Measures</u> <u>Secondary Outcome Measures</u>				
	 AUC_{0-tz} and C_{max} of empagliflozin, AUC_{0-tz} and C_{max} of metformin AUC_{0-infinity} of empagliflozin, AUC_{0-infinity} of metformin 				
Feeding state (Metformin dose) ^a	Fasted (1000mg), Fed (1000mg), Fasted (1500mg)				
Metformin dosing regimen ^a	Oral, single dose				
Maximum daily metformin dose ^a	1000/1500 mg				
Metformin formulation ^a	Extended-release tablet				
Daytime of metformin administration ^{b,d}	08:00 hours				
Metformin plasma sampling schedule ^{a,b,d}	20 min (08:20 hours), 40 min (08:40 hours), 1 h (09:00 hours), 1.33 h (09:20 hours), 1.67 h (09:40 hours), 2 h (10:00 hours), 2.5 h (10:30 hours), 3 h				
	(11:00 hours), 4 h (12:00 hours), 5 h (13:00 hours), 6 h (14:00 hours), 7 h (15:00 hours), 8 h (16:00 hours), 9 h (17:00 hours), 10 h (18:00 hours), 12 h				
	(20:00 hours), 16 h (00:00 hours), 24 h (08:00 hours), 36 h (20:00 hours), 48 h (08:00 hours) and 72 h (08:00 hours) after metformin administration				

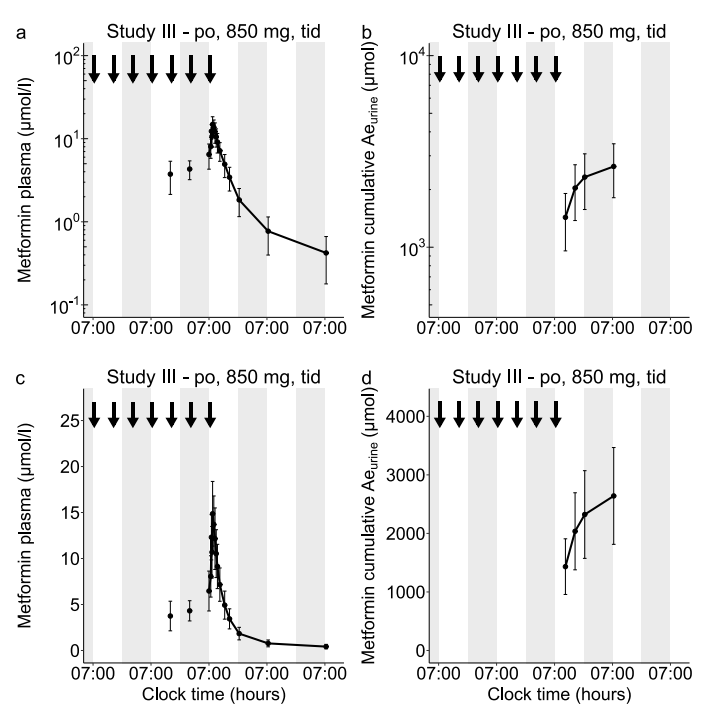
a Information extracted from https://clinicaltrials.gov/ct2/show/NCT01975220, b Information extracted from the study report, c values for age, weight and height are given as mean (range), d planned time, actual administration and sampling time is known and was used for model development. AUC₀₋₇₂, area under the concentration-time curve in plasma over the time interval 0 to 72 hours; AUC_{0-infinity}, area under the concentration-time curve in plasma over the time interval from 0 extrapolated to infinity based on predicted last concentration values; AUC_{0-tz}, area under the concentration-time curve in plasma over the time interval from 0 to the last quantifiable data point; C_{max}, maximum concentration; FDC, fixed dose combination



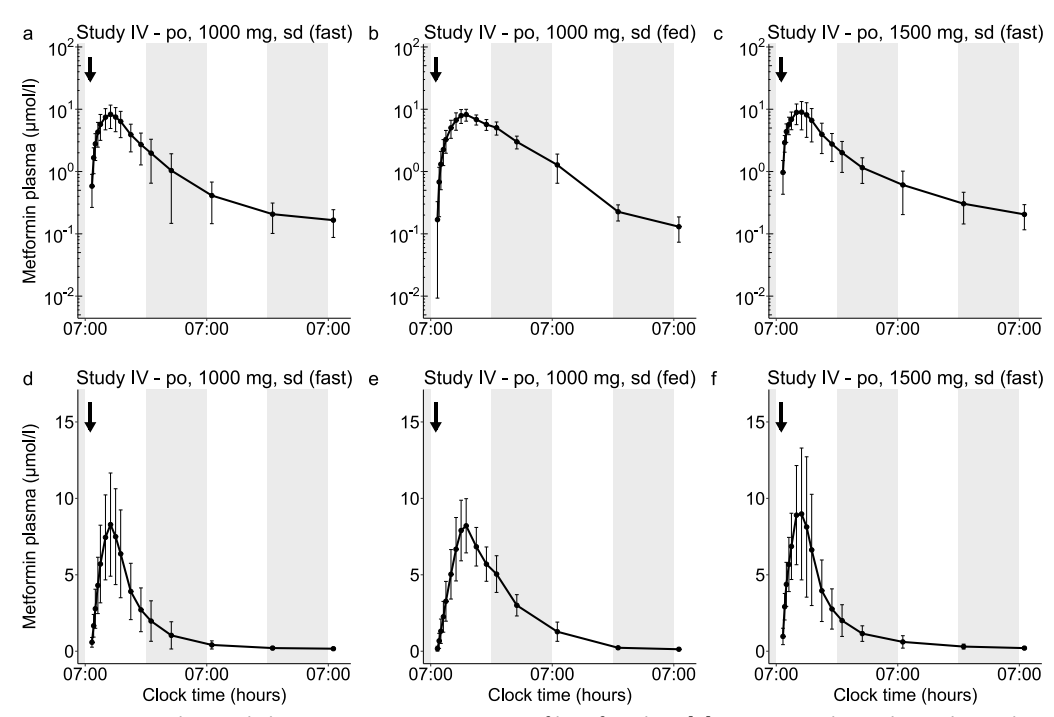
ESM Fig 1. Mean observed plasma concentration-time profiles for all administered regimen of study I [1]. Upper panel: semilogarithmic plots (concentration presented on decadic logarithm scale), lower panel: linear plots. Metformin was administered as (a—d) and (f—i) extended-release or (e, j) immediate-release tablet. Data are shown as arithmetic means ± SD. Black arrows indicate drug administration. Grey areas indicate night-time. bid, twice daily; po, oral; qd, once daily



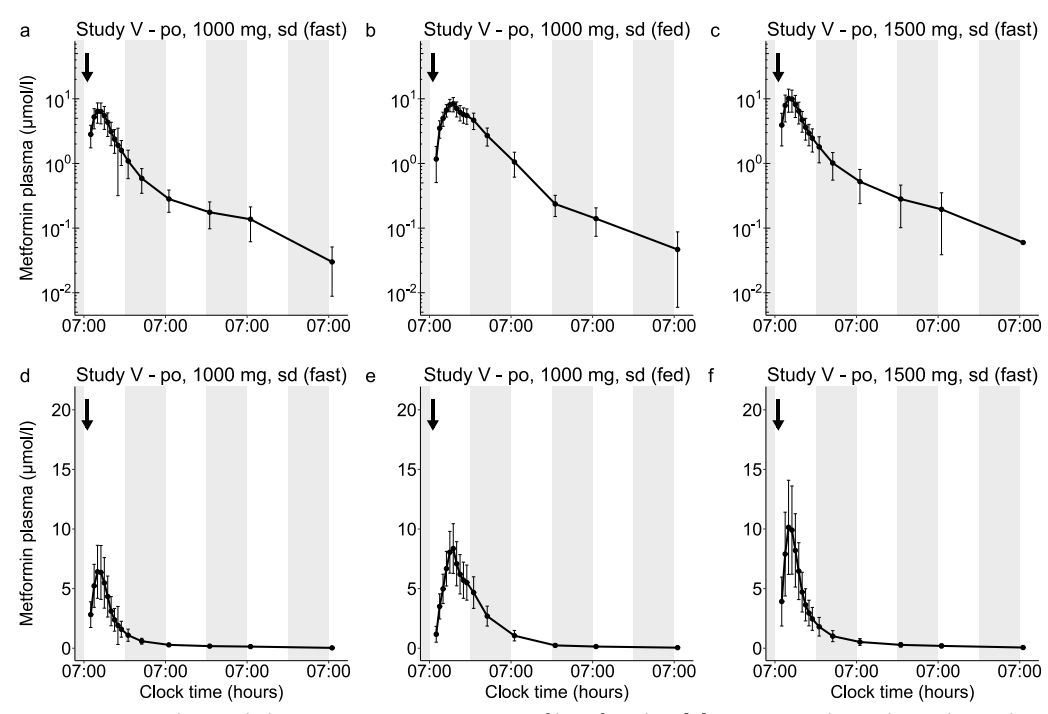
ESM Fig 2. Mean observed (**a, c**) plasma and (**b, d**) urine concentration-time profiles of study II [2]. Upper panel: semilogarithmic plots (concentration presented on decadic logarithm scale), lower panel: linear plots. Metformin was administered as immediate-release tablet. Data are shown as arithmetic means ± SD. Black arrows indicate drug administration. Grey areas indicate night-time. Ae_{urine}, amount excreted unchanged in urine; bid, twice daily; po, oral



ESM Fig 3. Mean observed (a, c) plasma and (b, d) urine concentration-time profiles of study III [3]. Upper panel: semilogarithmic plots (concentration presented on decadic logarithm scale), lower panel: linear plots. Metformin was administered as immediate-release tablet. Data are shown as arithmetic means \pm SD. Black arrows indicate drug administration. Grey areas indicate night-time. Ae_{urine}, amount excreted unchanged in urine; po, oral; tid, three times daily



ESM Fig 4. Mean observed plasma concentration-time profiles of study IV [4]. Upper panel: semilogarithmic plots (concentration presented on decadic logarithm scale), lower panel: linear plots. Metformin was administered as extended-release tablet. Data are shown as arithmetic means ± SD. Black arrows indicate drug administration. Grey areas indicate night-time. fast, fasted state; fed, fed state; po, oral; sd, single dose



ESM Fig 5. Mean observed plasma concentration-time profiles of study V [5]. Upper panel: semilogarithmic plots (concentration presented on decadic logarithm scale), lower panel: linear plots. Metformin was administered as extended-release tablet. Data are shown as arithmetic means ± SD. Black arrows indicate drug administration. Grey areas indicate night-time. fast, fasted state; fed, fed state; po, oral; sd, single dose

1.2 Statistical analysis

Individual plasma measurements were analysed separately for differences between trough plasma concentration (C_{trough}) values measured immediately before the next dose in the morning (' $C_{trough,morning}$ ') and the evening (' $C_{trough,evening}$ '). $C_{trough,morning}$ and $C_{trough,evening}$ were calculated average for each individual, and differences were compared using a paired t test. Additionally, a linear mixed model with random effect on study participant was applied to account for intra- and interindividual variability, including unequal numbers of measurements in the morning and the evening for each individual. The same procedure was applied to compare maximum plasma concentration (C_{max}) values measured after the morning dose (' $C_{max,morning}$ ') and the evening dose (' $C_{max,evening}$ '). For all statistical analyses, the significance level α was set to 0.05 (5%).

1.3 Non-linear mixed effects (NLME) pharmacokinetic modelling

NLME pharmacokinetic modelling was performed using NONMEM (NONMEM version 7.4.3, ICON Development Solutions, Ellicott City, MD, USA), allowing estimation of population medians for pharmacokinetic model parameters with simultaneous quantification of interindividual variability and residual (unexplained) variability. Calculation of pharmacokinetic parameters, quantitative model performance analysis, and generation of plots were accomplished using R 4.0.2 (R Core Team. R: A language and environment for statistical computing. R Foundation for Statistical Computing, Vienna, Austria) and RStudio 1.2.5033 (RStudio, Inc., Boston, MA, USA).

Model selection and hypothesis rating (model with time-of-day variation) was based on the precision of parameter estimates, the objective function value (OFV) provided by NONMEM [6] and visual inspection of goodness-of-fit plots (plotting predicted plasma and urine concentrations vs. observed values as well as conditional weighted residuals (CWRES) vs. time or predicted concentrations). One nested model was considered superior to another when the OFV was reduced by 3.84 units (Chi², p < 0.05, 1 degree of freedom) [7]. The First-Order Conditional Estimation with Interaction (FOCE-I) method was applied. To additionally evaluate the model performance of the model without versus with time-of-day variation, predicted and observed C_{trough} and C_{max} ratios (morning vs. evening) were compared including calculation of geometric mean fold errors (GMFEs) of C_{trough} and C_{max} ratio predictions as quantitative measure according to ESM Equation 1.

GMFE =
$$10^x$$
; $x = \frac{1}{m} \sum_{i=1}^{m} \left| log_{10} \left(\frac{predicted PK parameter_i}{observed PK parameter_i} \right) \right|$ (1)

where predicted PK parameter $_i$ = predicted C_{trough} or C_{max} ratio, observed PK parameter $_i$ = corresponding observed C_{trough} or C_{max} ratio and m = number of studies. Overall GMFEs of \leq 2 were considered reasonable predictions.

1.4 Literature-informed mechanistic physiologically based pharmacokinetic (PBPK) modelling

The previously published PBPK model [8] was developed in PK-Sim® and during this analysis extended in MoBi® (Open systems pharmacology suite 8.0, http://www.open-systems-pharmacology.org/). Calculation of pharmacokinetic parameters, quantitative model performance analysis, and generation of plots were accomplished using R 4.0.2 (R Core Team. R: A language and environment for statistical computing. R Foundation for Statistical Computing, Vienna, Austria) and RStudio 1.2.5033 (RStudio, Inc., Boston, MA, USA).

Virtual twins of study individuals were generated according to the demographic information, with corresponding ethnicity, sex, age, body weight, height and GFR, if reported. Metformin transporters were implemented in agreement with current literature, utilising the PK-Sim® expression database [9] to define their relative expression in the different organs of the body. Details on the expression of drug transporters implemented to model the pharmacokinetics of metformin are summarised in ESM Table 6. In all virtual individuals, enterohepatic circulation (EHC) was enabled (EHC continuous fraction set to 1) by assuming a continuous flow of the bile to the duodenum.

Model performance was evaluated by (1) comparison of predicted and observed plasma concentration time-profiles, (2) comparison of predicted and observed plasma concentration values in goodness-of-fit plots, (3) calculation of mean relative deviations (MRDs) of plasma concentration predictions according to ESM Equation 2, (4) comparison of predicted and observed C_{trough} and C_{max} ratios (morning vs. evening) and (5) calculation of GMFEs of C_{trough} and C_{max} ratio predictions.

MRD =
$$10^{x}$$
; $x = \sqrt{\frac{1}{k} \sum_{i=1}^{k} (\log_{10} c_{\text{predicted},i^{-}} \log_{10} c_{\text{observed},i})^{2}}$ (2)

where $c_{predicted,i}$ = predicted plasma concentration, $c_{observed,i}$ = corresponding observed plasma concentration and k = number of observed values. Overall MRD values \leq 2 were considered reasonable predictions.

ESM Table 6. System-dependent parameters

Transporter	Ref. Conc. (μmol/l) ^a	Expression profileb	Localisation	Direction	Half life [h]
MATE1	0.13 ^c [10, 11]	Kidney only [12, 13]	Apical	Efflux	36 (liver)
OCT1	0.16 ^d [14, 15]	Array [16] ^e	Basolateral ^f	Influx	36 (liver), 23 (intestine)
OCT2	0.19 ^c [10, 11]	EST [17]	Basolateral	Influx	36 (liver)
PMAT	1.00 ^g [18]	RT-PCR [19] ^e	Basolateral ^f	Influx	36 (liver), 23 (intestine)

Array, ArrayExpress measured expression profile; EST, expressed sequence tag measured expression profile; MATE, multidrug and toxin extrusion protein; OCT, organic cation transporter; PMAT, plasma membrane monoamine transporter; ref. conc., reference concentration; RT-PCR, reverse transcription-polymerase chain reaction measured expression profile

 $^{^{\}text{a}}$ mean reference concentration $\mu\text{mol/I}$ in the tissue of highest expression

b relative expression in the different organs (PK-Sim expression database profile)

calculated from transporter per mg membrane protein x 26.2 mg human kidney microsomal protein per g kidney [10]

^d calculated from transporter per mg membrane protein x 37.0 mg membrane protein per g liver [14]

e large intestinal mucosa → 0

f apical in enterocytes

 $^{^{\}rm g}$ transport rate constant (k $_{\rm cat}$) was optimised according to [18]

2 ESM Results

2.1 Statistical analysis

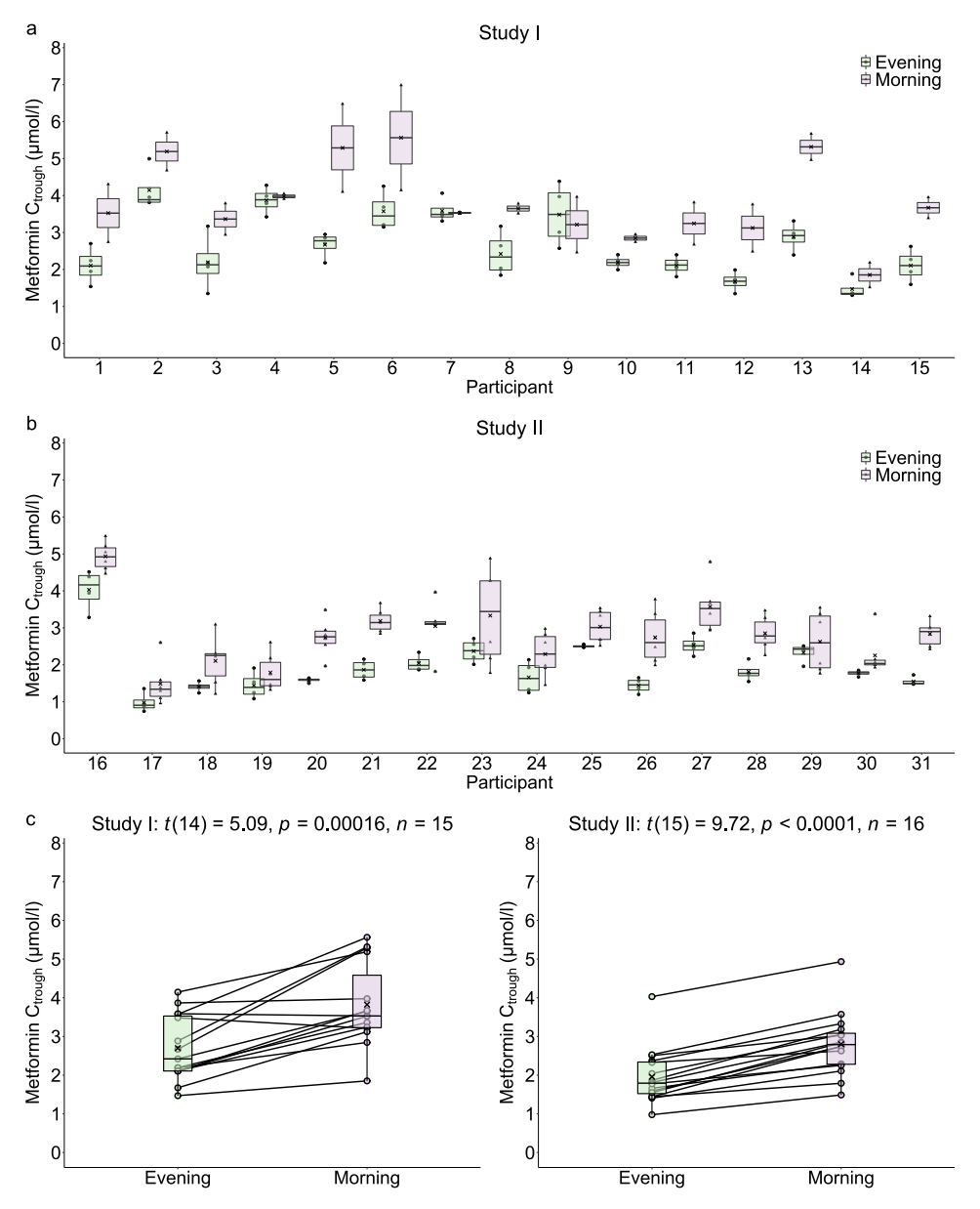


Fig 6. Intra- and interindividual variability of trough plasma concentration (C_{trough}) measurements from studies I and II [1, 2], including paired t test results. Boxes represent the distance between first and third quartiles (IQR). Whiskers range from smallest to highest value (< 1.5 × IQR).

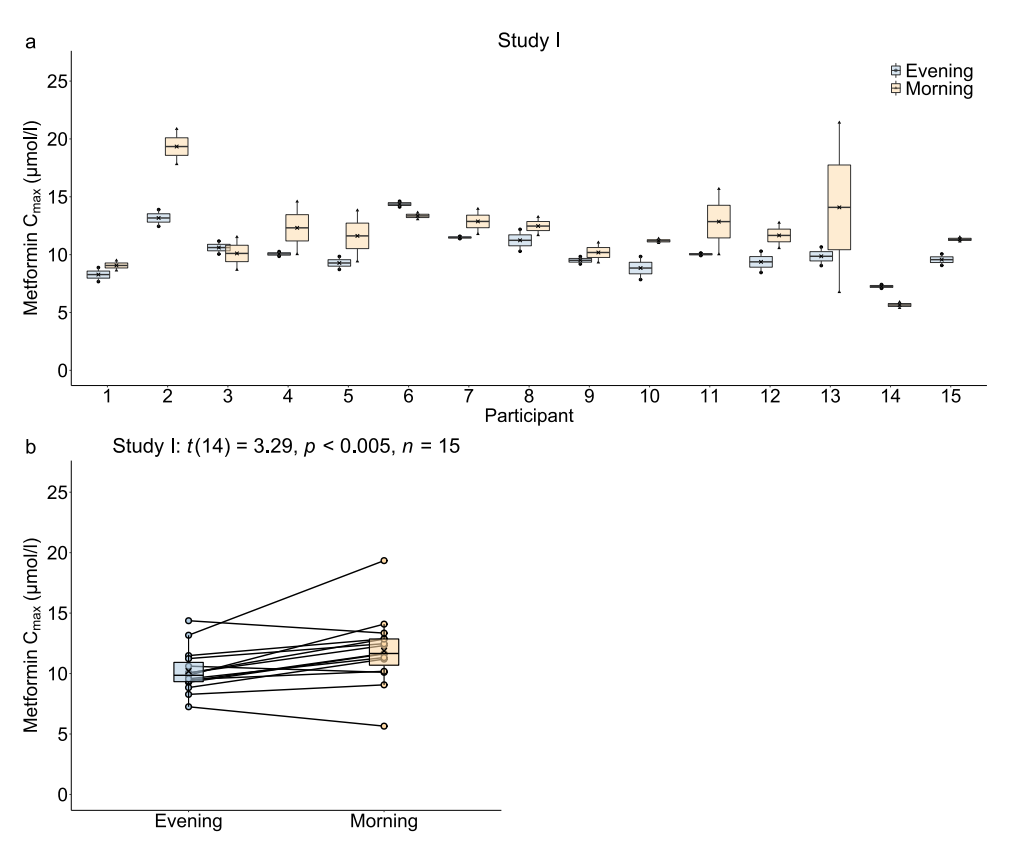


Fig 7. Intra- and interindividual variability of maximum plasma concentration (C_{max}) measurements from study I [1], including paired t test results. Boxes represent the distance between first and third quartiles (IQR). Whiskers range from smallest to highest value (< 1.5 × IQR).

2.2 NLME pharmacokinetic modelling

The volumes of distribution were 41.1 I for central (V_2) and 129 I for peripheral (V_3) compartments, respectively. The physiologically described rhythm of the GFR was implemented by multiplication of a sine function with clearance. The amplitude and a time shift of the sine function were estimated as 21% and 12.3 h (acrophase at 17:43 hours), respectively. Interindividual variability was found on the clearance, the volume of distribution and the bioavailability. Implementation of food, formulation and dose as significant covariates partly explained the interindividual variability and the related parameters were reduced about 14.2%, 75.0% and 51.5% for clearance, volume of distribution and bioavailability, respectively. Administration after food intake leads to a 1.91-fold higher bioavailability and a 0.63-fold lower absorption rate constant but 5.10-fold increased release duration for the extended-release formulation. The bioavailability of the extended-release formulation was 1.09-fold higher compared to the immediate-release formulation. The dose was implemented as a covariate using an exponential function according to ESM Equation 3, leading to a decreased bioavailability by administration of higher doses metformin. All estimated parameter values are summarised in ESM Table 7. All model parameters were precisely estimated with residual standard errors < 25%. Observed versus model predicted metformin concentrations are randomly distributed around the line of identity, indicating good descriptive properties of the final pharmacokinetic model.

F1 = estimated rel. F1 ×
$$(\frac{\text{dose}}{1000})^{-0.117}$$
 (3)

where F1 = absolute bioavailability, estimated rel. F1 = estimated relative bioavailability and dose = metformin dose.

ESM Table 7. NLME pharmacokinetic model parameters

		Value (RSE)			
Parameter	Unit	Without time-of-day variation	With time-of-day variation	Description	
ΔΟΒV			-660.39	Drop in objective function value	
Fixed effects					
CL	l/h	27.7 (14%)	28.9 (10%)	Clearance	
V_2	I	19.1 (15%)	41.1 (9%)	Central volume of distribution	
k_{a}	1/h	0.261 (3%)	0.280 (4%)	Absorption rate constant	
V_3	1	133 (15%)	129 (12%)	Peripheral volume of distribution	
Q	l/h	6.18 (16%)	6.01 (11%)	Intercompartimental clearance	
F1	%	0.181 (19%)	0.191 (19%)	Absolute bioavailability	
TDEL	h	-	12.3 (1%)	Timeshift of the sine function	
AMP	-	-	0.21 (7%)	Amplitude of the sine function	
D1_bioequivalence	h	2.49 (9%)	5.12 (3%)	Duration of the release of the extended-release formulation (study I)	
D1_phase_I	h	2.38 (7%)	1.18 (6%)	Duration of the release of the extended-release formulation (studies IV and V)	
Factor_D1_fed	-	2.54 (8.3%)	5.12 (3%)		
Factor_F1_ER	-	1 (3%)	1.09 (3%)		
Factor_k _a _fed	-	0.681 (4%)	0.631 (5%)		
Exponent_F1_dose	-	-0.134 (16%)	-0.117 (17%)		
Random effects					
IIV CL	%CV	68.5 (7%)	62.5 (8%)	Interindividual variability on clearance	
IIV V ₂	%CV	137.3 (7%)	91 (11%)	Interindividual variability on volume of distribution	
IIV F1	%CV	61 (9%)	63.3 (15%)	Interindividual variability on bioavailabitiy	
Residual effects					
PRV	%	32 (4%)	30.1 (9%)	Proportional residual variability of bioequivalence study (plasma concentration) (study I)	
PRV	%	32.9 (2%)	31.6 (2 %)	Proportional residual variability of phase I trials (plasma	
PRV	%	56.8 (12%)	55 (11%)	concentration) (studies II–V) Proportional residual variability of phase I trials (urine concentration) (studies II and III)	

RSE, relative standard error

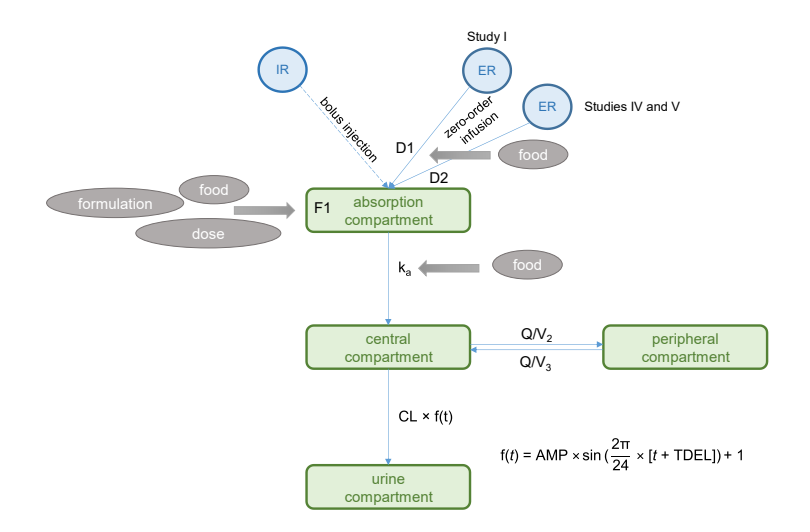
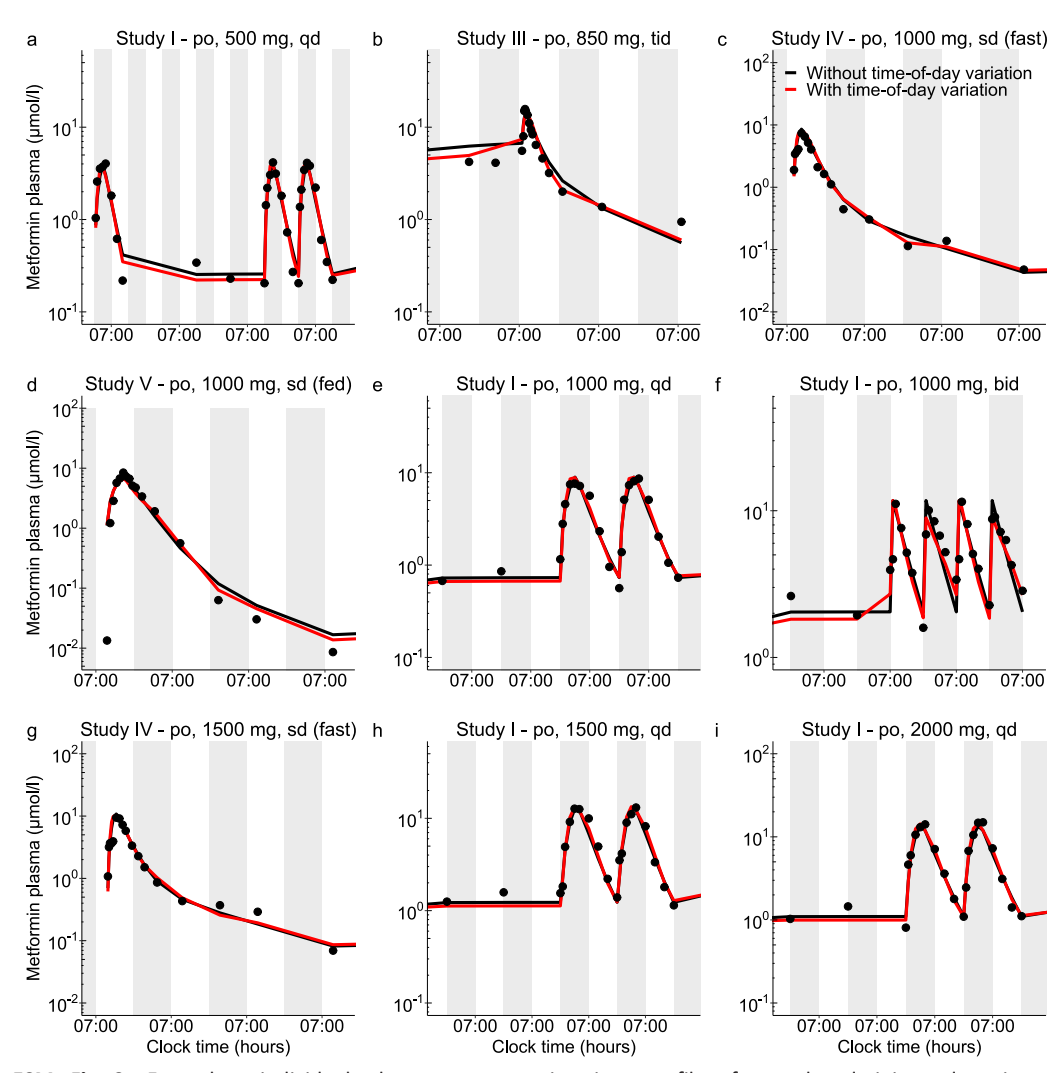


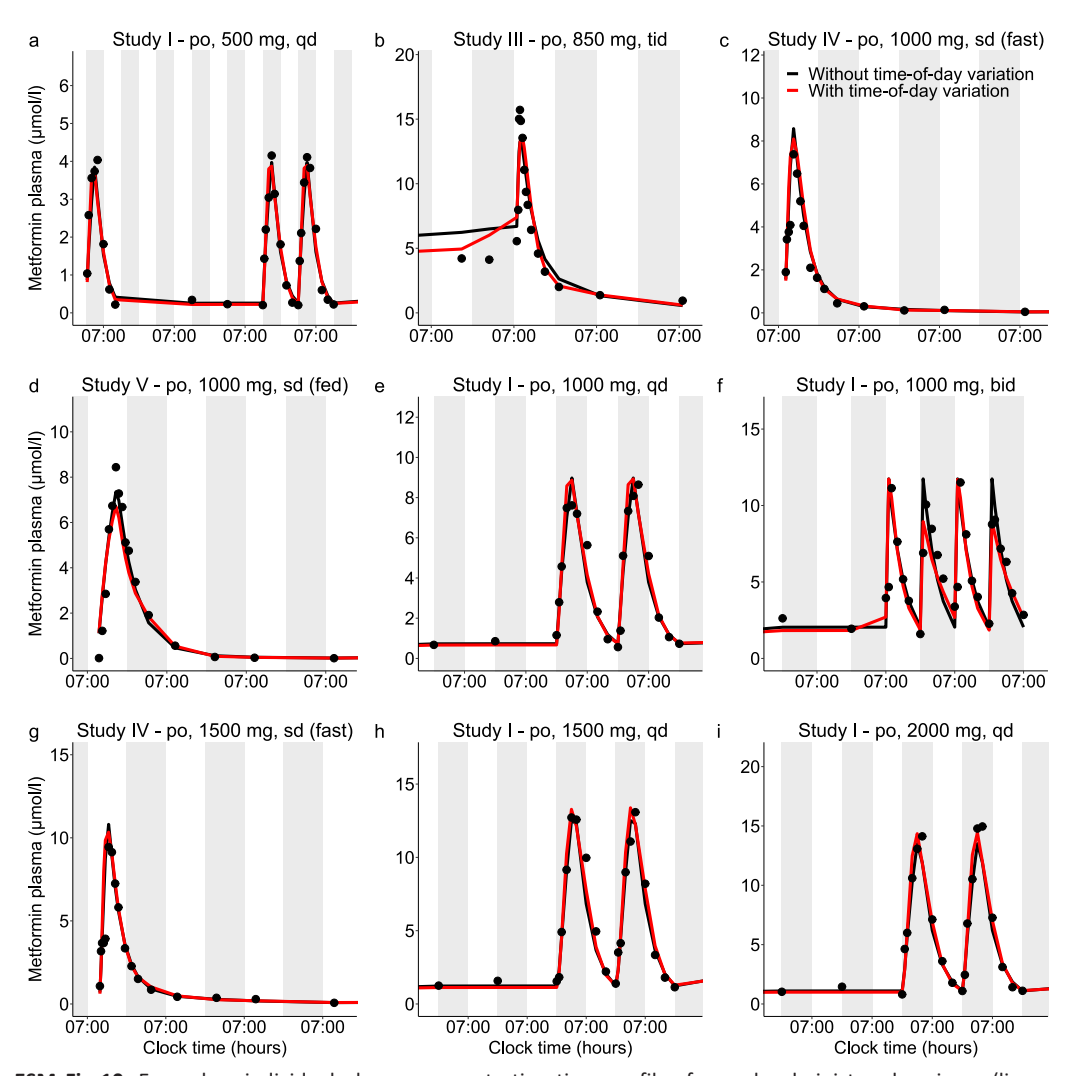
Fig 8. Structure of the final metformin NLME pharmacokinetic model. AMP, amplitude; CL, clearance; D, duration of release of the formulation; ER, extended-release; F1, absolute bioavailability; IR, immediate-release; k_a, absorption rate constant; Q, intercompartimental clearance; t, time; TDEL, shift in time; V, volume of distribution

2.2.1 NLME pharmacokinetic model plots

2.2.1.1 Metformin plasma concentration-time profiles

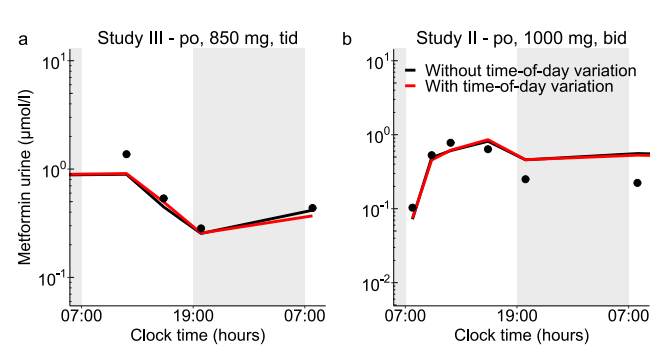


ESM Fig 9. Exemplary individual plasma concentration-time profiles for each administered regimen (semilogarithmic plots, i.e. concentration presented on decadic logarithm scale). Metformin was administered as (a, c, d, e, g, h, i) extended-release or (b, f) immediate-release tablet. Observed data from studies I-V [1–5] are shown as dots, predictions are shown as lines (black: without time-of-day variation). Grey areas indicate night-time. bid, twice daily; fast, fasted state; fed, fed state; po, oral; sd, single dose; tid, three times daily; qd, once daily

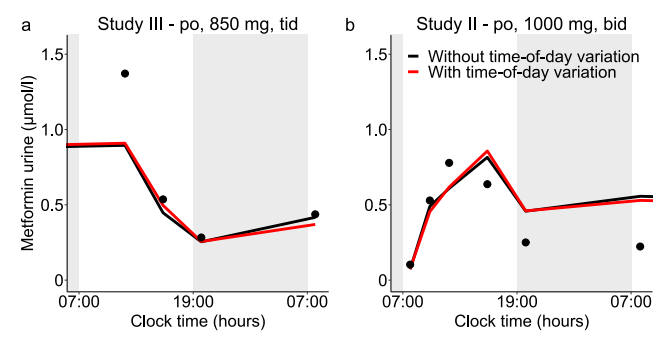


ESM Fig 10. Exemplary individual plasma concentration-time profiles for each administered regimen (linear plots). Metformin was administered as (a, c, d, e, g, h, i) extended-release or (b, f) immediate-release tablet. Observed data from studies I-V [1–5] are shown as dots, predictions are shown as lines (black: without time-of-day variation, red: with time-of-day variation). Grey areas indicate night-time. bid, twice daily; fast, fasted state; fed, fed state; po, oral; sd, single dose; tid, three times daily; qd, once daily

2.2.1.2 Metformin urine concentration-time profiles

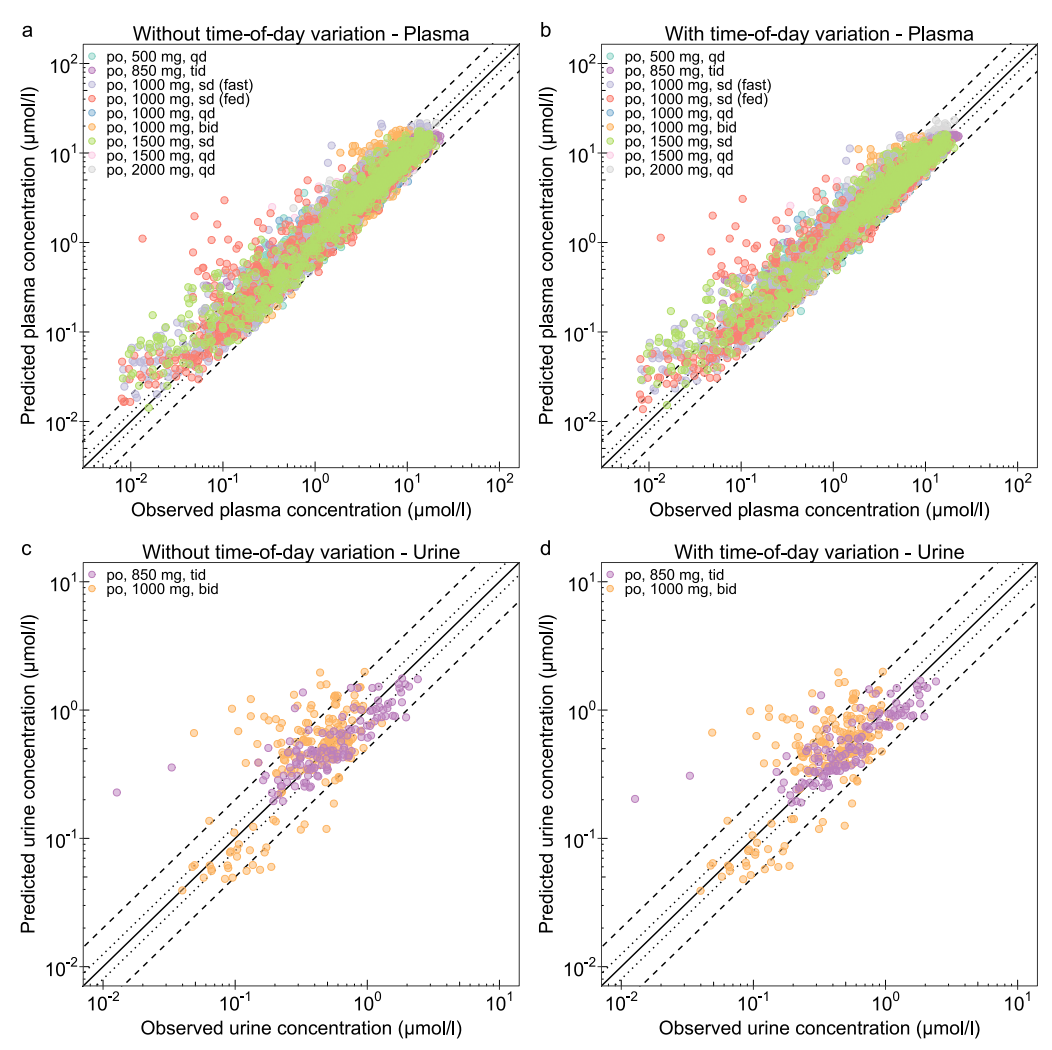


ESM Fig 11. Exemplary individual urine concentration-time profiles (semilogarithmic plots, i.e. concentration presented on decadic logarithm scale). Observed data from studies II and III [2, 3] are shown as dots, predictions are shown as lines (black: without time-of-day variation, red: with time-of-day variation). Grey areas indicate night-time. bid, twice daily; po, oral; tid, three times daily

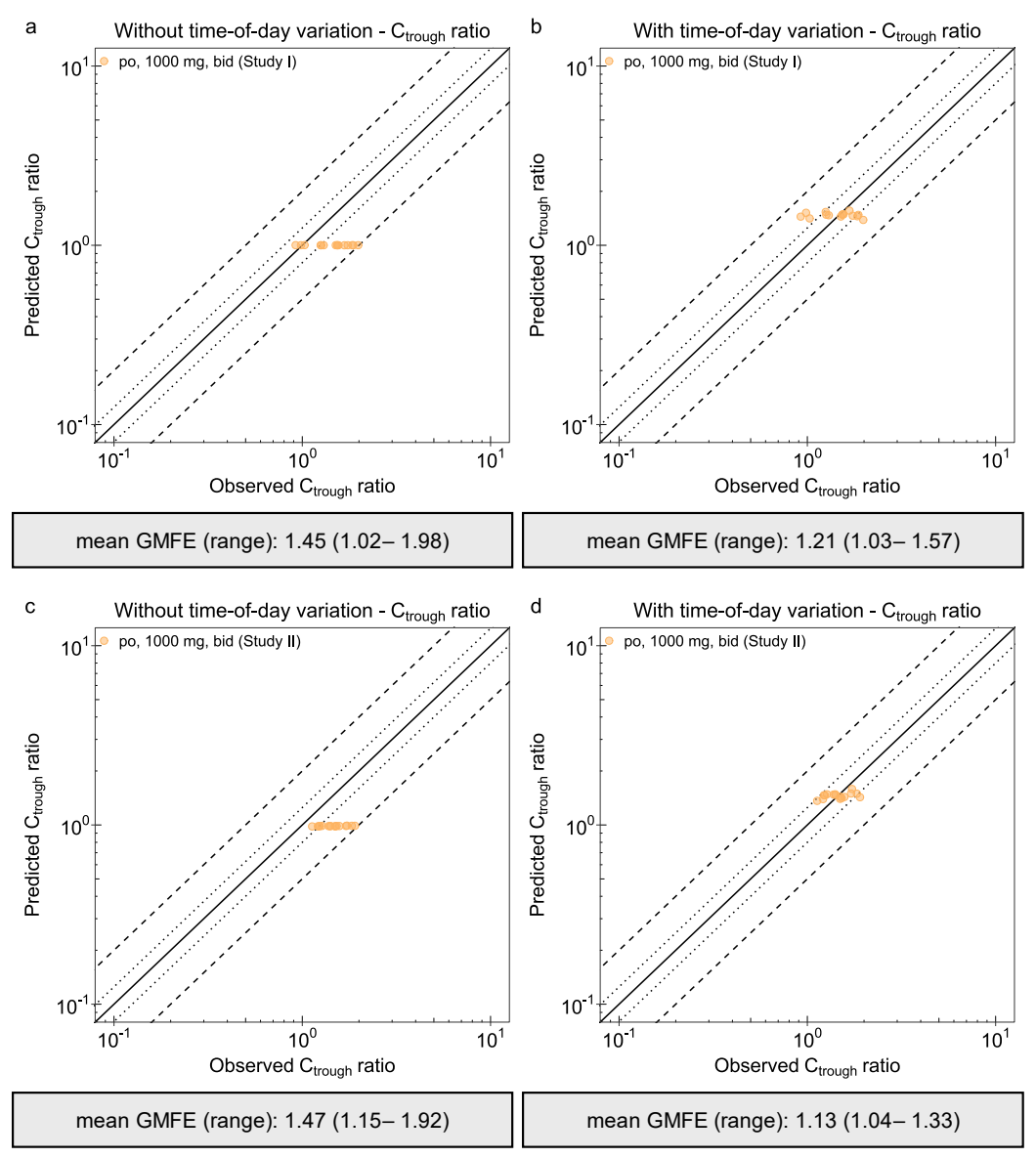


ESM Fig 12. Exemplary individual urine concentration-time profiles (linear plots). Observed data from studies II and III [2, 3] are shown as dots, predictions are shown as lines (black: without time-of-day variation, red: with time-of-day variation). Grey areas indicate night-time. bid, twice daily; po, oral; tid, three times daily

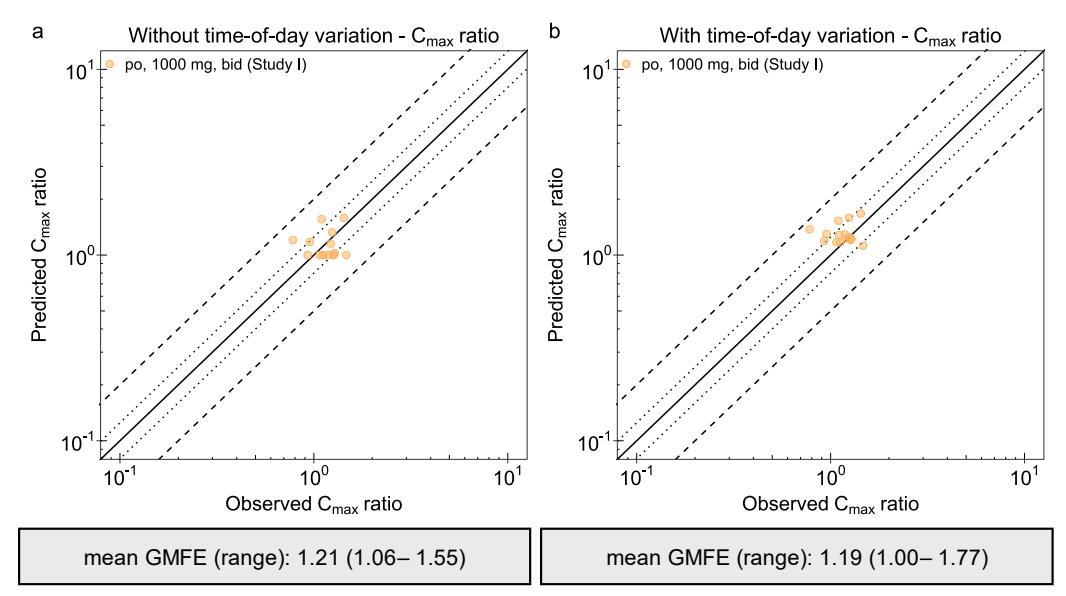
2.2.1.3 Metformin goodness-of-fit plots



ESM Fig 13. Goodness-of-fit plots, showing NLME pharmacokinetic model predictions compared to observed metformin (**a**—**b**) plasma and (**c**—**d**) urine concentrations of individuals from studies I-V [1–5], receiving either metformin extended- or immediate-release formulations. Predictions are shown for the model (**a**, **c**) without and (**b**, **d**) with time-of-day variation. The straight black line marks the line of identity. Dotted lines indicate 0.8- to 1.25-fold and dashed lines indicate 0.5- to 2-fold acceptance limits. bid, twice daily; fast, fasted state; fed, fed state; po, oral; sd, single dose; tid, three times daily; qd, once daily

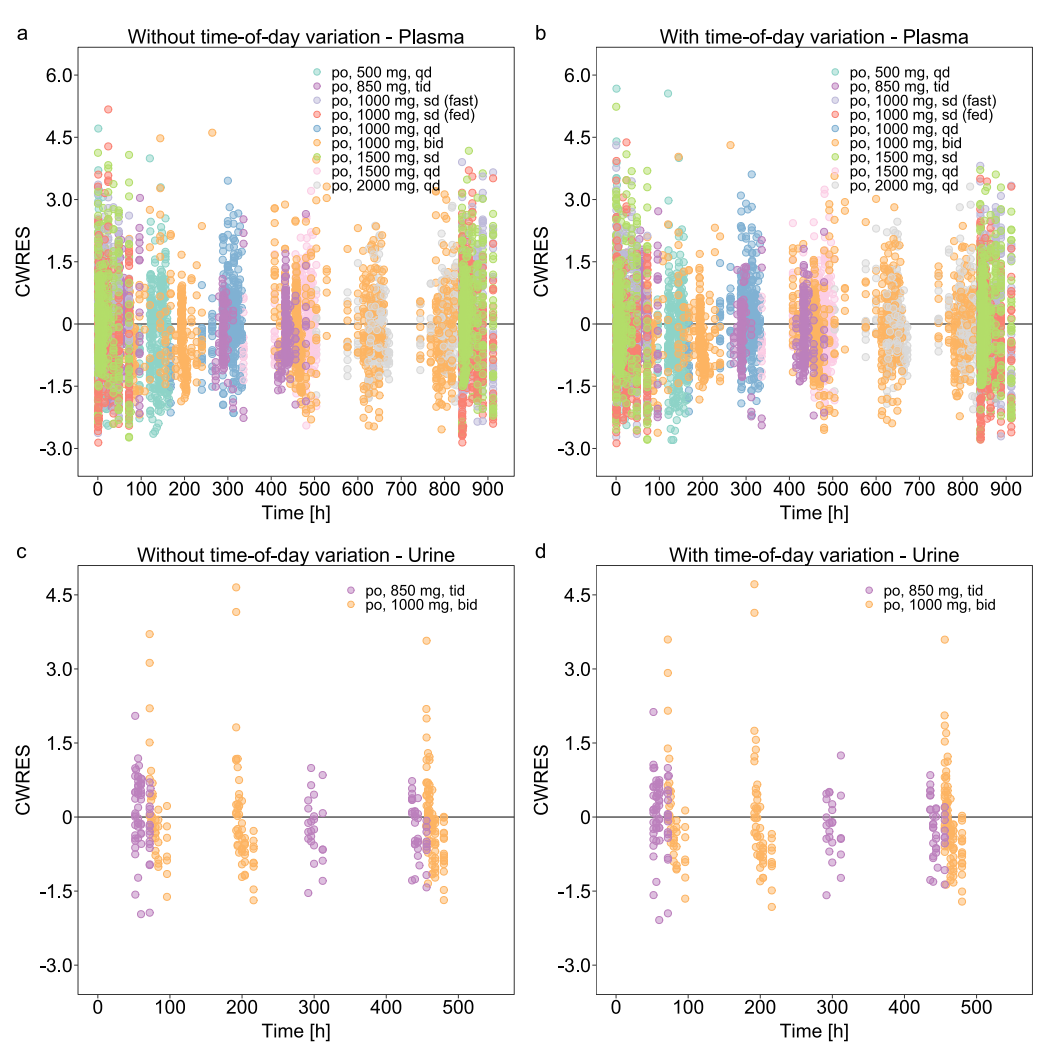


ESM Fig 14. Goodness-of-fit plots, showing NLME pharmacokinetic model predictions compared to observed metformin C_{trough} ratios (morning/evening) from studies I and II [1, 2], receiving twice daily 1000 mg of metformin immediate-release formulation ((**a–b**) study I and (**c–d**) study II), comparing the model (**a–c**) without and (**b–d**) with time-of-day variation. The straight black line marks the line of identity. Dotted lines indicate 0.8- to 1.25-fold and dashed lines indicate 0.5- to 2-fold acceptance limits. bid, twice daily; GMFE, geometric mean fold error; po, oral



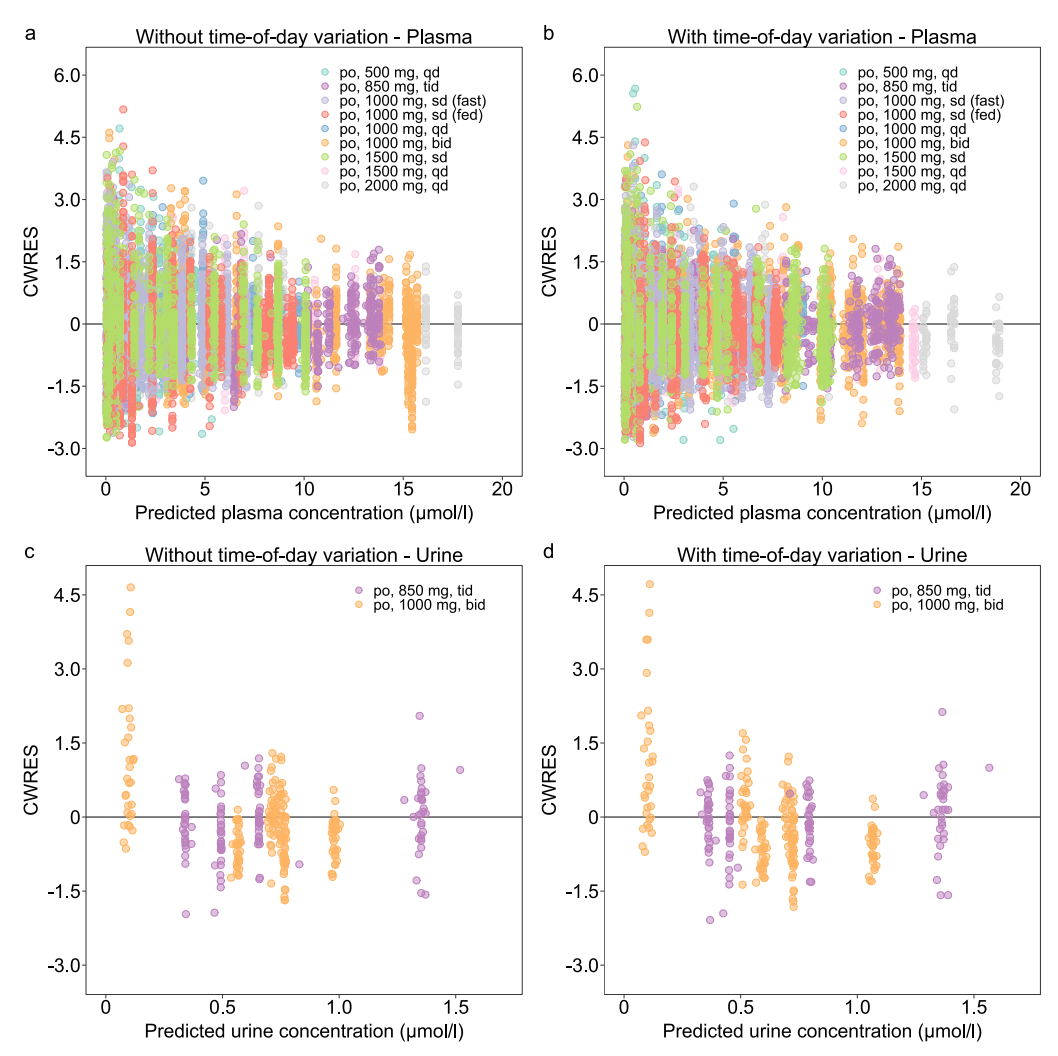
ESM Fig 15. Goodness-of-fit plots, showing NLME pharmacokinetic model predictions compared to observed metformin C_{max} ratios (morning/evening) from studies I and II [1, 2], receiving twice daily 1000 mg of metformin immediate-release formulation (study I), comparing the model (a) without and (b) with time-of-day variation. The straight black line marks the line of identity. Dotted lines indicate 0.8- to 1.25-fold and dashed lines indicate 0.5- to 2-fold acceptance limits. bid, twice daily; GMFE, geometric mean fold error; po, oral

2.2.1.4 Conditional weighted residuals vs. time



ESM Fig 16. NLME pharmacokinetic model conditional weighted residuals (CWRES) vs. time for the model (a, c) without and (b, d) with time-of-day variation taking (a—b) metformin plasma concentrations and (c—d) metformin urine concentrations from studies I-V [1–5] into account. bid, twice daily; fast, fasted state; fed, fed state; po, oral; sd, single dose; tid, three times daily; qd, once daily

2.2.1.5 Conditional weighted residuals vs. prediction



ESM Fig 17. NLME pharmacokinetic model conditional weighted residuals (CWRES) vs. prediction for the model (a, c) without and (b, d) with time-of-day variation taking (a-b) metformin plasma concentrations and (c-d) metformin urine concentrations from studies I-V [1–5] into account. bid, twice daily; fast, fasted state; fed, fed state; po, oral; sd, single dose; tid, three times daily; qd, once daily

2.3 Literature-informed mechanistic PBPK modelling

2.3.1 Literature search

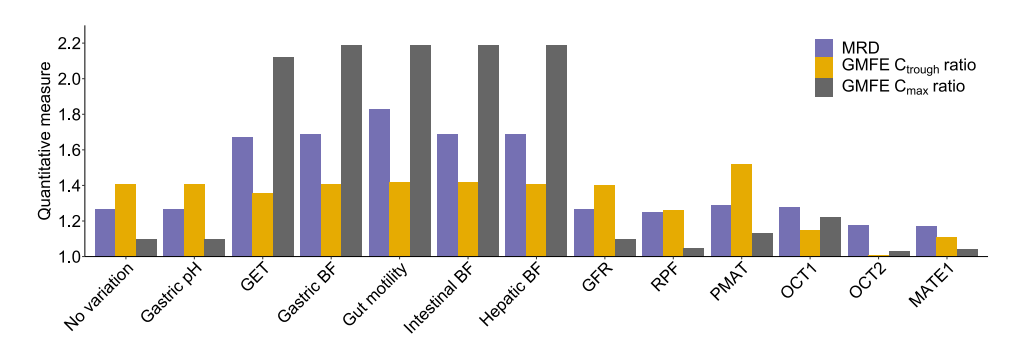
ESM Table 8. Time-of-day variation of pharmacokinetic-related processes and physiological conditions according to Dallmann et al. [20]

ADME process	Amplitude (%)	Acrophase (Clock time, hours)	Reference
Absorption			
Gastric pH	35	09:00	[21]
Gastric emptying time	20 (solid), 7 (liquid) ^a	20:00 ^b	[22]
Gut motility	56	14:00	[23]
Blood flow to GIT	15	04:00	[24]
Distribution			
Hepatic blood flow	15	04:00	[24]
Excretion			
Glomerular filtration rate	13	15:01	[25–27]
Renal plasma flow	12	17:22	[25–27]

^a Amplitudes calculated for emptying half-times, ^b meals were given at 08:00 and 20:00 hours. GIT, gastrointestinal tract

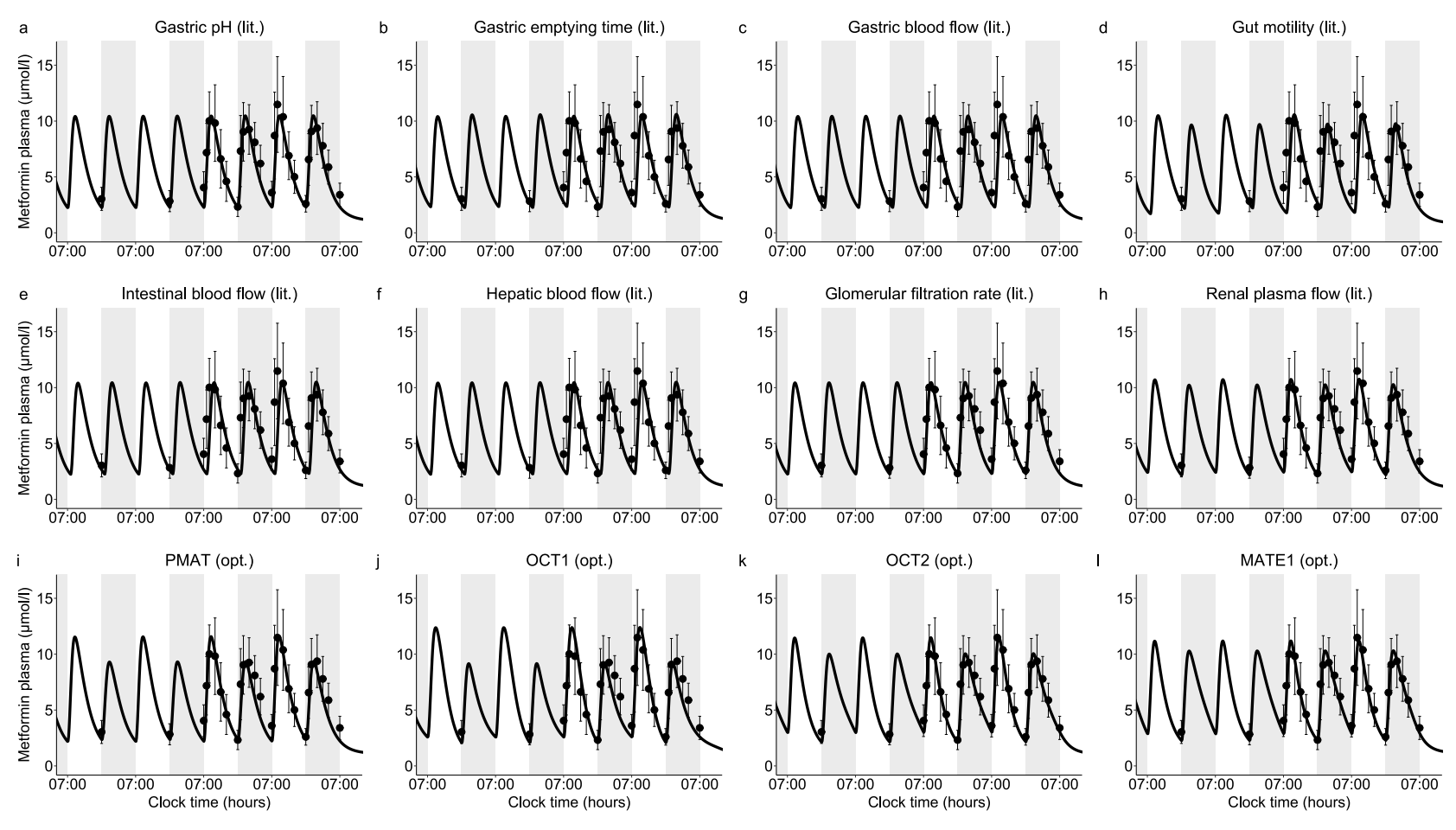
2.3.2 Hypothesis testing

Daily variation of processes and physiological conditions identified during literature search were rated quantitatively (ESM Fig 18) and graphically regarding prediction accuracy (ESM Fig 19).



ADME process	MRD	GMFE C _{trough} ratio	GMFE C _{max} ratio
No time-of-day variation	1.27	1.41	1.10
Absorption			
Gastric pH (lit.)	1.27	1.41	1.10
Gastric emptying time (lit.)	1.67	1.36	2.12
Gastric blood flow (lit.)	1.69	1.41	2.19
Gut motility (lit.)	1.83	1.42	2.19
Intestinal blood flow (lit.)	1.69	1.42	2.19
Distribution			
Hepatic blood flow (lit.)	1.69	1.41	2.19
Excretion			
Glomerular filtration rate (lit.)	1.27	1.40	1.10
Renal plasma flow (lit.)	1.25	1.26	1.05
Transporter			
PMAT (opt.)	1.29	1.52	1.13
OCT1 (opt.)	1.28	1.15	1.22
OCT2 (opt.)	1.18	1.01	1.03
MATE1 (opt.)	1.17	1.11	1.04

ESM Fig 18. Hypothesis testing with the PBPK model, assuming rhythmic physiological processes. BF, blood flow; C_{max}, maximum plasma concentration; C_{trough}, trough plasma concentration; GET, gastric emptying time; GMFE, geometric mean fold error; lit, literature; MATE, multidrug and toxin extrusion protein; MRD, mean relative deviation; OCT, organic cation transporter; opt, optimised; PMAT, plasma membrane monoamine transporter; RPF, renal plasma flow



ESM Fig 19. PBPK model predictions alongside observed data of study I [1] (1000 mg twice daily immediate-release administration in the fed state), assuming a daily oscillation of different processes and physiological conditions. Observed data are shown as dots ± SD, predictions are shown as lines. Grey areas indicate night-time. lit, literature; MATE, multidrug and toxin extrusion protein; OCT, organic cation transporter; opt, optimised; PMAT, plasma membrane monoamine transporter

2.3.3 Final PBPK model parameters (with daily oscillation)

Individual plasma concentration-time profiles show high interindividual variability. Therefore, organic cation transporter (OCT) 2 transport rate constant (k_{cat}) values were optimised for every individual. Additionally, OCT2 amplitude and time shift were optimised (after inclusion of rhythmic GFR and RPF) with the help of individual profiles (n=26) (ESM Table 10). A correlation plot of OCT2 k_{cat} values, amplitude and time shift (sine function describing daily oscillation) is shown in ESM Fig 20, where no correlation has been detected.

ESM Table 9. Drug-dependent parameters of the metformin PBPK model adopted from Hanke et al.[8]

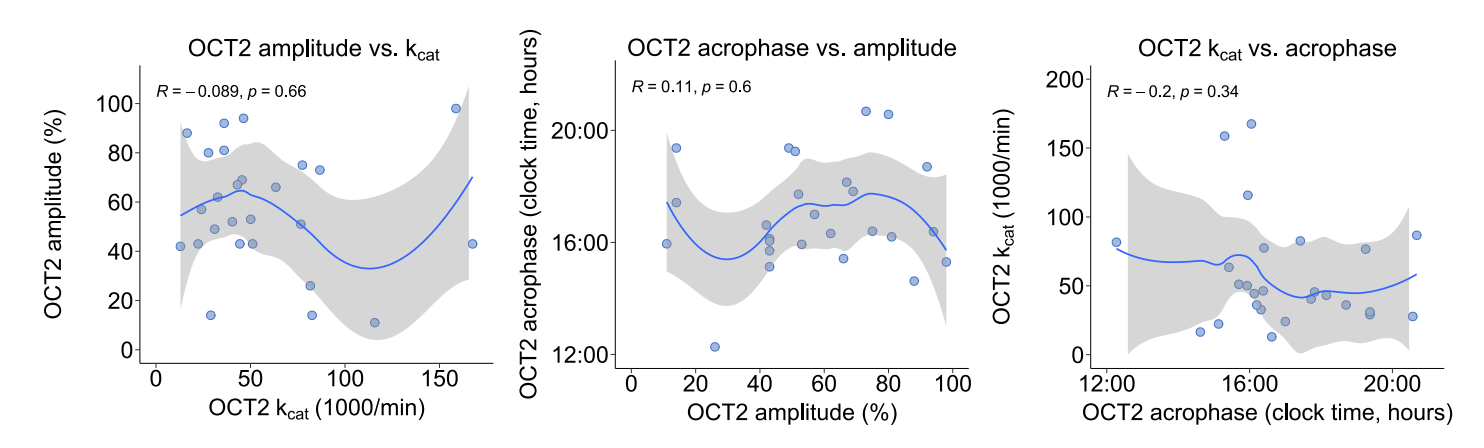
Parameter	Value	Unit	Source	Literature	Reference	Description
MW	129.16	g/mol	Literature	129.16	[28]	Molecular weight
pKa ₁ (base)	2.80		Literature	2.80	[29]	Acid dissociation constant
pKa₂ (base)	11.50		Literature	11.50	[29]	Acid dissociation constant
Solubility (pH 6.8)	350.90	g/l	Literature	350.90	[29]	Solubility
logP	-1.43		Literature	-1.43	[30]	Lipophilicity
fu	100	%	Literature	100	[31–33]	Fraction unbound plasma
B/P ratio	-		Optimised	Time-dependent	[31]	Blood/plasma concentration ratio
MATE1 K _M	283.00	μmol/l	Literature	283.00	[34]	Michaelis-Menten constant
MATE1 k _{cat}	165.69	1/min	Optimised	-	-	Transport rate constant
OCT1 K _M	1180.00	μmol/l	Literature	1180.00	[35]	Michaelis-Menten constant
OCT1 k _{cat}	641.19	1/min	Optimised	-	-	Transport rate constant
OCT2 K _M	810.00	μmol/l	Literature	810.00	[35]	Michaelis-Menten constant
OCT2 k _{cat}	5.17×10^4	1/min	Optimised	-	-	Transport rate constant
PMAT K _M	367.57	μmol/l	Optimised	1320.00	[36]	Michaelis-Menten constant
PMAT k _{cat}	76.47	1/min	Optimised	-	-	Transport rate constant
PMAT Hill	3.00		Literature	2.64	[36]	Hill coefficient
GFR fraction	1		Assumed	-	-	Fraction of filtered drug in the urine
EHC continuous fraction	1		Assumed	-	-	Fraction of bile continually released
Partition coefficients	Diverse		Calculated	PK-Sim	[37]	Cell to plasma partition coefficients
Cellular permeability	2.30×10^{-4}	cm/min	Calculated	CDS norm.	[38]	Plasma permeability into the cellular space
Intestinal permeability	8.49×10^{-7}	cm/min	Optimised	1.87×10^{-7}	Calculated	Transcellular intestinal permeability
Basolat. small intest. permeability	1.16×10^{-5}	cm/min	Optimised	1.11×10^{-6}	Calculated	Basolateral permeability out of the mucosa
Basolat. large intest. permeability	0	cm/min	Assumed	1.11×10^{-6}	Calculated	Basolateral permeability out of the mucosa
Formulation	IR fast/IR fed ^a		Optimised	=	[8, 39, 40]	Formulation used in predictions

^a IR fast: Weibull function with a dissolution time of 7.90 minutes and a dissolution shape of 1.36 (extracted from [39]), IR fed: Weibull function with a dissolution time of 7.90 minutes and a dissolution shape of 0.11 (both optimised) [8, 40], ER fed: Weibull function with a dissolution time of 402.80 minuted and a dissolution shape of 1.35 (both optimised) [1, 41, 42]. basolat., basolateral; CDS, norm. charge-dependent Schmitt normalised to PK-Sim calculation method; EHC, enterohepatic circulation; ER, extended-release formulation; intest., intestinal; IR, immediate-release formulation; MATE, multidrug and toxin extrusion protein; OCT, organic cation transporter; PK-Sim, PK-Sim standard calculation method; PMAT, plasma membrane monoamine transporter

ESM Table 10. System- and drug-dependent PBPK model parameters to cover time-of-day dependent and interindividual variability

Parameter –		Value		•		_,	
	mean	range	Unit	Source	Literature	Reference	Description
GFR amplitude	13	-	%	Literature	13	[25–27]	Amplitude sine function
GFR acrophase	15:01	-	Clock time, hours	Literature	15:01	[25–27]	Acrophase sine function
RPF amplitude	12	-	%	Literature	12	[25–27]	Amplitude sine function
RPF acrophase	17:22	-	Clock time, hours	Literature	17:22	[25–27]	Acrophase sine function
OCT2 k _{cat}	5.77×10^4	$1.29 \times 10^4 - 1.68 \times 10^5$	1/min	Optimised	-	-	Individual transport rate constant
OCT2 amplitude	57	11–98	%	Optimised	-	-	Individual amplitude sine function
OCT2 acrophase	16:54	12:16 -20:41 hours	Clock time, hours	Optimised	-	-	Individual acrophase sine function

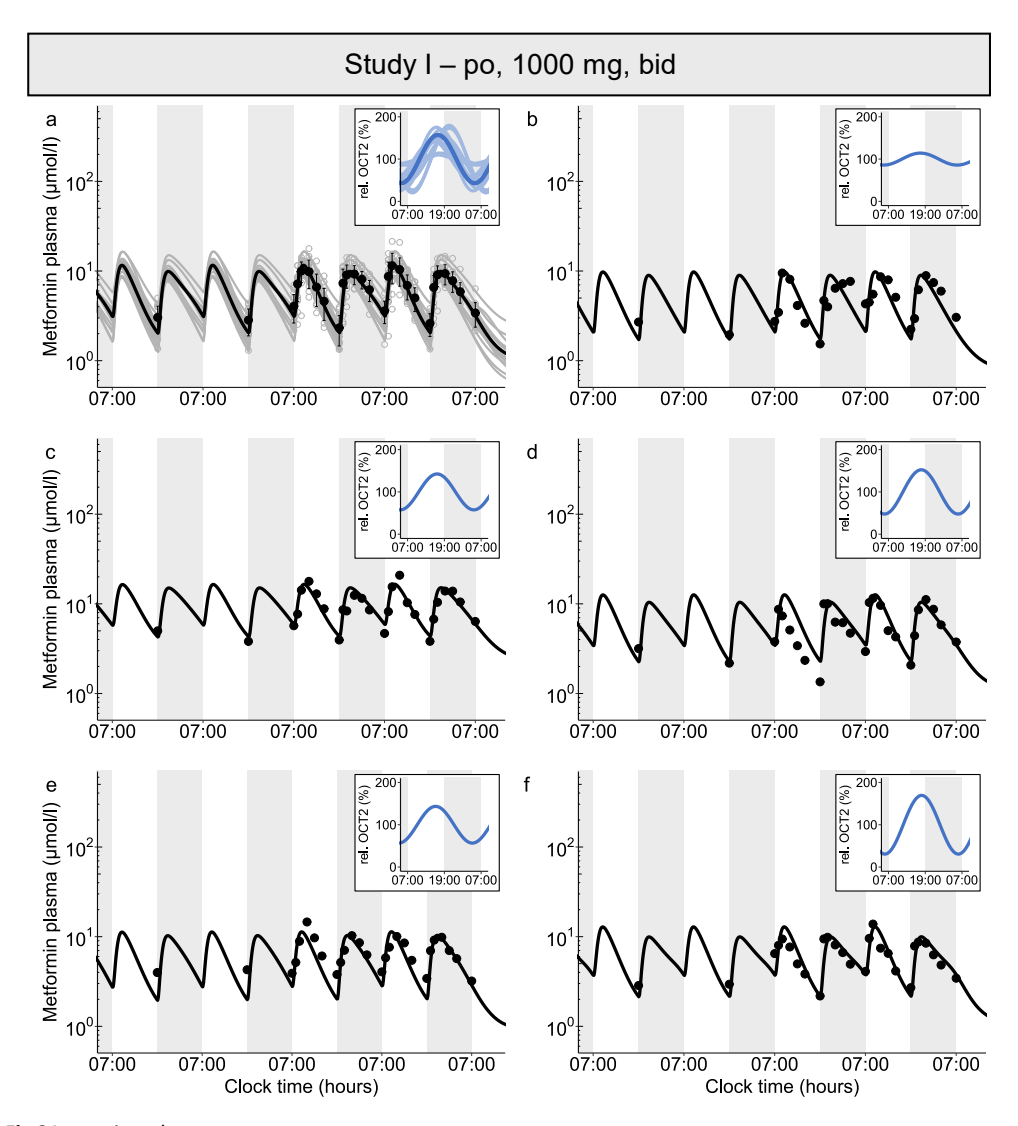
A 24-hour phase was assumed for the sine function. OCT, organic cation transporter; RPF, renal plasma flow



ESM Fig 20. Correlation plots of individual PBPK modelled OCT2 k_{cat}, amplitude and time shift values to cover daily oscillation (*n*=26). k_{cat}, transport rate constant; OCT, organic cation transporter

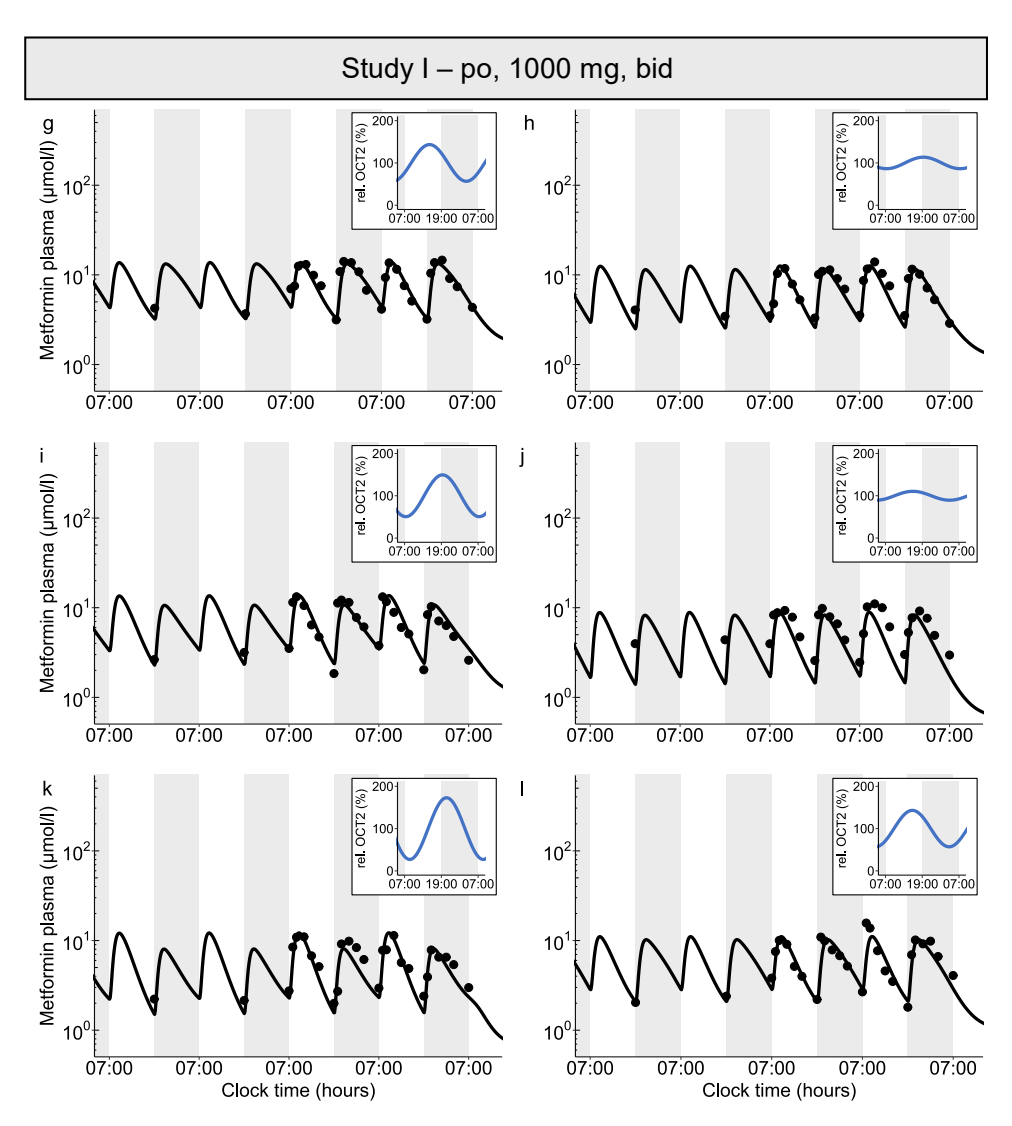
2.3.4 PBPK model plots

2.3.4.1 Metformin plasma concentration-time profiles

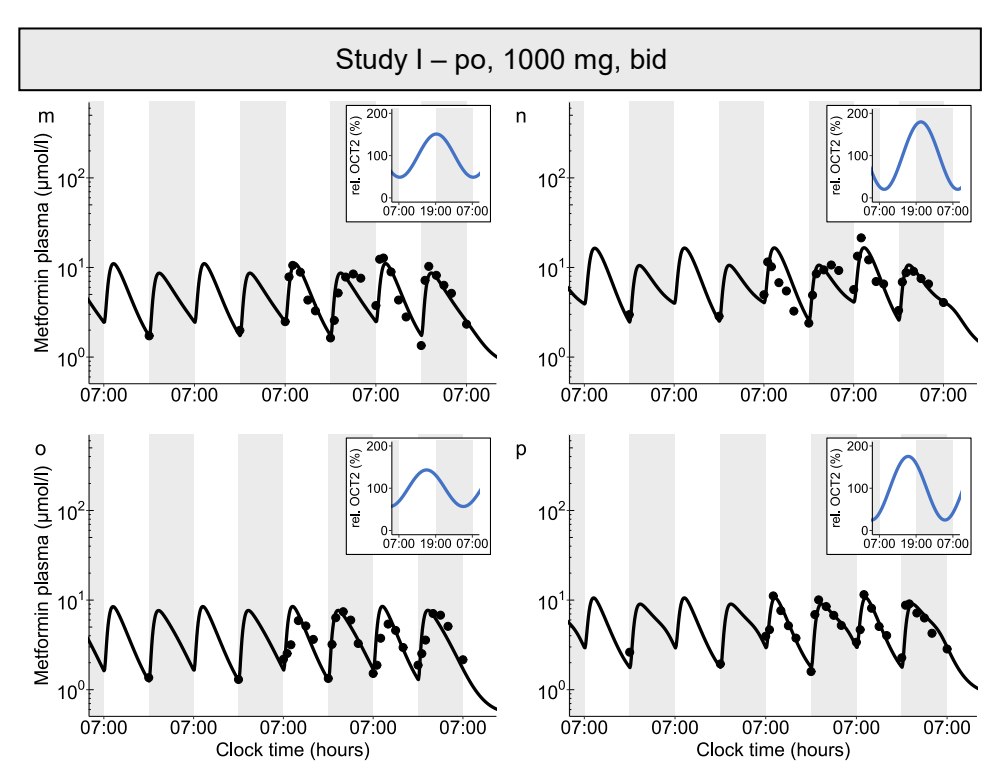


ESM Fig 21. continued

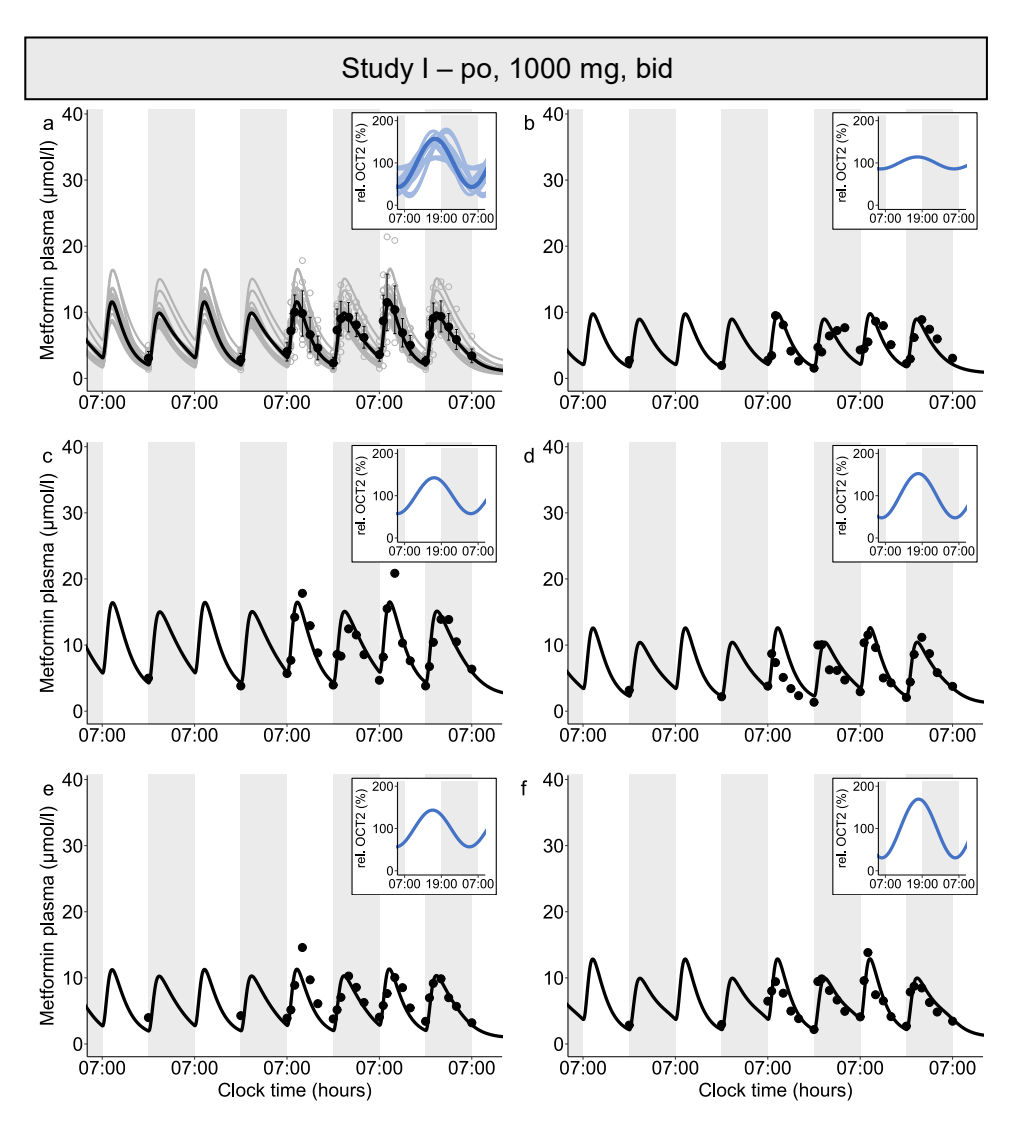
2-35



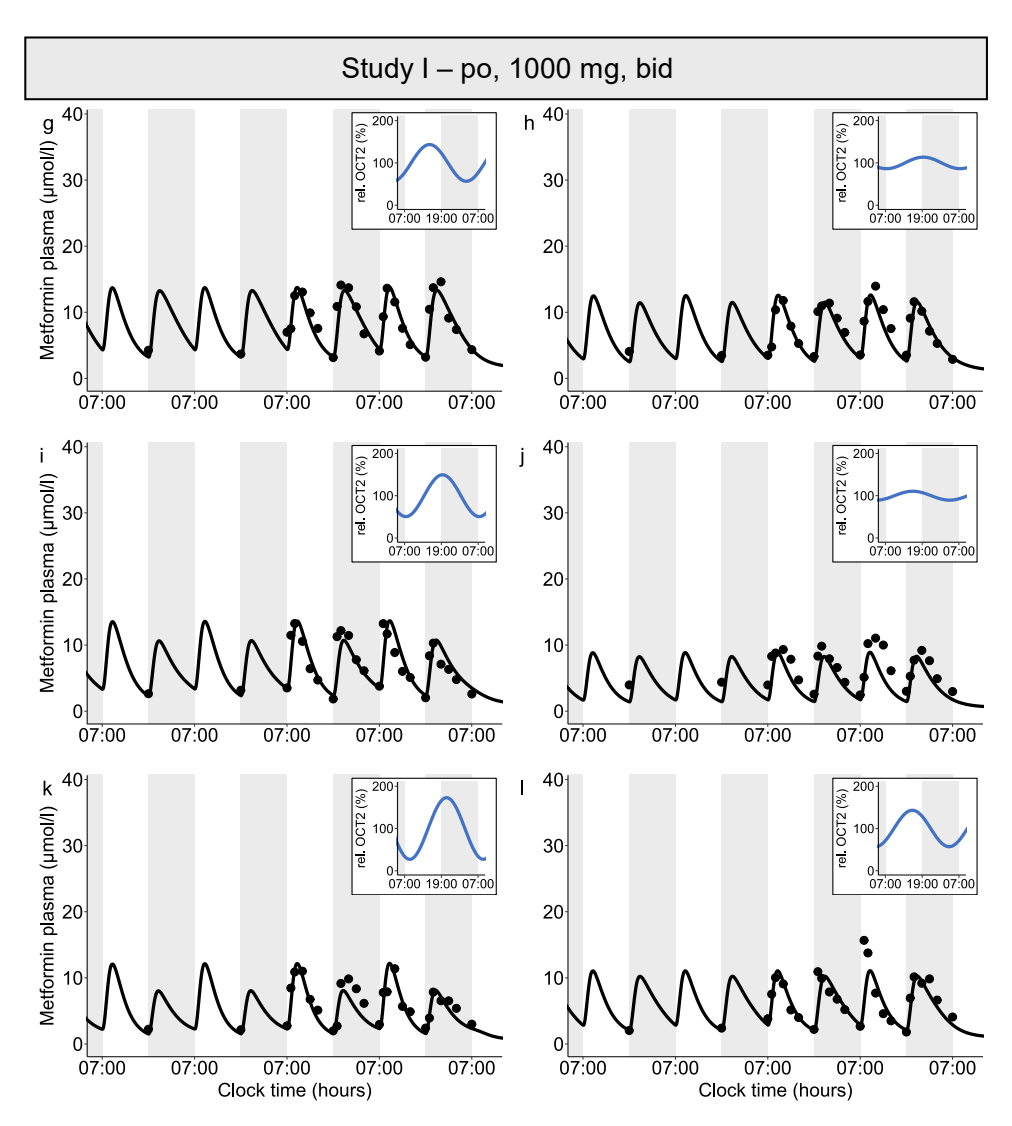
ESM Fig 21. continued



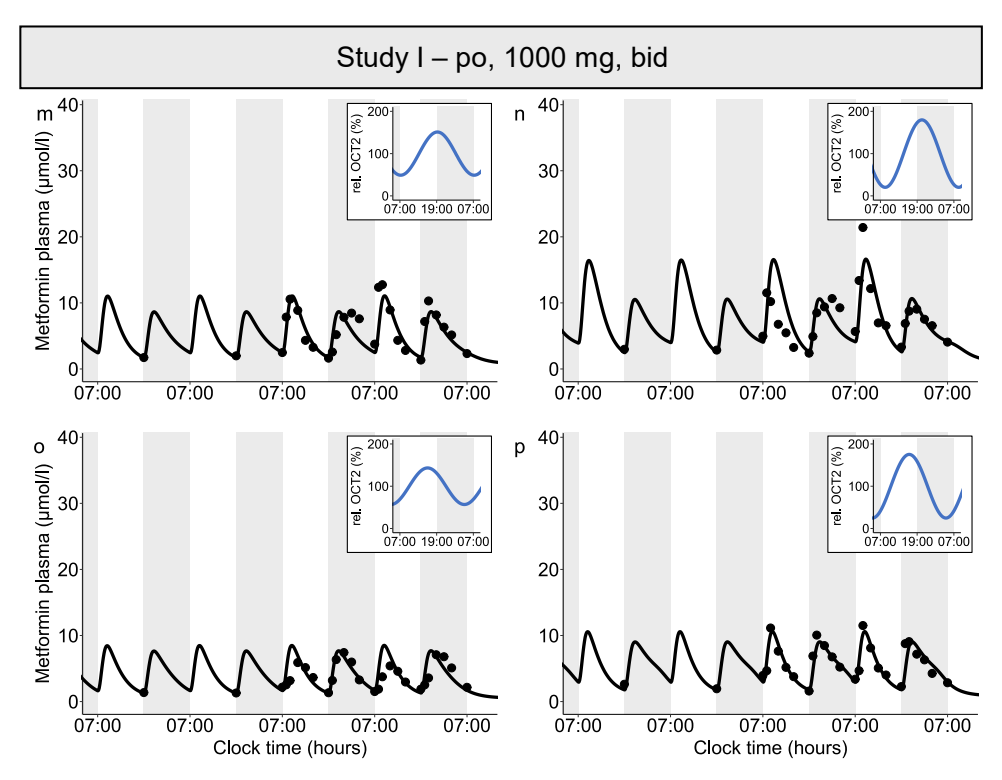
ESM Fig 21. PBPK model predictions compared to observed (a) mean and (b-p) individual plasma concentration-time profiles of metformin after twice daily administration of 1000 mg metformin immediate-release formulation in the fed state (semilogarithmic plots, i.e. concentration presented on decadic logarithm scale, training dataset). Predictions are shown as lines. Observed data from study I are shown as dots ± SD [1]. Grey areas indicate night-time. Inserts depict optimised mean and individual relative OCT2 expression, respectively. bid, twice daily; OCT, organic cation transporter; po, oral



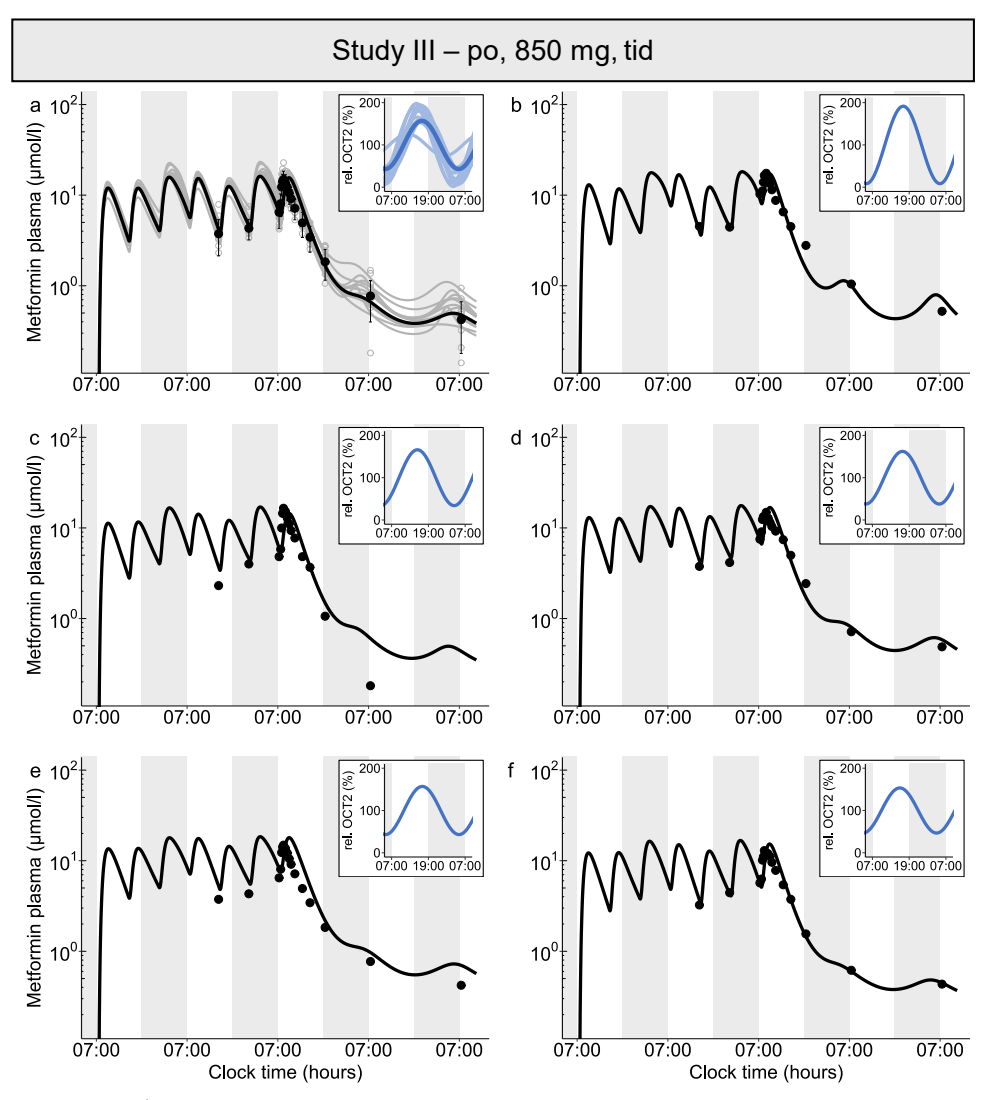
ESM Fig 22. continued



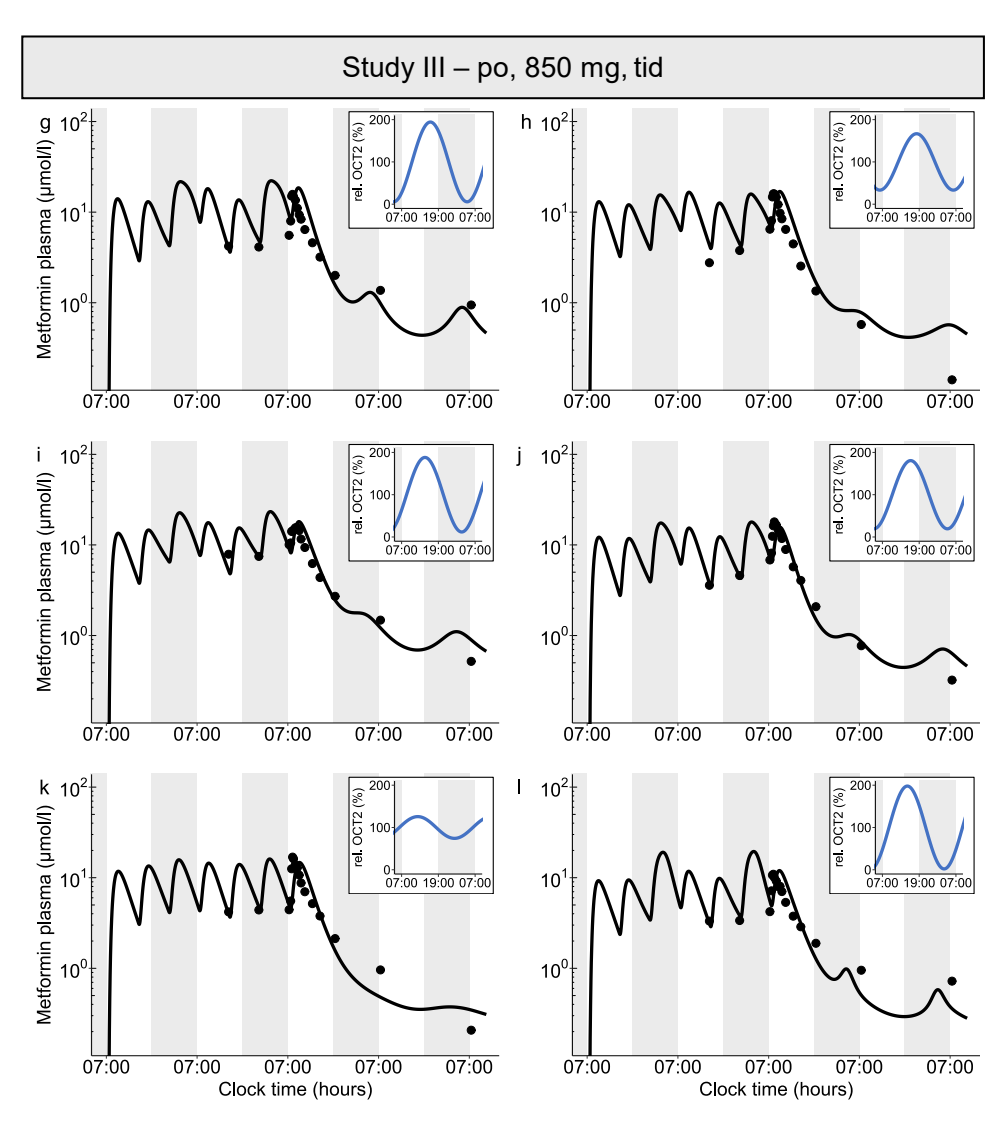
ESM Fig 22. continued



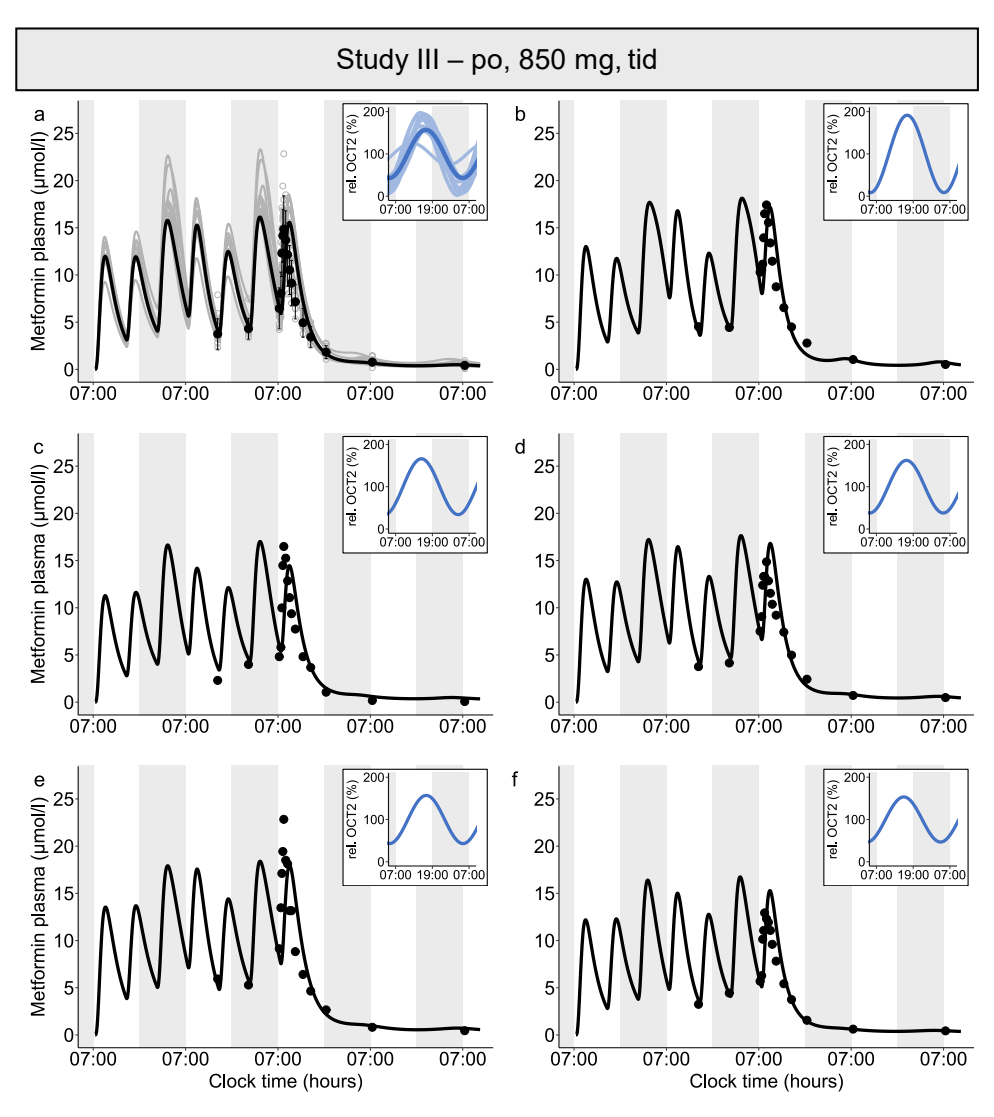
ESM Fig 22. PBPK model predictions compared to observed (a) mean and (**b–p**) individual plasma concentration-time profiles of metformin after twice daily administration of 1000 mg metformin immediate-release formulation in the fed state (linear plots, training dataset). Predictions are shown as lines. Observed data from study I are shown as dots ± SD [1]. Grey areas indicate night-time. Inserts depict optimised mean and individual relative OCT2 expression, respectively. bid, twice daily; OCT, organic cation transporter; po, oral



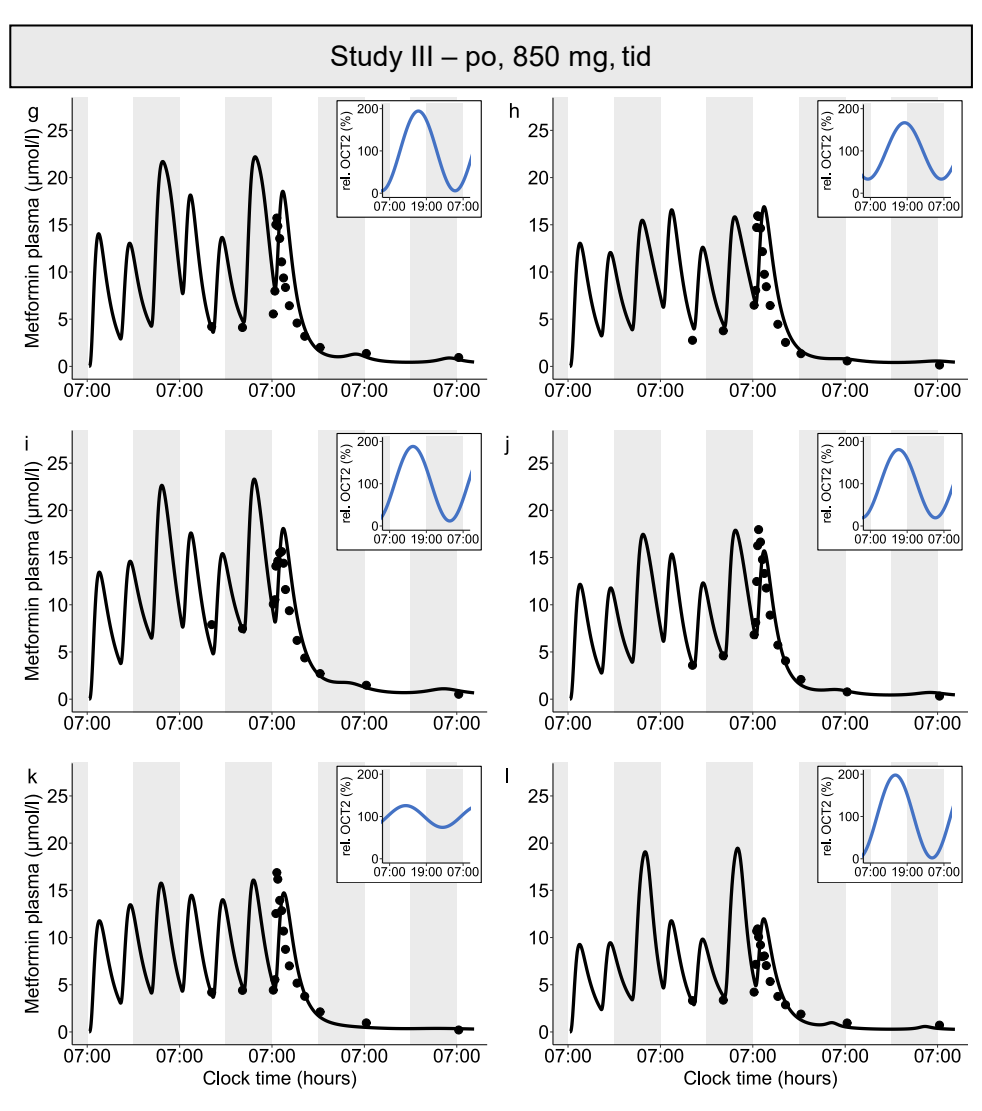
ESM Fig 23. continued



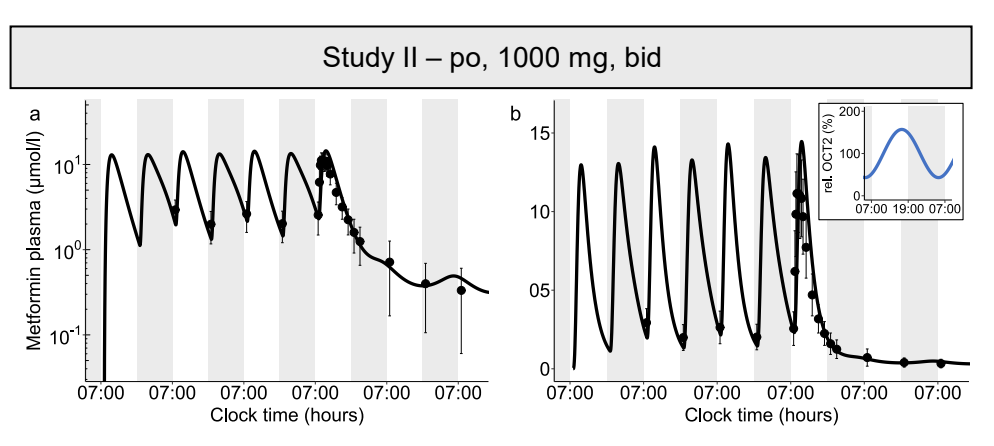
ESM Fig 23. PBPK model predictions compared to observed (a) mean and (b–l) individual plasma concentration-time profiles of metformin after three times daily administration of 850 mg immediate-release formulation (first six doses in fed state, last dose in fasted state) (semilogarithmic plots, i.e. concentration presented on decadic logarithm scale, training dataset). Predictions are shown as lines. Observed data from study III are shown as dots ± SD [3]. Grey areas indicate night-time. Inserts depict optimised mean and individual relative OCT2 expression, respectively. OCT, organic cation transporter; po, oral; tid, three times daily



ESM Fig 24. continued

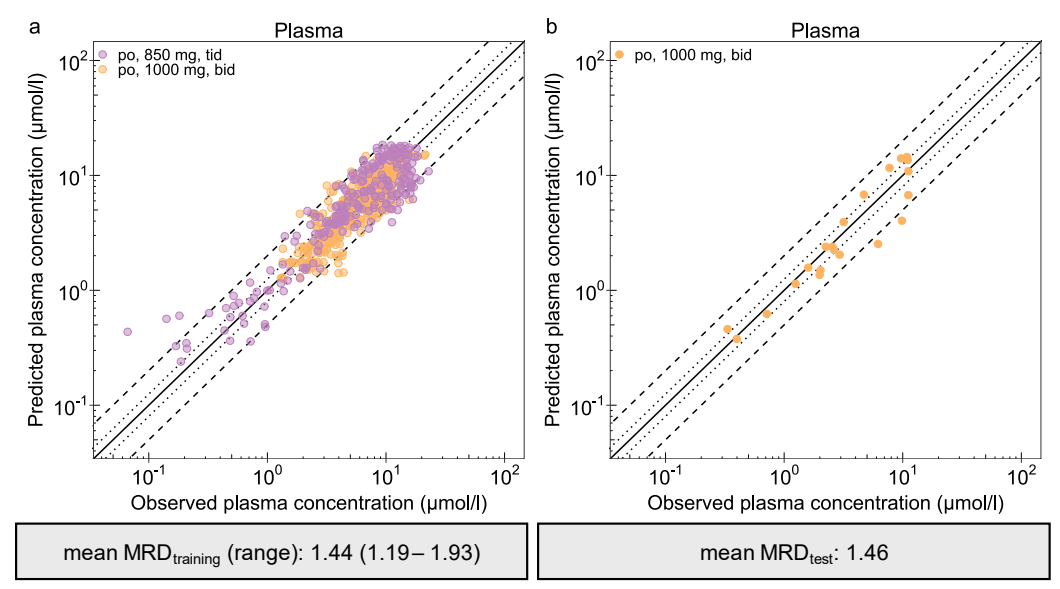


ESM Fig 24. PBPK model predictions compared to observed (a) mean and (b-l) individual plasma concentration-time profiles of metformin after three times daily administration of 850 mg immediate-release formulation (first six doses in fed state, last dose in fasted state) (linear plots, training dataset). Predictions are shown as lines. Observed data from study III are shown as dots ± SD [3]. Grey areas indicate night-time. Inserts depict optimised mean and individual relative OCT2 expression, respectively. OCT, organic cation transporter; po, oral; tid, three times daily

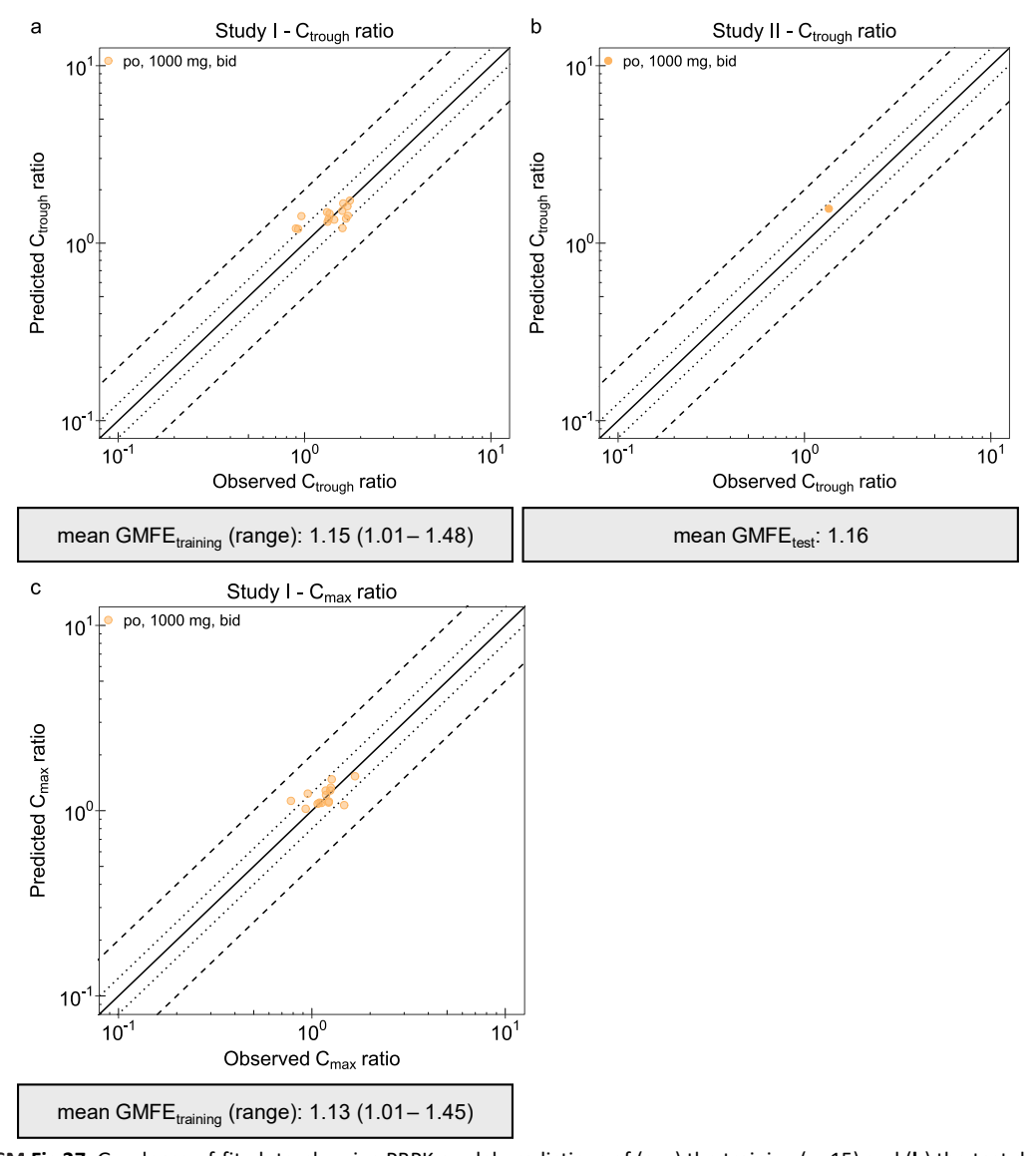


ESM Fig 25. PBPK model predictions compared to observed mean concentration-time profiles of metformin after twice daily administration of 1000 mg metformin immediate-release formulation in the fed state ((a) semilogarithmic plot, i.e. concentration presented on decadic logarithm scale, (b) linear plot, test dataset). Predictions are shown as lines. Observed data from study II are shown as dots ± SD [2]. Grey areas indicate night-time. Insert depicts optimised mean relative OCT2 expression. bid, twice daily; OCT, organic cation transporter; po, oral

2.3.4.2 Metformin goodness-of-fit plots



ESM Fig 26. Goodness-of-fit plots, showing PBPK model predictions of (a) the training (n=26) and (b) the test dataset (mean profile) compared to observed metformin plasma concentrations following either twice daily 1000 mg or three times daily 850 mg of metformin immediate-release formulation (study I-III [1–3]). The straight black line marks the line of identity. Dotted lines indicate 0.8- to 1.25-fold and dashed lines indicate 0.5- to 2-fold acceptance limits. bid, twice daily; MRD, mean relative deviation; po, oral; tid, three times daily



ESM Fig 27. Goodness-of-fit plots, showing PBPK model predictions of (a, c) the training (*n*=15) and (b) the test dataset (mean profile) compared to observed metformin (a—b) C_{trough} or (c) C_{max} ratios (morning/evening), following twice daily 1000 mg of metformin immediate-release formulation (studies I and II [1, 2]). The straight black line marks the line of identity. Dotted lines indicate 0.8- to 1.25-fold and dashed lines indicate 0.5- to 2-fold acceptance limits. bid, twice daily; GMFE, geometric mean fold error; po, oral

3 ESM References

- Timmins P, Donahue S, Meeker J, Marathe P (2005) Steady-state pharmacokinetics of a novel extended-release metformin formulation. Clin Pharmacokinet 44(7):721–729. https://doi.org/10.2165/00003088-200544070-00004
- 2. Boehringer Ingelheim Pharma GmbH & Co. KG (2014) Relative Bioavailability BI 10773 and Metformin in Healthy Male Volunteers. ClinicalTrials.gov Identifier: NCT02172248. National Library of Medicine, Bethesda MD; https://clinicaltrials.gov/ct2/show/NCT02172248. Accessed 13 Sep 2022
- 3. Boehringer Ingelheim Pharma GmbH & Co. KG (2014) Bioavailability of BI 1356 BS and Metformin After Co-administration Compared to the Bioavailability of BI 1356 BS Alone and Metformin Alone in Healthy Male Volunteers. ClinicalTrials.gov Identifier: NCT02183506. National Library of Medicine, Bethesda MD; https://clinicaltrials.gov/ct2/show/NCT02183506. Accessed 13 Sep 2022
- Boehringer Ingelheim Pharma GmbH & Co. KG (2013) Relative Bioavailability of 2 Fixed Dose Combinations of Linagliptin/Metformin Compared With Single Tablets. ClinicalTrials.gov Identifier: NCT01845077. National Library of Medicine, Bethesda MD; https://www.clinicaltrials.gov/ct2/show/NCT01845077. Accessed 13 Sep 2022
- Boehringer Ingelheim Pharma GmbH & Co. KG (2013) Relative Bioavailability of 2 Fixed Dose Combinations of Empagliflozin/Metformin Compared With Single Tablets. ClinicalTrials.gov Identifier: NCT01975220. National Library of Medicine, Bethesda MD; https://clinicaltrials.gov/ct2/show/NCT01975220. Accessed 13 Sep 2022
- 6. Akaike H (1974) A new look at the statistical model identification. IEEE Trans Automat Contr 19(6):716–723. https://doi.org/10.1109/TAC.1974.1100705
- 7. Beal S, Sheiner L (1998) NONMEM Users Guides. San Francisco: NONMEM Project Group University of California
- 8. Hanke N, Türk D, Selzer D, et al (2020) A comprehensive whole-body physiologically based pharmacokinetic drug—drug—gene interaction model of metformin and cimetidine in healthy adults and renally impaired individuals. Clin Pharmacokinet 59(11):1419—1431. https://doi.org/10.1007/s40262-020-00896-w
- Open Systems Pharmacology Suite Community. (2018) PK-Sim® Ontogeny Database Documentation,
 Version
 7.3. https://github.com/Open-Systems-Pharmacology/OSPSuite.Documentation/blob/master/PK-Sim Ontogeny Database Version 7.3.pdf.
 Accessed 24 Aug 2020
- Scotcher D, Billington S, Brown J, et al (2017) Microsomal and cytosolic scaling factors in dog and human kidney cortex and application for in vitro-in vivo extrapolation of renal metabolic clearance.
 Drug Metab Dispos 45(5):556–568. https://doi.org/10.1124/dmd.117.075242
- 11. Prasad B, Johnson K, Billington S, et al (2016) Abundance of drug transporters in the human kidney

- cortex as quantified by quantitative targeted proteomics. Drug Metab Dispos 44(12):1920–1924. https://doi.org/10.1124/dmd.116.072066
- 12. Otsuka M, Matsumoto T, Morimoto R, Arioka S, Omote H, Moriyama Y (2005) A human transporter protein that mediates the final excretion step for toxic organic cations. Proc Natl Acad Sci U S A 102(50):17923–17928
- Masuda S, Terada T, Yonezawa A, et al (2006) Identification and functional characterization of a new human kidney-specific H+/organic cation antiporter, kidney-specific multidrug and toxin extrusion 2.
 J Am Soc Nephrol 17(8):2127–2135. https://doi.org/10.1681/ASN.2006030205
- 14. Prasad B, Evers R, Gupta A, et al (2014) Interindividual variability in hepatic organic anion-transporting polypeptides and P-glycoprotein (ABCB1) protein expression: quantification by liquid chromatography tandem mass spectroscopy and influence of genotype, age, and sex. Drug Metab Dispos 42(1):78–88. https://doi.org/10.1124/dmd.113.053819
- 15. Wang L, Prasad B, Salphati L, et al (2015) Interspecies variability in expression of hepatobiliary transporters across human, dog, monkey, and rat as determined by quantitative proteomics. Drug Metab Dispos 43(3):367–374. https://doi.org/10.1124/dmd.114.061580
- 16. Kolesnikov N, Hastings E, Keays M, et al (2015) ArrayExpress update-simplifying data submissions.

 Nucleic Acids Res 43(D1):D1113–D1116. https://doi.org/10.1093/nar/gku1057
- 17. Expressed Sequence Tags (EST) from UniGene. National Center for Biotechnology Information (NCBI). https://www.ncbi.nlm.nih.gov/unigene
- Meyer M, Schneckener S, Ludewig B, Kuepfer L, Lippert J (2012) Using expression data for quantification of active processes in physiologically based pharmacokinetic modeling. Drug Metab Dispos 40(5):892–901. https://doi.org/10.1124/dmd.111.043174
- 19. Nishimura M, Naito S (2005) Tissue-specific mRNA expression profiles of human ATP-binding cassette and solute carrier transporter superfamilies. Drug Metab Pharmacokinet 20(6):452–477. https://doi.org/10.2133/dmpk.20.452
- Dallmann R, Brown SA, Gachon F (2014) Chronopharmacology: New insights and therapeutic implications. Annu Rev Pharmacol Toxicol 54(1):339–361. https://doi.org/10.1146/annurevpharmtox-011613-135923
- 21. Vaughn B, Rotolo S, Roth H (2014) Circadian rhythm and sleep influences on digestive physiology and disorders. ChronoPhysiology Ther 4:67–77. https://doi.org/10.2147/CPT.S44806
- 22. Goo RH, Moore JG, Greenberg E, Alazraki NP (1987) Circadian variation in gastric emptying of meals in humans. Gastroenterology 93(3):515–518. https://doi.org/10.1016/0016-5085(87)90913-9
- 23. Kumar D, Wingate D, Ruckebusch Y (1986) Circadian variation in the propagation velocity of the migrating motor complex. Gastroenterology 91(4):926–930. https://doi.org/10.1016/0016-5085(86)90696-7
- 24. Lemmer B, Nold G (1991) Circadian changes in estimated hepatic blood flow in healthy subjects. Br J

- Clin Pharmacol 32(5):627-629. https://doi.org/10.1111/j.1365-2125.1991.tb03964.x
- 25. Wesson LG (1964) Electrolyte excretion in relation to diurnal cycles of renal function. Medicine (Baltimore) 43(5):547–592. https://doi.org/10.1097/00005792-196409000-00002
- Koopman MG, Koomen GCM, Krediet RT, de Moor EA, Hoek FJ, Arisz L (1989) Circadian rhythm of glomerular filtration rate in normal individuals. Clin Sci 77(1):105–111. https://doi.org/10.1042/cs0770105
- 27. van Acker BAC, Koomen GCM, Koopman MG, Krediet RT, Arisz L (1992) Discrepancy between circadian rhythms of inulin and creatinine clearance. J Lab Clin Med 120(3):400–410
- 28. Wishart DS, Knox C, Guo AC, et al (2006) DrugBank: a comprehensive resource for in silico drug discovery and exploration. Nucleic Acids Res 34(Database issue):D668-D672. https://doi.org/10.1093/nar/gkj067
- 29. Desai D, Wong B, Huang Y, et al (2014) Surfactant-mediated dissolution of metformin hydrochloride tablets: Wetting effects versus ion pairs diffusivity. J Pharm Sci 103(3):920–926. https://doi.org/10.1002/jps.23852
- 30. Graham GG, Punt J, Arora M, et al (2011) Clinical pharmacokinetics of metformin. Clin Pharmacokinet 50(2):81–98. https://doi.org/10.2165/11534750-000000000-00000
- 31. Tucker GT, Casey C, Phillips PJ, Connor H, Ward JD, Woods HF (1981) Metformin kinetics in healthy subjects and in patients with diabetes mellitus. Br J Clin Pharmacol 12(2):235–246. https://doi.org/10.1111/j.1365-2125.1981.tb01206.x
- 32. Pentikäinen PJ, Neuvonen PJ, Penttilä A (1979) Pharmacokinetics of metformin after intravenous and oral administration to man. Eur J Clin Pharmacol 16(3):195–202. https://doi.org/10.1007/BF00562061
- 33. Sirtori CR, Franceschini G, Galli-Kienle M, et al (1978) Disposition of metformin (N,N-dimethylbiguanide) in man. Clin Pharmacol Ther 24(6):683–693. https://doi.org/10.1002/cpt1978246683
- 34. Yin J, Duan H, Wang J (2016) Impact of substrate-dependent inhibition on renal organic cation transporters hOCT2 and hMATE1/2-K-mediated drug transport and intracellular accumulation. J Pharmacol Exp Ther 359(3):401–410. https://doi.org/10.1124/jpet.116.236158
- 35. Chen Y, Li S, Brown C, et al (2009) Effect of genetic variation in the organic cation transporter 2 on the renal elimination of metformin. Pharmacogenet Genomics 19(7):497–504. https://doi.org/10.1097/FPC.0b013e32832cc7e9
- Zhou M, Xia L, Wang J (2007) Metformin transport by a newly cloned proton-stimulated organic cation transporter (plasma membrane monoamine transporter) expressed in human intestine. Drug Metab Dispos 35(10):1956–1962. https://doi.org/10.1124/dmd.107.015495
- 37. Willmann S, Lippert J, Schmitt W (2005) From physicochemistry to absorption and distribution: predictive mechanistic modelling and computational tools. Expert Opin Drug Metab Toxicol 1(1):159–168. https://doi.org/10.1517/17425255.1.1.159

- Open Systems Pharmacology Suite Community. Open Systems Pharmacology Documentation. https://docs.open-systems-pharmacology.org/working-with-pk-sim/pk-sim-documentation. Accessed 22 Jan 2022
- 39. Block LC, Schemling LO, Couto AG, Mourão SC, Bresolin TMB (2008) Pharmaceutical equivalence of metformin tablets with various binders. Rev Ciências Farm Básica e Apl 29(1):29–35
- 40. Sambol NC, Brookes LG, Chiang J, et al (1996) Food intake and dosage level, but not tablet vs solution dosage form, affect the absorption of metformin HCl in man. Br J Clin Pharmacol 42(4):510–512. https://doi.org/10.1111/j.1365-2125.1996.tb00017.x
- 41. Buse JB, DeFronzo RA, Rosenstock J, et al (2015) The primary glucose-lowering effect of metformin resides in the gut, not the circulation. Results from short-term pharmacokinetic and 12-week doseranging studies. Diabetes Care 39(2):198–205. https://doi.org/10.2337/dc15-0488
- 42. Idkaidek N, Arafat T (2011) Metformin IR versus XR pharmacokinetics in humans. J Bioequiv Availab 03(10):233–235. https://doi.org/10.4172/jbb.1000092

A 2: Project III appendix
Supplementary material to Project III

Supplementary online material

Alternative Treatment Regimens with the PCSK9 Inhibitors Alirocumab and Evolocumab: A Pharmacokinetic and Pharmacodynamic Modeling Approach

Nina Scherer; Christiane Dings; Michael Böhm, M.D.; Ulrich Laufs, M.D.; Thorsten Lehr, Ph.D.

Supplemental Figure S1:

Goodness of fit plots for alirocumab (left) and evolocumab (right) for the pharmacokinetic (upper) and pharmacodynamic (lower) population predicted vs. observed. The black lines indicate the lines of identity. LDLc, low density lipoprotein cholesterol.

Supplemental Figure S2:

VPCs: Observed and model predicted PK and PD data after single dose administration (upper and middle) and multiple dose administration (lower) of alirocumab. Circle indicates the observations, line and bands indicate the predicted median and 90% confidence interval of the predictions of 5000 individuals. LDLc, low density lipoprotein cholesterol; QnWxm, dosing once every n weeks for m times; s.c., subcutaneous.

Supplemental Figure S3:

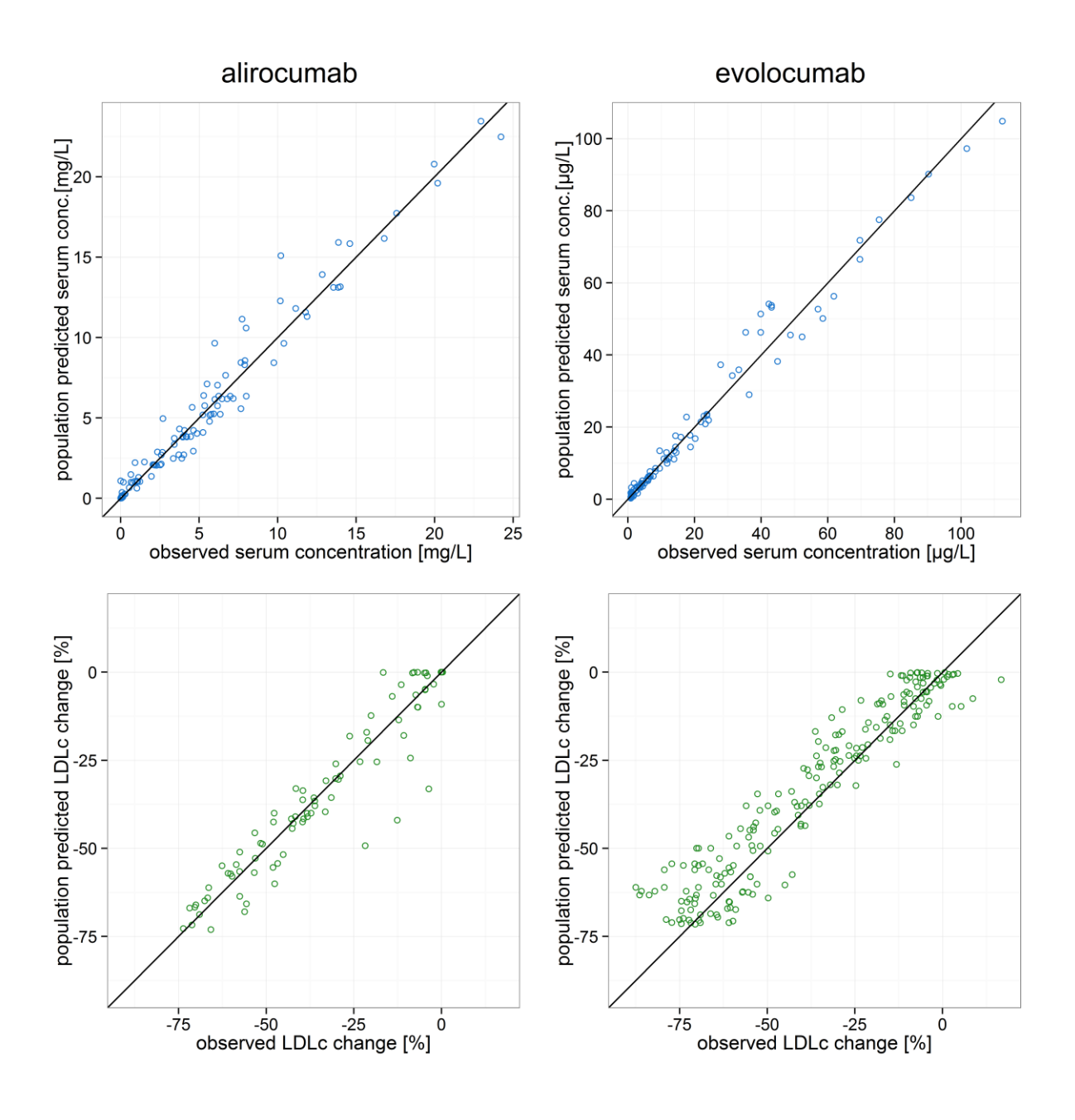
VPCs: Observed and model predicted PK and PD data after single dose administration (upper) and multiple dose administration (lower) of evolocumab. Circle indicates the observations, line and bands indicate the predicted median and 90% confidence interval of the predictions of 5000 individuals. LDLc, low density lipoprotein cholesterol; QnWxm, dosing once every n weeks for m times; s.c., subcutaneous; i.v., intravenous.

Supplemental Table S1:

Overview over the available data for model development. Administration was subcutaneous unless specified otherwise. i.v., intravenous.

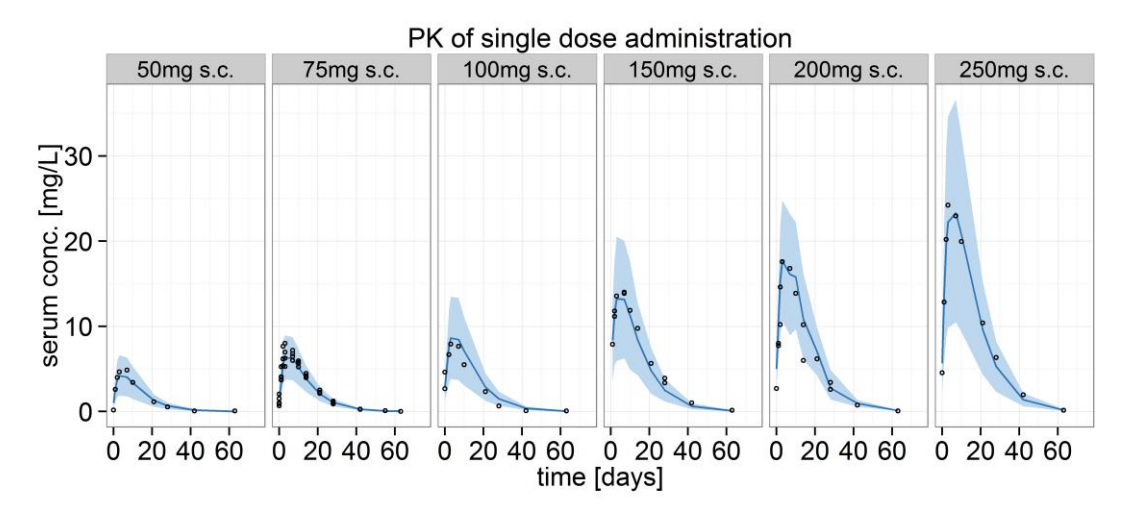
References (Supplementary)

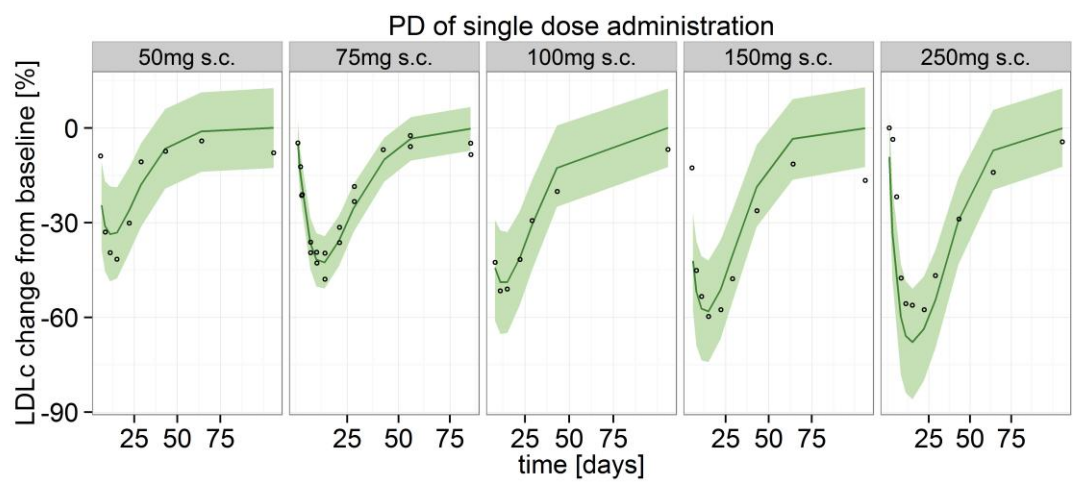
- Chung SM, Earp J, Vaidyanathan J, Mehrotra N. Center for Drug Evaluation and Research Clinical Pharmacology and Biopharmaceutics Review (Praluent- Alirocumab) (Application Number 125559Orig1s000) [Internet]. 2014. Available from: http://www.accessdata.fda.gov/drugsatfda_docs/nda/2015/125559Orig1s000ClinPharmR.pdf
- 2. Stein EA, Mellis S, Yancopoulos GD, Stahl N, Logan D, Smith WB, et al. Effect of a Monoclonal Antibody to PCSK9 on LDL Cholesterol. J Chem Inf Model. 2012;366(25):1108–18.
- Smith JP. Food and Drug Administration Center for Drug Evaluation and Research. Briefing
 Document: Praluent (alirocumab) injection [Internet]. The Endocrinologic and Metabolic Drugs
 Advisory Committee Meeting. 2015. Available from:
 http://www.fda.gov/downloads/AdvisoryCommittees/CommitteesMeetingMaterials/Drugs/Endo
 crinologicandMetabolicDrugsAdvisoryCommittee/UCM449865.pdf
- 4. Lunven C, Paehler T, Poitiers F, Brunet A, Rey J, Hanotin C, et al. A randomized study of the relative pharmacokinetics, pharmacodynamics, and safety of alirocumab, a fully human monoclonal antibody to PCSK9, after single subcutaneous administration at three different injection sites in healthy subjects. Cardiovasc Ther. 2014;32(6):297–301.
- Suryanarayana S, Earp J, Mehrotra N, Jaya V. Center for Drug Evaluation and Research Clinical Pharmacology and Biopharmaceutics Review (Repatha- Evolocumab) (Application Number 125559Orig1s000). 2014; Available from: http://www.accessdata.fda.gov/drugsatfda docs/nda/2015/125522Orig1s000ClinPharmR.pdf
- Dias CS, Shaywitz AJ, Wasserman SM, Smith BP, Gao B, Stolman DS, et al. Effects of AMG 145 on low-density lipoprotein cholesterol levels: Results from 2 randomized, double-blind, placebocontrolled, ascending-dose phase 1 studies in healthy volunteers and hypercholesterolemic subjects on statins. J Am Coll Cardiol. 2012;60(19):1888–98.
- 7. Amgen Inc. EMDAC Meeting Briefing Document (Evolocumab) Background Information for Endocrinologic and Metabolic Drugs Advisory Committee [Internet]. 2015. Available from: http://www.fda.gov/downloads/AdvisoryCommittees/CommitteesMeetingMaterials/Drugs/EndocrinologicandMetabolicDrugsAdvisoryCommittee/UCM450072.pdf

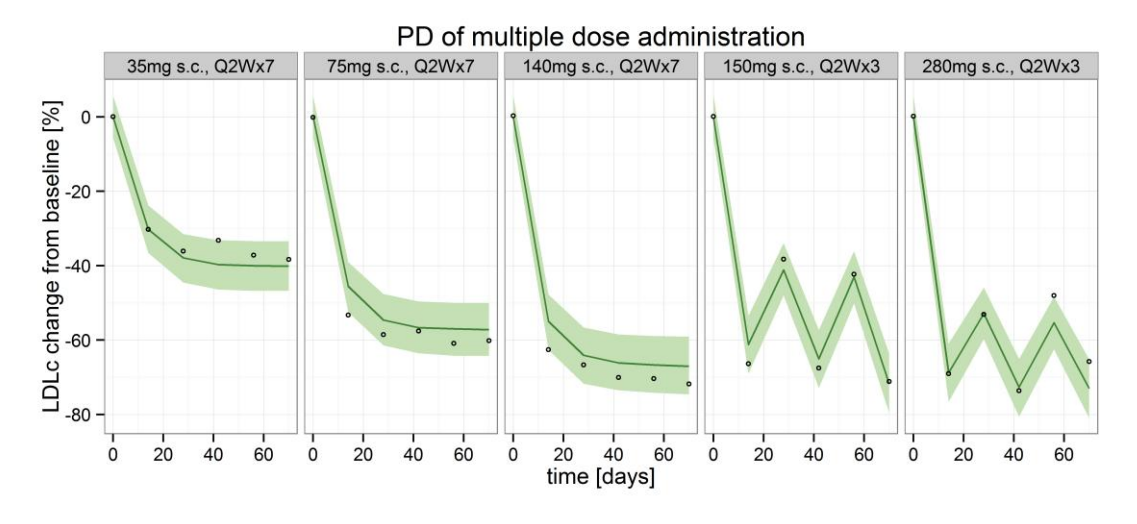


Supplemental Figure S 1: Goodness of fit plots for alirocumab (left) and evolocumab (right) for the pharmacokinetic (upper) and pharmacodynamic (lower) population predicted vs. observed. The black lines indicate the lines of identity. LDLc, low density lipoprotein cholesterol.

VPC of alirocumab

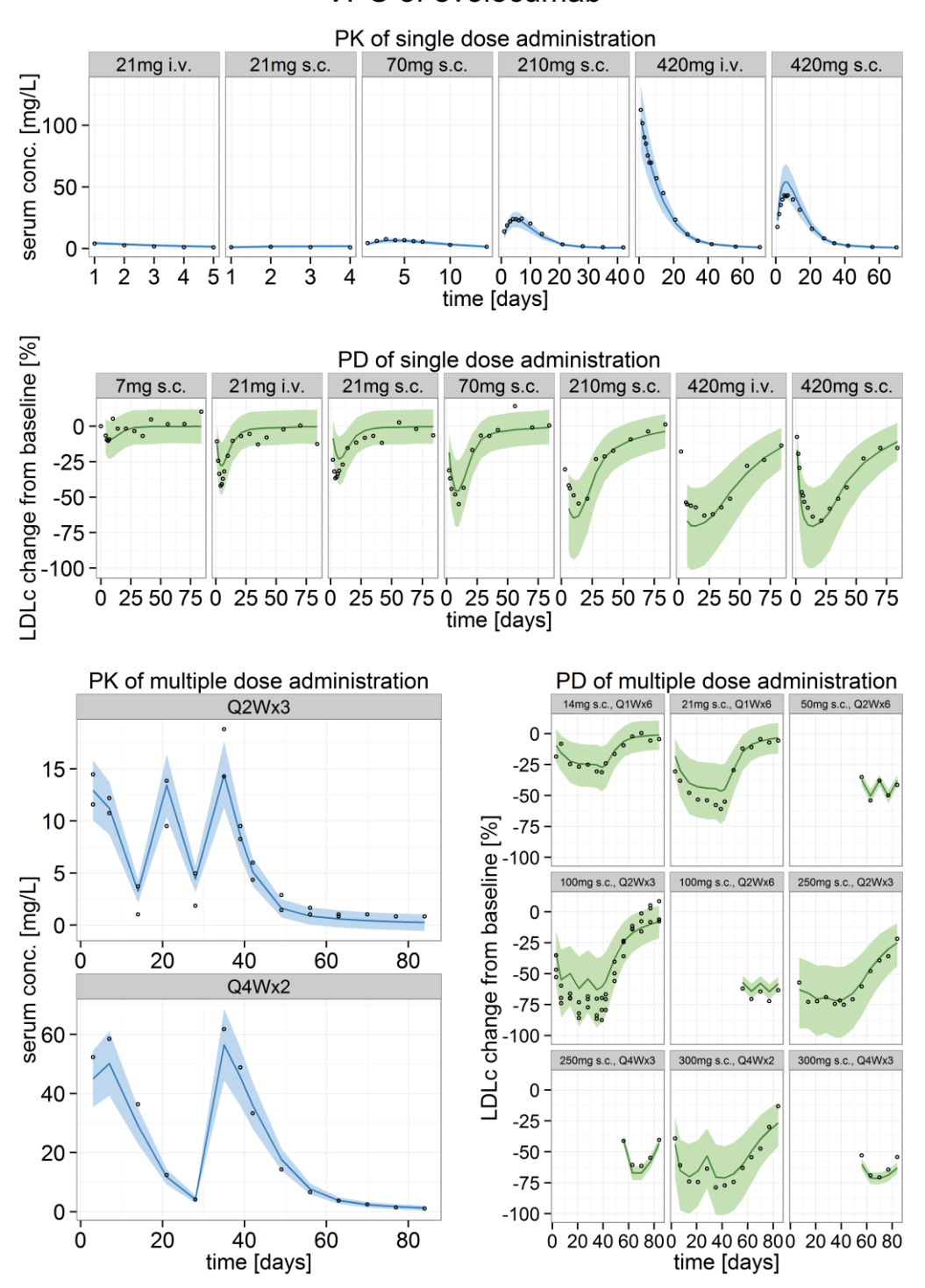






Supplemental Figure S 2 VPCs: Observed and model predicted PK and PD data after single dose administration (upper and middle) and multiple dose administration (lower) of alirocumab. Circle indicates the observations, line and bands indicate the predicted median and 90% confidence interval of the predictions of 5000 individuals. LDLc, low density lipoprotein cholesterol; QnWxm, dosing once every n weeks for m times; s.c., subcutaneous.

VPC of evolocumab



Supplemental Figure S 3: VPCs: Observed and model predicted PK and PD data after single dose administration (upper) and multiple dose administration (lower) of evolocumab. Circle indicates the observations, line and bands indicate the predicted median and 90% confidence interval of the predictions of 5000 individuals. LDLc, low density lipoprotein cholesterol; QnWxm, dosing once every n weeks for m times; s.c., subcutaneous; i.v., intravenous.

Supplemental Table S 1: Overview over the available data for model development. Administration was subcutaneous unless specified otherwise. i.v., intravenous.

alirocumab

study number**	references	SD/MD	PK	PD	doses [mg] (n)	statin co- medication
NCT01074372	(93–95)	SD	Х	Х	50 (6), 100 (6),	no
					150 (5), 250 (6)	
NCT01785329	(96)	SD	Χ	Χ	75 (20)	no
NCT01670734	(95)	SD	Χ		75 (8)	no
NCT01448239	(95)	SD	Χ		200 (12)	no
NCT01161082	(95)	SD	Χ		150 (8)	no
			Х		200 (10)	yes (dose not
						stratified)
NCT01288443	(93)	MD		Χ	50 Q2W (30),	yes (dose not
					100 Q2W (31),	stratified)
					150 Q2W (29),	
					200 Q4W (28),	
					300 Q4W (30)	

evolocumab:

study number**	references	SD/MD	PK	PD	doses [mg] (n)	statin co- medication
20080397	(97,98)	SD	Χ	Х	7 (6), 21 (6),	no
					70 (6), 210 (6),	
					420 (6), 21 i.v. (6),	
					420 i.v. (6)	
20080398	(97,98)	MD		Χ	14 QW (6)	yes (low dose
				Χ	35 QW (6)	statin)
			Χ	Χ	140 Q2W (6)	
				Χ	280 Q2W (6)	
			X	Χ	420 Q4W (6)	
			X	Χ	140 Q2W (9)	yes (high dose
						statin)
			Χ	Χ	140 Q2W (4)	yes (dose not
						stratified)
20101154,	(99)	MD		Χ	70 Q2W (124),	yes (dose not
20101155,					140 Q2W (121),	stratified)
20090158,					280 Q4W (155),	
20090159					420 Q4W (211)	

^{*}SD, single dose; MD, multiple dose; PK, pharmacokinetic; PD, pharmacodynamic; i.v., intravenious; n, number of subjects from which mean curves are calculated

^{**}in case of several study numbers, mean curves were derived from data of several studies

Appendix B:

B1: Conference Abstracts

Pharmacokinetic and Pharmacodynamic Modeling of Alirocumab and Evolocumab, two fully human monoclonal antibodies targeting PCSK9.

Nina Scherer, Christiane Dings, Michael Böhm, Ulrich Laufs and Thorsten Lehr. 25th Population Approach Group Europe (PAGE) meeting, 2016, Lisbon, Portugal.

Mathematical modeling of glucose, insulin and c-peptide during the OGTT in prediabetic subjects: a DIRECT study.

Christiane Dings, Nina Scherer, Jan Freijer, Valerie Nock, Thorsten Lehr. 26th Population Approach Group Europe (PAGE) meeting, 2017, Budapest, Hungary.

A population pharmacokinetic (PK) model of metformin regarding immediate and extended release formulations under fasted and fed conditions.

Nina Scherer, Christiane Dings, Jan Freijer, Valerie Nock, Thorsten Lehr. 26th Population Approach Group Europe (PAGE) meeting, 2017, Budapest, Hungary.

Mathematical modelling of glucose tolerance tests describing glucose, insulin and C-peptide levels in different cohorts: an IMI DIRECT study.

Christiane Dings, <u>Nina Scherer</u>, Valerie Nock, Anita Hennige, Ewan Pearson, Paul W. Franks, Thorsten Lehr, for the IMI-DIRECT consortium.

54th European Association for the Study of Diabetes (EASD) meeting, 2018, Berlin, Germany.

Mathematical modeling of the oral glucose tolerance test in pre-diabetic patients: An IMI DIRECT study

Christiane Dings, Nina Scherer, Iryna Sihinevich, Valerie Nock, Anita M. Hennige, Ewan R. Pearson, Paul W. Franks and Thorsten Lehr for the IMI DIRECT consortium. 28th Population Approach Group Europe (PAGE) meeting, 2019, Stockholm, Sweden

Mathematical Modeling of Glucose Homeostasis in Morbidly Obese Diabetic Patients Undergoing Roux-en-Y Gastric Bypass Surgery: An IMI DIRECT

Study Iryna Sihinevich, Christiane Dings, <u>Nina Scherer</u>, Valerie Nock, Anita M. Hennige, Violeta Raverdy, Francois Pattou and Thorsten Lehr for the IMI DIRECT consortium. *28th Population Approach Group Europe (PAGE) meeting, 2019*, Stockholm, Sweden.

B2: Book Chapters

Daniel Moj, Melanie I. Titze, <u>Nina Scherer</u>, Torsten Lehr. "Onkologie" in Pharmakogenetik und Therapeutisches Drug Monitoring: Diagnostische Bausteine für die individualisierte Therapie

Hanns-Georg Klein and Ekkehard Haen.

Berlin, Boston: De Gruyter, 2018. https://doi.org/10.1515/9783110352900

Danksagung

An dieser Stelle möchte ich allen von Herzen "Danke" sagen, die mich während meiner Promotionszeit auf verschiedenste Art und Weise begleitet, motiviert und unterstützt haben.

Mein besonderer Dank gilt Prof. Dr. Thorsten Lehr, der mir die Möglichkeit gab, meine Dissertation in seiner Arbeitsgruppe anzufertigen und mich mit seiner Begeisterung für die Pharmakometrie angesteckt hat. Thorsten's fortwährende Unterstützung, seine Anregungen und Rückmeldungen über viele Jahre hinweg haben maßgeblich zum Gelingen dieser Arbeit beigetragen.

Ebenso danke ich Prof. Dr. Marc Schneider für die Übernahme des Zweitgutachtens und die bereichernden Diskussionen während meines Projekts.

Mein herzlicher Dank gilt allen Kolleginnen und Kollegen des Arbeitskreises der Klinischen Pharmazie, für ihre Unterstützung, die anregenden Diskussionen und die angenehmen Gespräche während gemeinsamer Kaffeepausen. Herausheben möchte ich insbesondere Dr. Christiane Dings, Iryna Sihinevich und Katharina Götz, sowie die beiden (Büro-)Hunden Linux und Lina, die mich in allen Lebenslagen erlebt, ertragen, motiviert, aufgebaut und unterstützt haben. Die gemeinsame Zeit bleibt unvergessen.

Ich danke dem Graduiertenprogramm PharMetrX, insbesondere Prof. Dr. Charlotte Kloft und Prof. Dr. Wilhelm Huisinga, für die Möglichkeit, ein umfassendes Wissen im Bereich der Modellierung zu erlangen.

Dem gesamten IMI DIRECT Consortium danke ich für die lehrreiche Zeit. Der interdisziplinäre Austausch mit Fachleuten aus verschiedenen Bereichen war für mich äußerst bereichernd und hat mir wertvolle Impulse für meinen weiteren Lebensweg gegeben.

Mein weiterer Dank gilt den Co-Autorinnen und Co-Autoren meiner Manuskripte für ihre Unterstützung – ohne sie wäre diese Arbeit nicht zustande gekommen.

Ebenso möchte ich Dr. Stefan Rettig, Jana Brardt-Penzel und Bettina André-Dohmen danken, die mich auf meinem aktuellen beruflichen Weg begleiten, dabei stets fordern und fördern und immer großes Verständnis für dieses Projekt hatten.

Abschließend danke ich meinen Freunden und meiner Familie für ihre Unterstützung. Mit dem Abschluss dieser Dissertation endet nicht nur ein wissenschaftliches Projekt, sondern auch eine intensive Lebensphase, die ich ohne die Unterstützung vieler besonderer Menschen nicht hätte bewältigen können. Mein tief empfundener Dank gilt meiner Mutter Heike, die mich von Anfang an bis heute mit Liebe, Geduld und Ermutigung begleitet hat. Ihr Vertrauen in mich war stets ein Anker, besonders in Momenten des Zweifelns. Ebenso danke ich meinem Vater Karl Heinz, der mir stets das Gefühl gab, dass alles gut werden würde und mit regelmäßiger Essensversorgung auch in stressigen Schreib- und Lebensphasen für Entlastung sorgte.

Ein ganz besonderer Dank gebührt meiner besseren Hälfte Daniel. Mit seiner liebevollen Gelassenheit, seinem Humor und seiner Fähigkeit, mich in den richtigen Momenten aufzufangen, war er mein Fels in der Brandung. Wenn ich (nicht nur einmal) das Gefühl hatte, diese Arbeit nicht mehr zu Ende bringen zu können, war er da – mit einem offenen Ohr, einem Lächeln und der Erinnerung daran, warum ich diesen Weg gewählt habe. Nicht zuletzt hat mir unsere wundervolle Tochter Romy immer wieder gezeigt, wie man das Leben mit großer Wissbegier und unermüdlicher Freude entdecken kann. Ihre neugierige Art und ihr Sturkopf erinnerten mich oft an mich selbst und haben mich motiviert, dieses Projekt mit derselben Entschlossenheit zu vollenden. Zudem danke ich unserer zweiten Tochter, die ich derzeit unter meinem Herzen trage. Ihre bevorstehende Geburt hat mir die Kraft und Motivation gegeben, dieses Projekt nun erfolgreich abzuschließen.

Ohne die Unterstützung all dieser Menschen wäre diese Dissertation nicht möglich gewesen.